Astroparticle physics overview

Andrii Neronov
APC Paris & EPFL Lausanne

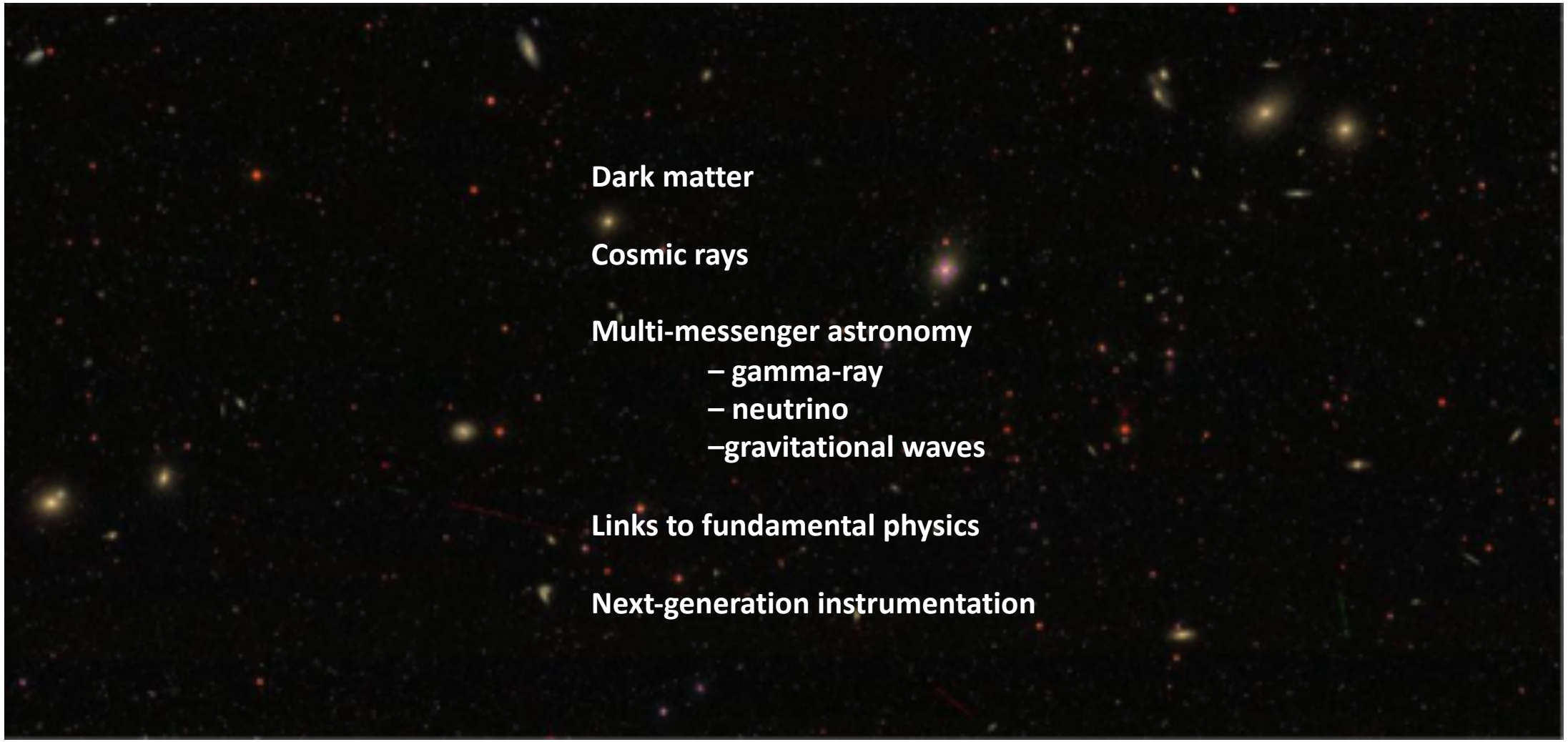

Dark matter in the Milky Way and other galaxies

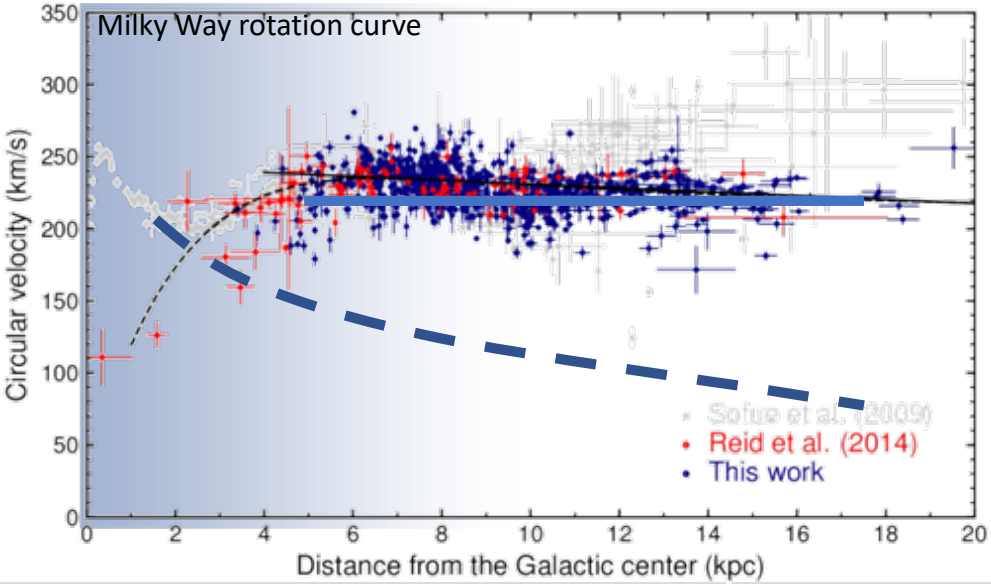

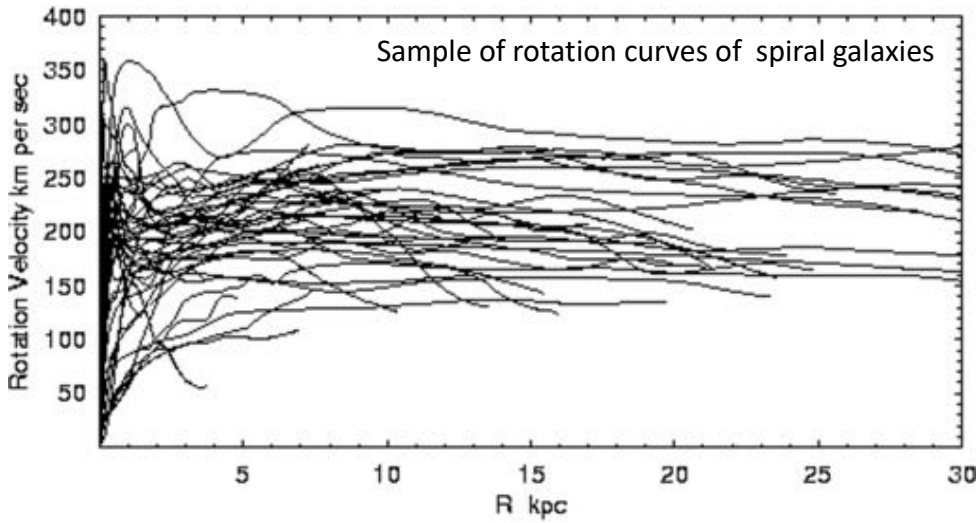

Matter content of galaxies can be measured from their dynamical properties.

$$m\ \vec{a} = \vec{F}$$

$$\frac{mv^2}{r} = \frac{G_N M(r) m}{r^2}$$

$$v(r) = \sqrt{\frac{G_N M(r)}{r}}$$

Measurements of rotation velocity of a galaxy as a function of distance from its center give mass profile $M(r)$.

Outside the galaxy, the rotation velocity is expected to decrease as $r^{-1/2}$.

This is not what is observed e.g. in the Milky Way. Instead, its rotation velocity stays approximately at the same level, $v \sim 230\ \mathrm{km/s}$ all the way up to $\sim 30\ \mathrm{kpc}$ from the center.

This suggest that the mass grows as $M \propto r$, but there is no visible matter at such large distances. The density of stellar disk decreases exponentially beyond $r_* \simeq 4\ \mathrm{kpc}$ distance

$$\rho_*(r) \propto e^{-\frac{r}{r_*}}$$

The same mass growth $M \propto r$ is observed in most of other spiral galaxies. The rotation curves remain flat well beyond the visible matter distribution.

Direct dark matter detection

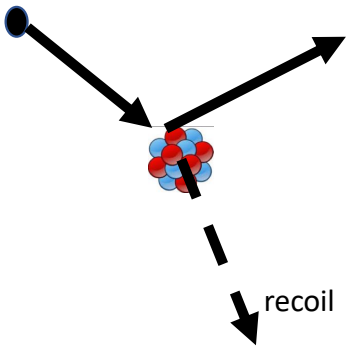

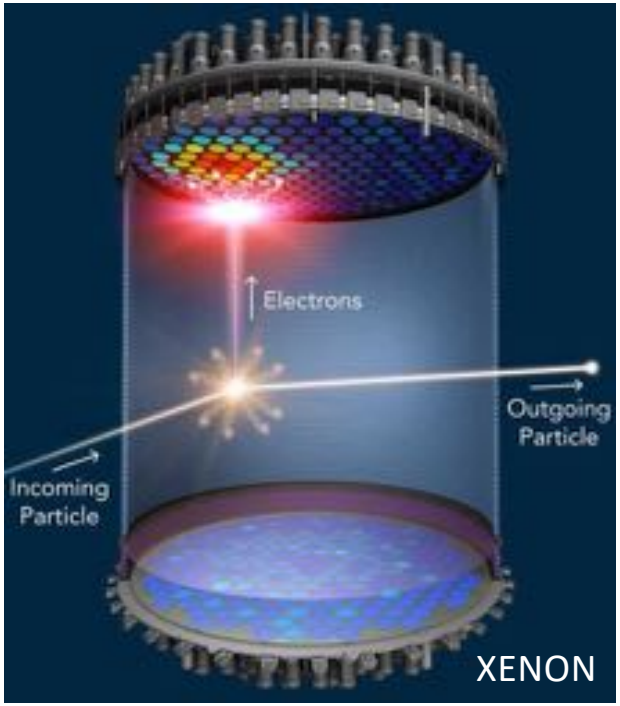

Close to the solar distance, the density of the dark and conventional (baryonic) matter are comparable,

$$\rho_{dm} \sim \rho_b \sim 0.3 \frac{\text{GeV}}{\text{cm}^3}$$

The density of dark matter particles of the mass m in the GeV-TeV range is

$$n_{dm} = \frac{\rho_{dm}}{m} \simeq 0.3 \left[\frac{m}{1\ \text{GeV}}\right]^{-1} \frac{1}{\text{cm}^3}$$

These particles are available everywhere (pass through every laboratory setup with velocities $v \sim \sqrt{G_N\, M/r} \sim 230\ \text{km/s}$.

Their kinetic energy is

$$E_{dm} \sim \frac{mv^2}{2} \simeq 0.3 \left[\frac{m}{1\ \text{GeV}}\right] \text{keV}$$

If the dark matter particles occasionally collide with atomic nuclei (or electrons?) they might deposit “recoil” energy up to E_{dm} in detector material.

This energy deposition can be measured. It is larger than ionisation energy of atoms.

- Dark matter interactions can excite atomic levels. De-exciting atoms would emit detectable **light** pulses.
- Dark matter interactions can produce free charges (e.g. electron-hole pairs in semiconductors). Free charges can be sampled as **current** pulses, if voltage is applied to detector.
- Dark matter interaction can excite the detector mechanically (**phonons**) ultimately causing slight increase in its **temperature**.

Direct dark matter detection

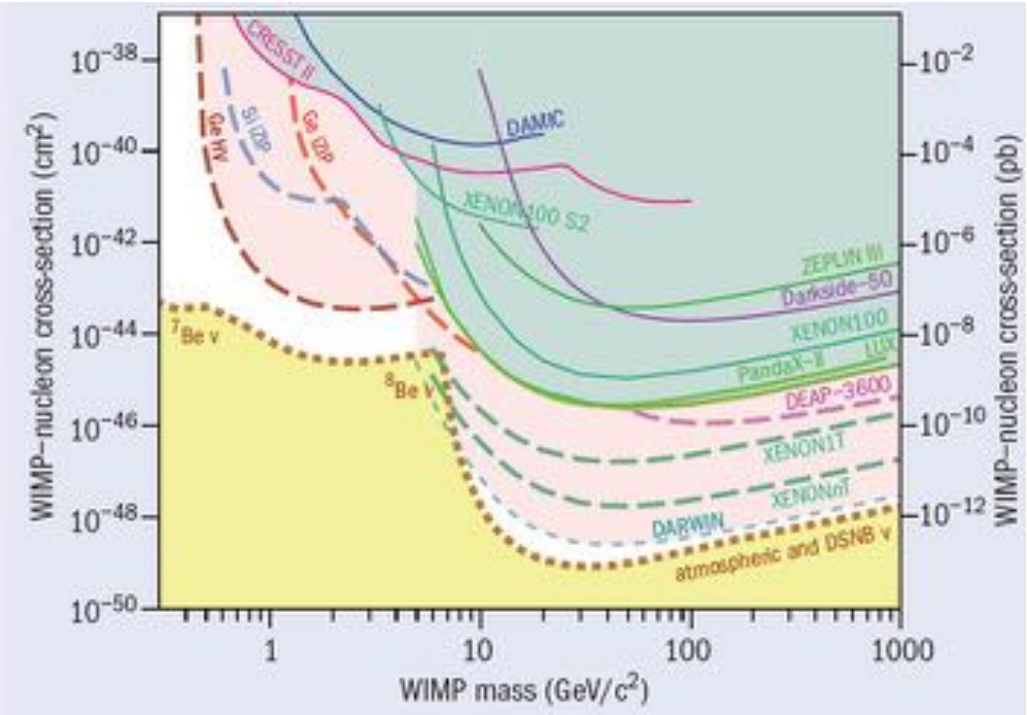

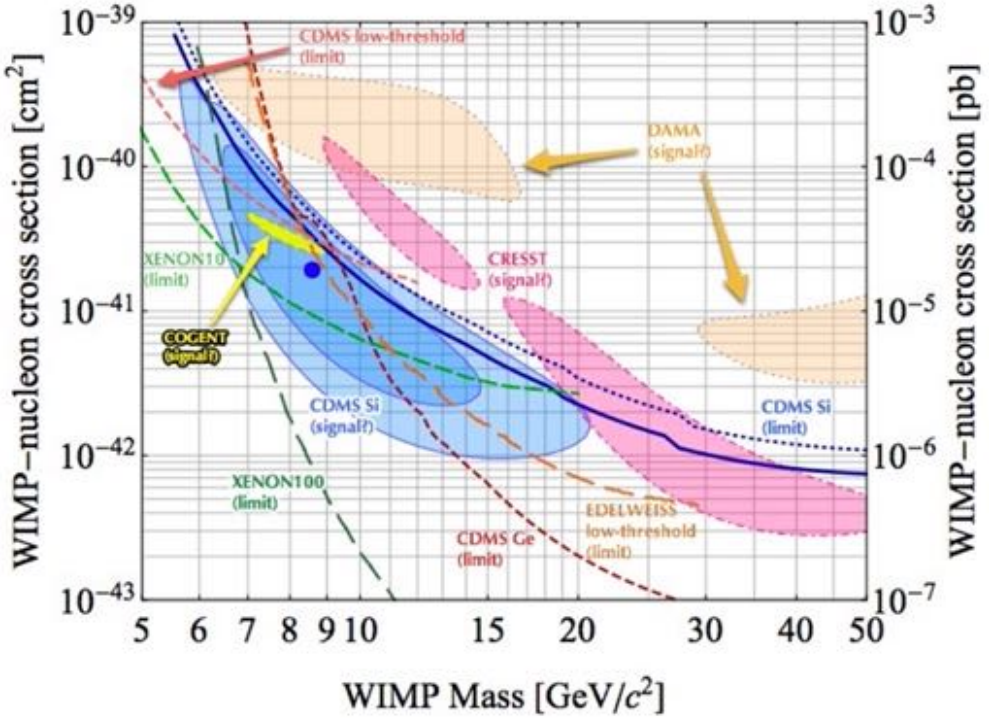

Up to now, no unambiguous signature of dark matter interactions in dark matter detectors has been found. Negative search results imply that WIMP interactions in detectors are rare. This suggests that the DM-nuclei interaction cross-section σ_{dm-N} is smaller than certain mass-dependent upper limit.

A number of experiments finds evidence for the signal, either in the form of candidate “events”, or in the form of annual modulation of the event rate.

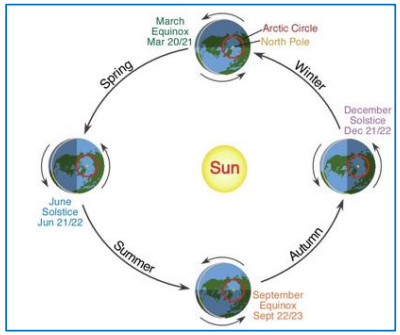

From laboratory experiments to astronomical observations

Motivation: laboratory experiments in particle physics designed to probe fundamental laws of Nature have limited reach. Astroparticle observations provide complementary possibilities for probing fundamental physics.

The ”new physics” effects (like e.g. detection of dark matter) are expected to appear as “unexplained anomalies” in the astronomical / astroparticle data (like e.g. behaviour of galaxy rotation curves). The discovery of “new physics” can be claimed only if the conventional astrophysics models of astronomical phenomena are well understood and and their uncertainties are under control.

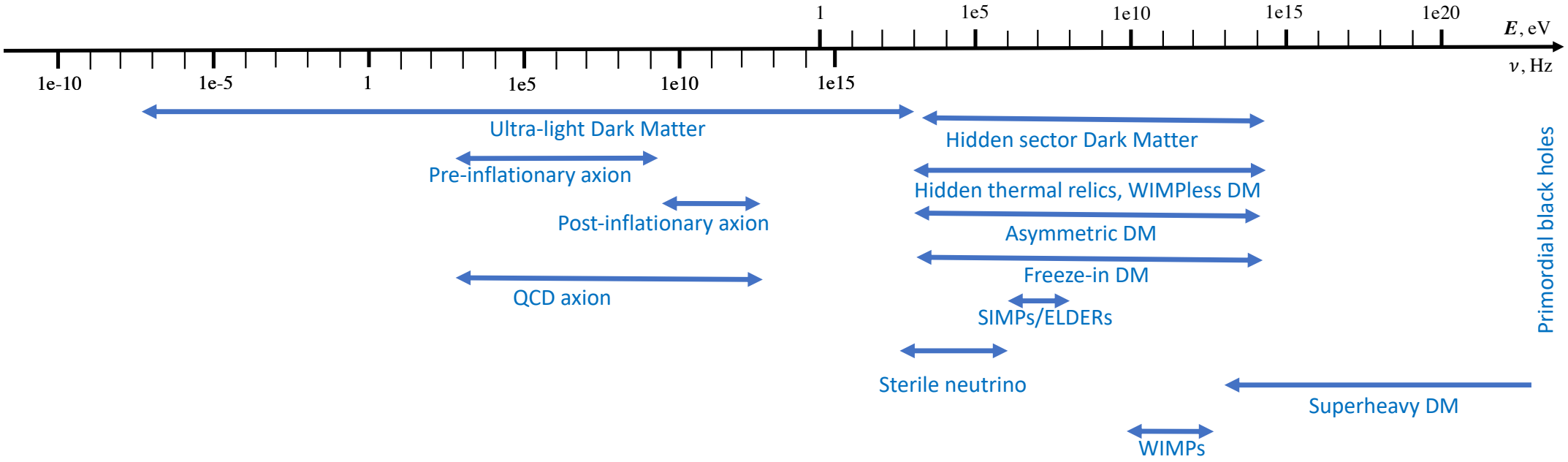

Astronomical and astroparticle observations

EM: electromagnetic

GW: gravitational wave

NU: neutrino

CR: cosmic ray

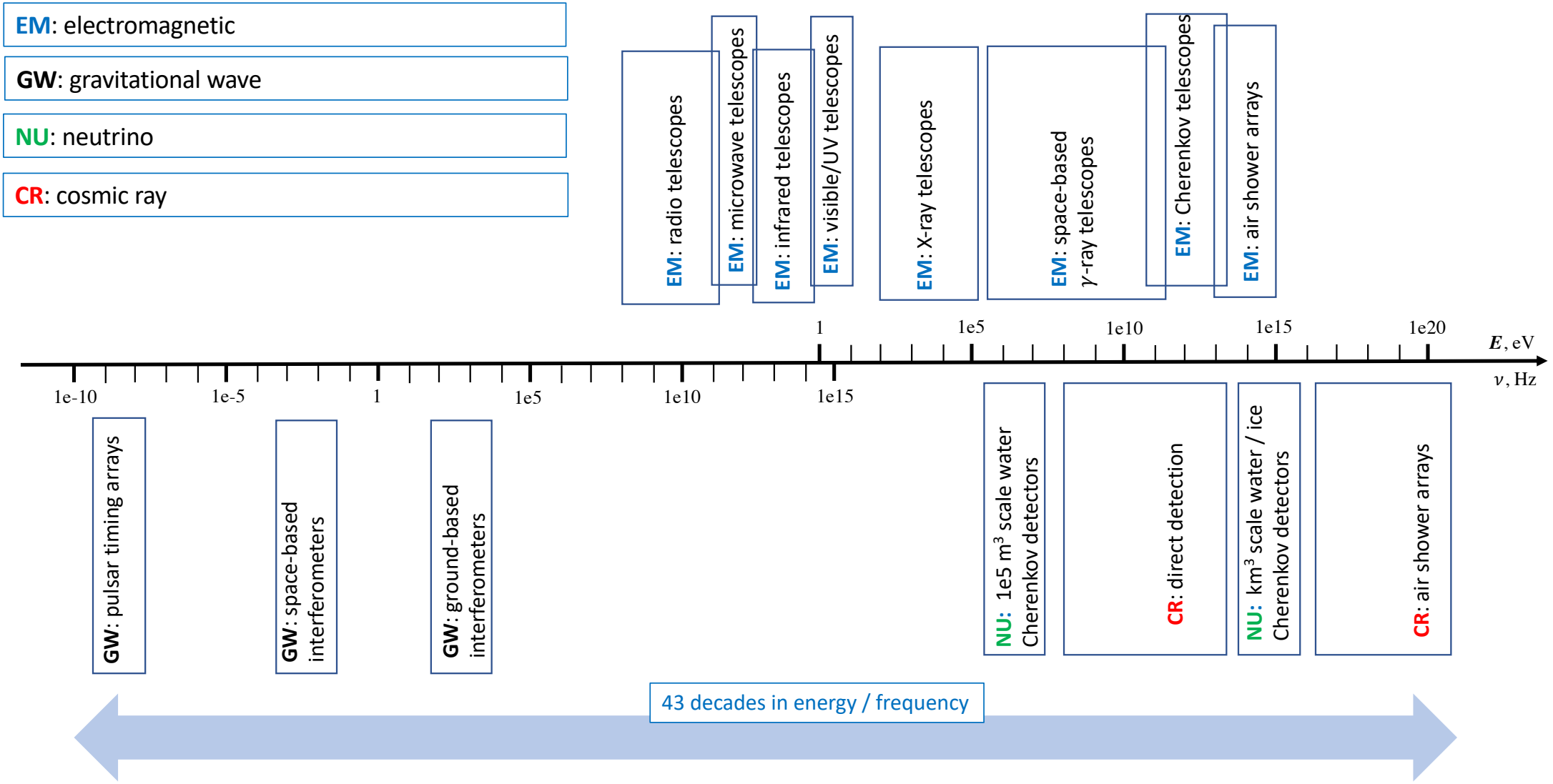

Astronomical and astroparticle observations

EM: electromagnetic

GW: gravitational wave

NU: neutrino

CR: cosmic ray

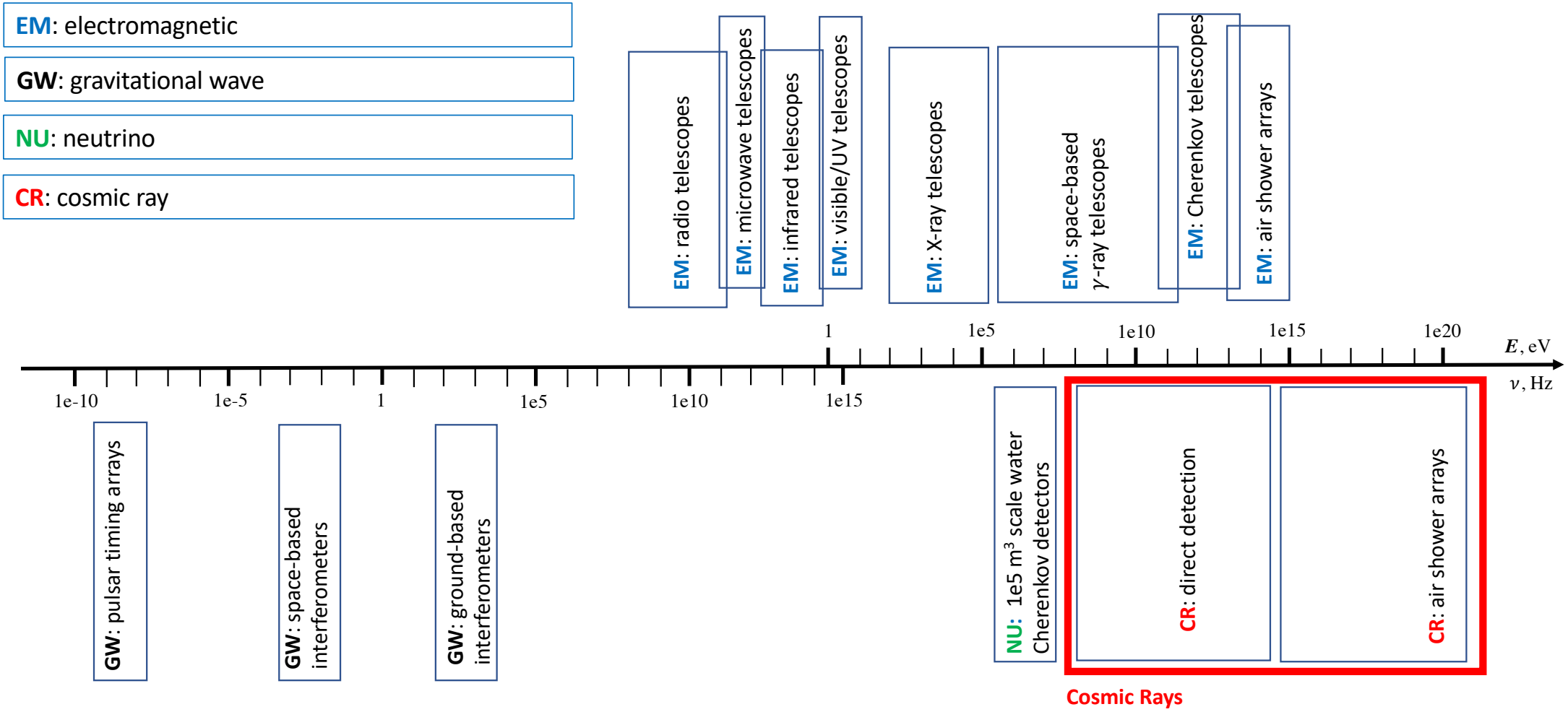

Cosmic ray physics

Cosmic Rays (CR) are high-energy particles coming from outside the Earth atmosphere. The bulk of the CR flux is in the GeV energy band. It is dominated by protons.

Cosmic ray spectrum is approximately a broken powerlaw,

$$\frac{\mathrm{d}N}{dE} \propto E^{-\Gamma}$$

With Γ varying in the range $\Gamma \sim 2.7$ below the "knee" in the energy range $E \sim 10^{15}$ eV softening to $\Gamma \sim 3$ in the range 10^{15} eV $< E <$ 10^{18} eV ("ankle") and hardening again between the ankle and a high-energy suppression (cut-off?) at about 10^{20} eV.

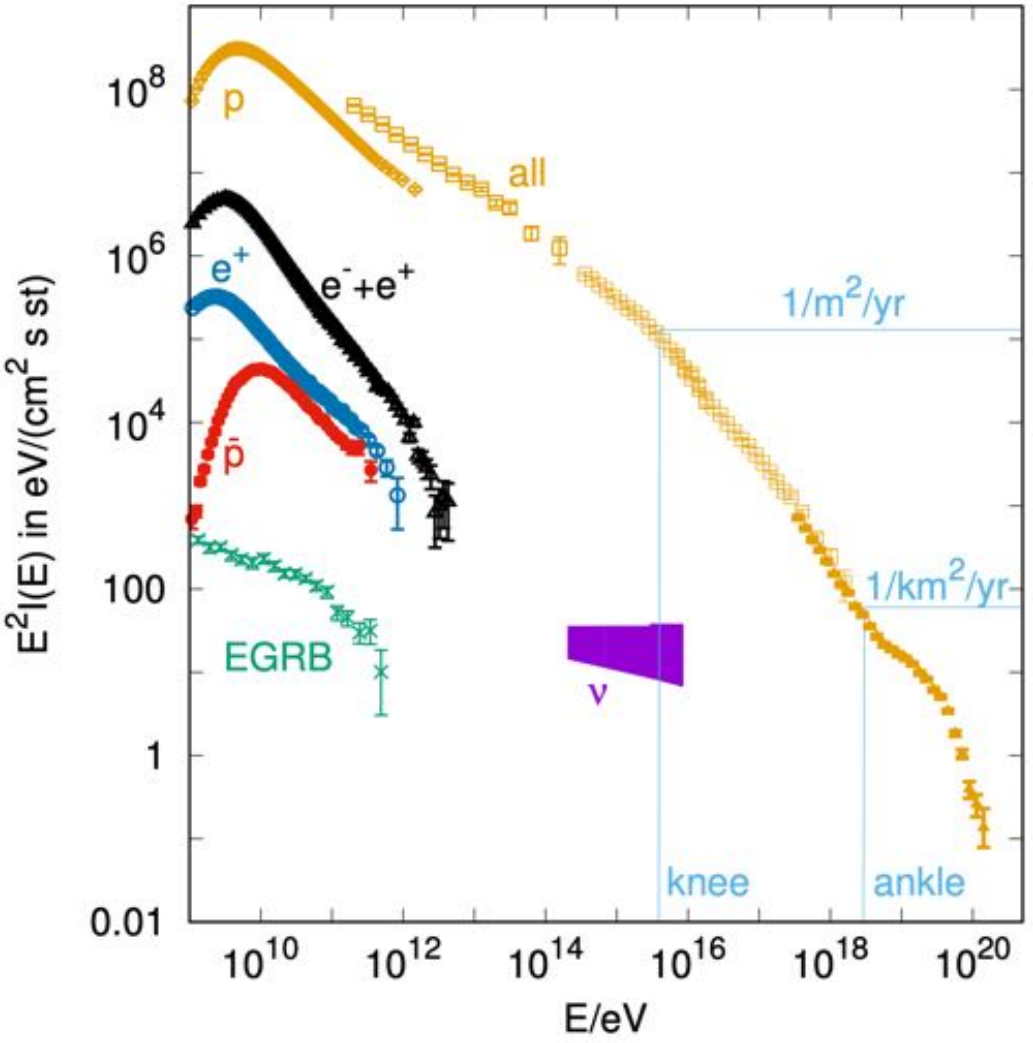

Cosmic ray physics

Cosmic Rays (CR) are high-energy particles coming from outside the Earth atmosphere. The bulk of the CR flux is in the GeV energy band. It is dominated by protons.

Cosmic ray spectrum is approximately a broken powerlaw,

$$\frac{\mathrm{d}N}{dE} \propto E^{-\Gamma}$$

With Γ varying in the range $\Gamma \sim 2.7$ below the "knee" in the energy range $E \sim 10^{15}$ eV softening to $\Gamma \sim 3$ in the range 10^{15} eV $< E <$ 10^{18} eV ("ankle") and hardening again between the ankle and a high-energy suppression (cut-off?) at about 10^{20} eV.

Apart from protons, CR flux contains atomic nuclei. Their spectra are also broken powerlaws, with spectral indexes Γ slightly different from that of protons.

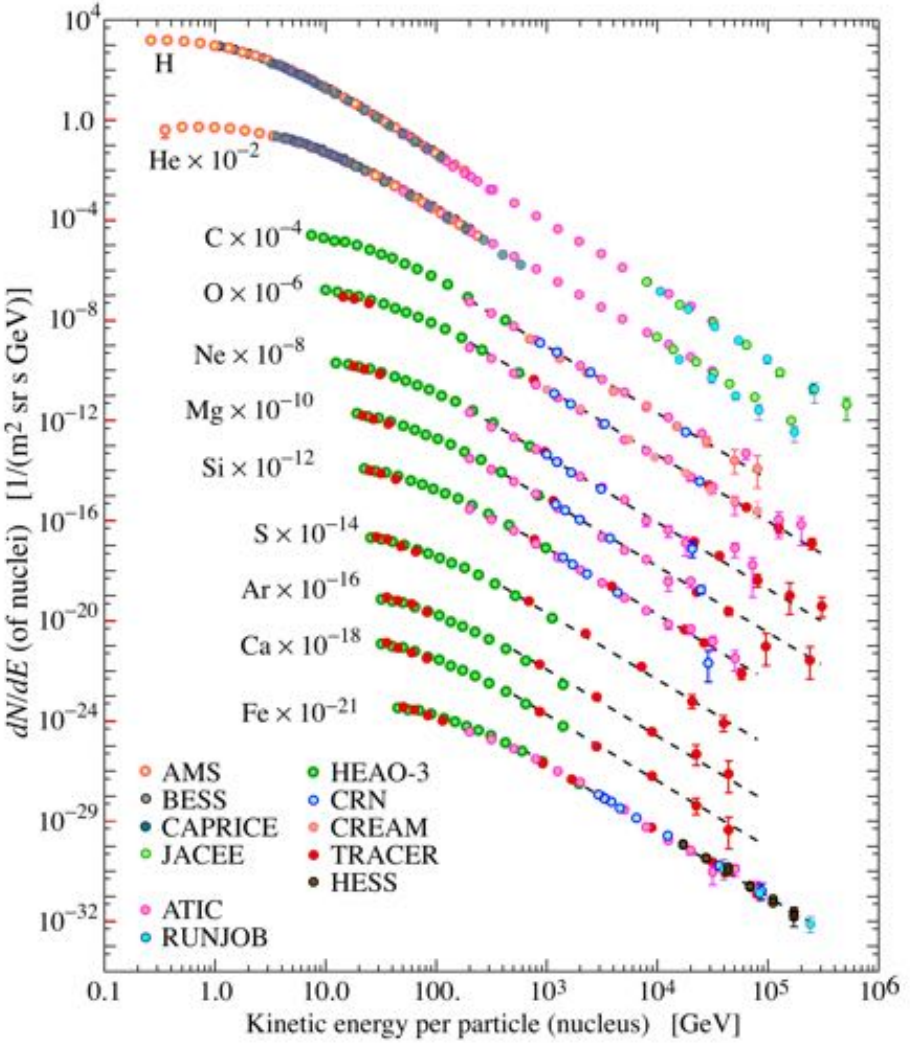

Cosmic ray physics

Cosmic Rays (CR) are high-energy particles coming from outside the Earth atmosphere. The bulk of the CR flux is in the GeV energy band. It is dominated by protons.

Cosmic ray spectrum is approximately a broken powerlaw,

$$\frac{\mathrm{d}N}{dE} \propto E^{-\Gamma}$$

With Γ varying in the range $\Gamma \sim 2.7$ below the "knee" in the energy range $E \sim 10^{15}$ eV softening to $\Gamma \sim 3$ in the range 10^{15} eV $< E <$ 10^{18} eV ("ankle") and hardening again between the ankle and a high-energy suppression (cut-off?) at about 10^{20} eV.

Apart from protons, CR flux contains atomic nuclei. Their spectra are also broken powerlaws, with spectral indexes Γ slightly different from that of protons.

Abundances of different nuclei in the CR flux carry information about

– physics of particle accelerators operating in (yet uncertain) astronomical sources of CRs;

– physics of propagation of CRs through interstellar and intergalactic medium;

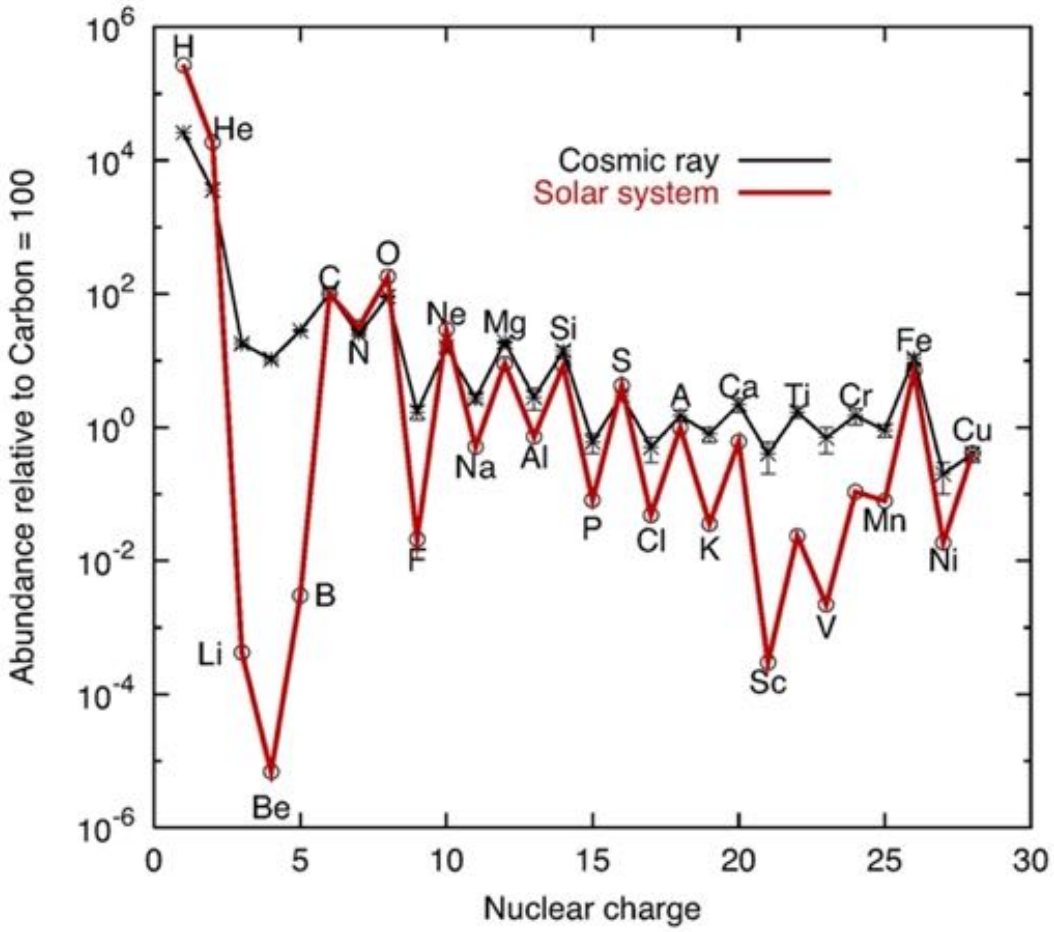

Cosmic ray physics

Cosmic Rays (CR) are high-energy particles coming from outside the Earth atmosphere. The bulk of the CR flux is in the GeV energy band. It is dominated by protons.

Cosmic ray spectrum is approximately a broken powerlaw,

$$\frac{\mathrm{d}N}{dE} \propto E^{-\Gamma}$$

With Γ varying in the range $\Gamma \sim 2.7$ below the "knee" in the energy range $E \sim 10^{15}$ eV softening to $\Gamma \sim 3$ in the range 10^{15} eV $< E <$ 10^{18} eV ("ankle") and hardening again between the ankle and a high-energy suppression (cut-off?) at about 10^{20} eV.

Apart from protons, CR flux contains atomic nuclei. Their spectra are also broken powerlaws, with spectral indexes Γ slightly different from that of protons.

Abundances of different nuclei in the CR flux carry information about
– physics of particle accelerators operating in (yet uncertain) astronomical sources of CRs;
– physics of propagation of CRs through interstellar and intergalactic medium;

Cosmic ray spectrum also has contribution from electrons, positrons, antiprotons.

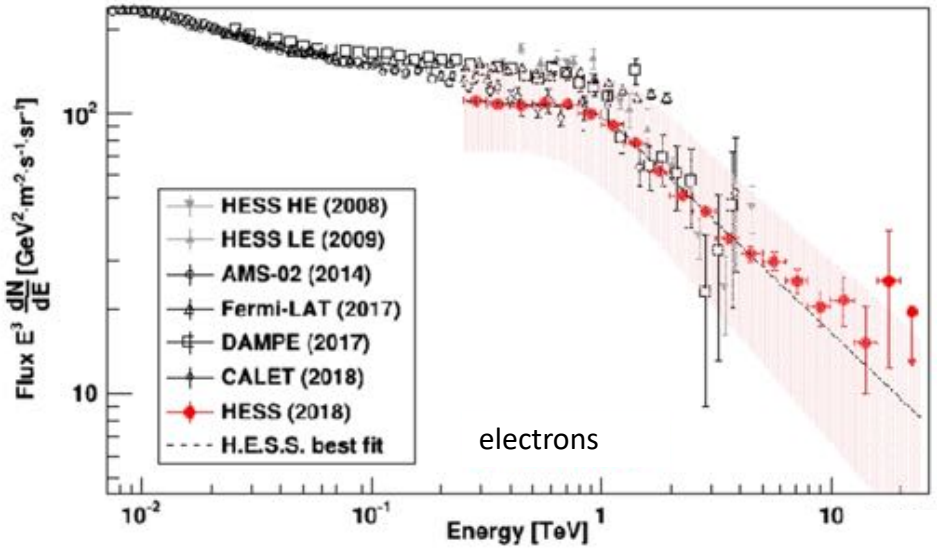

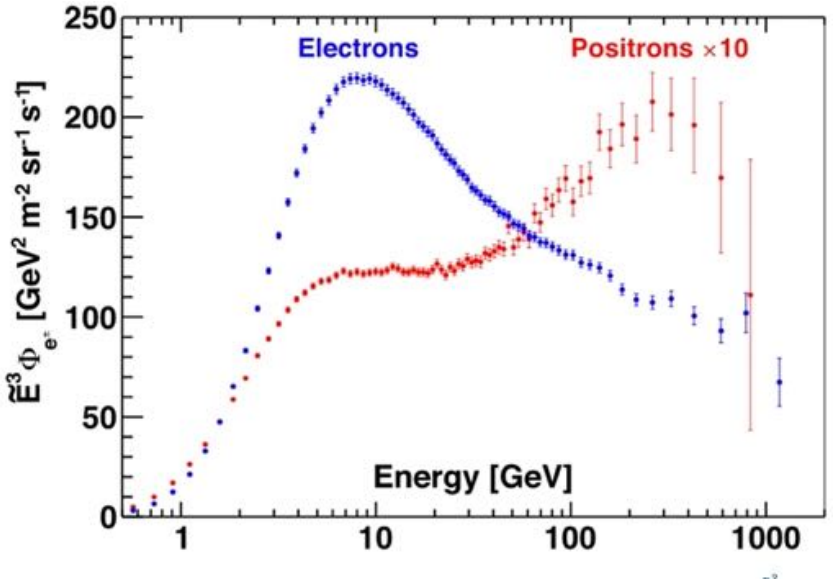

Cosmic ray physics

Cosmic Rays (CR) are high-energy particles coming from outside the Earth atmosphere. The bulk of the CR flux is in the GeV energy band. It is dominated by protons.

Cosmic ray spectrum is approximately a broken powerlaw,

$$\frac{\mathrm{d}N}{dE} \propto E^{-\Gamma}$$

With Γ varying in the range $\Gamma \sim 2.7$ below the "knee" in the energy range $E \sim 10^{15}$ eV softening to $\Gamma \sim 3$ in the range 10^{15} eV $< E <$ 10^{18} eV ("ankle") and hardening again between the ankle and a high-energy suppression (cut-off?) at about 10^{20} eV.

Apart from protons, CR flux contains atomic nuclei. Their spectra are also broken powerlaws, with spectral indexes Γ slightly different from that of protons.

Abundances of different nuclei in the CR flux carry information about

– physics of particle accelerators operating in (yet uncertain) astronomical sources of CRs;

– physics of propagation of CRs through interstellar and intergalactic medium;

– propagation of CRs through the Solar system.

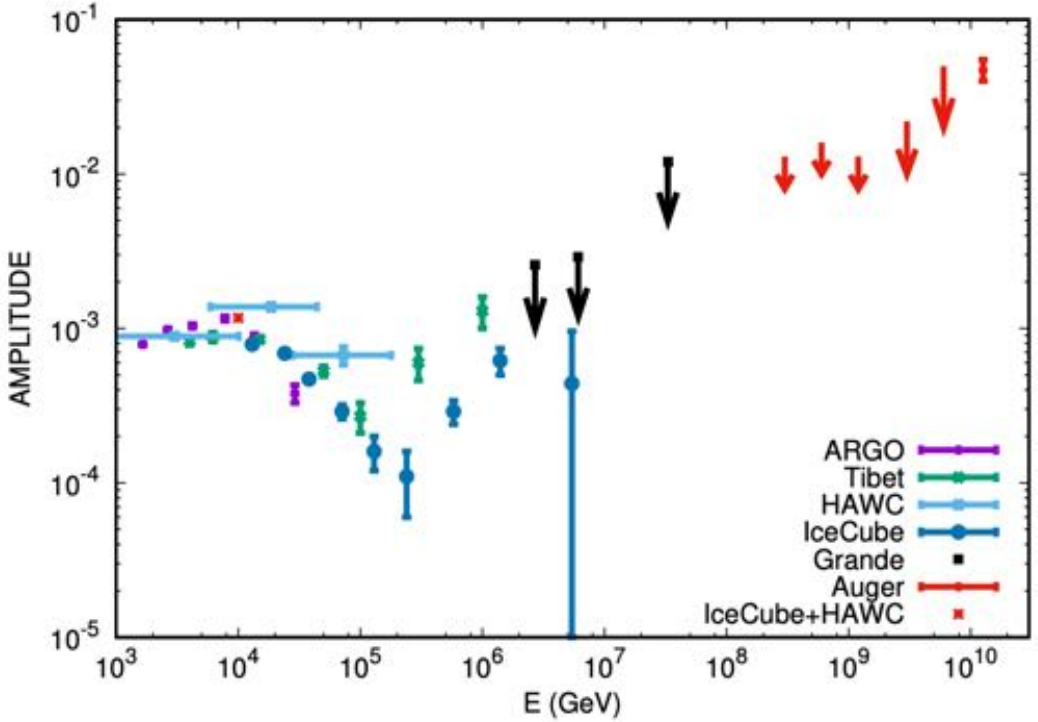

CR flux is approximately isotropic: the dipole anisotropy is at the level of $\sim 10^{-3}$ below the knee. It reaches several percent at 10^{19} eV in the Ultra-High-Energy Cosmic Ray (UHECR) band.

Cosmic ray detection

CR with energies much below the knee can be detected ”directly” using particle detectors on spacecrafts or high-altitude balloons .

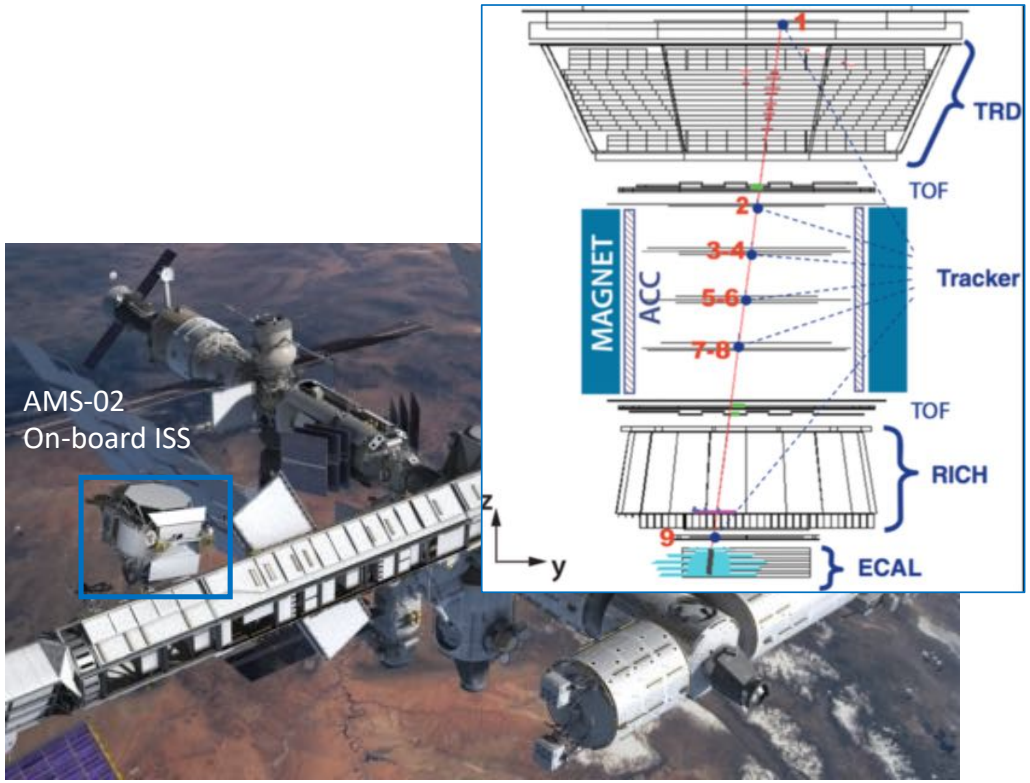

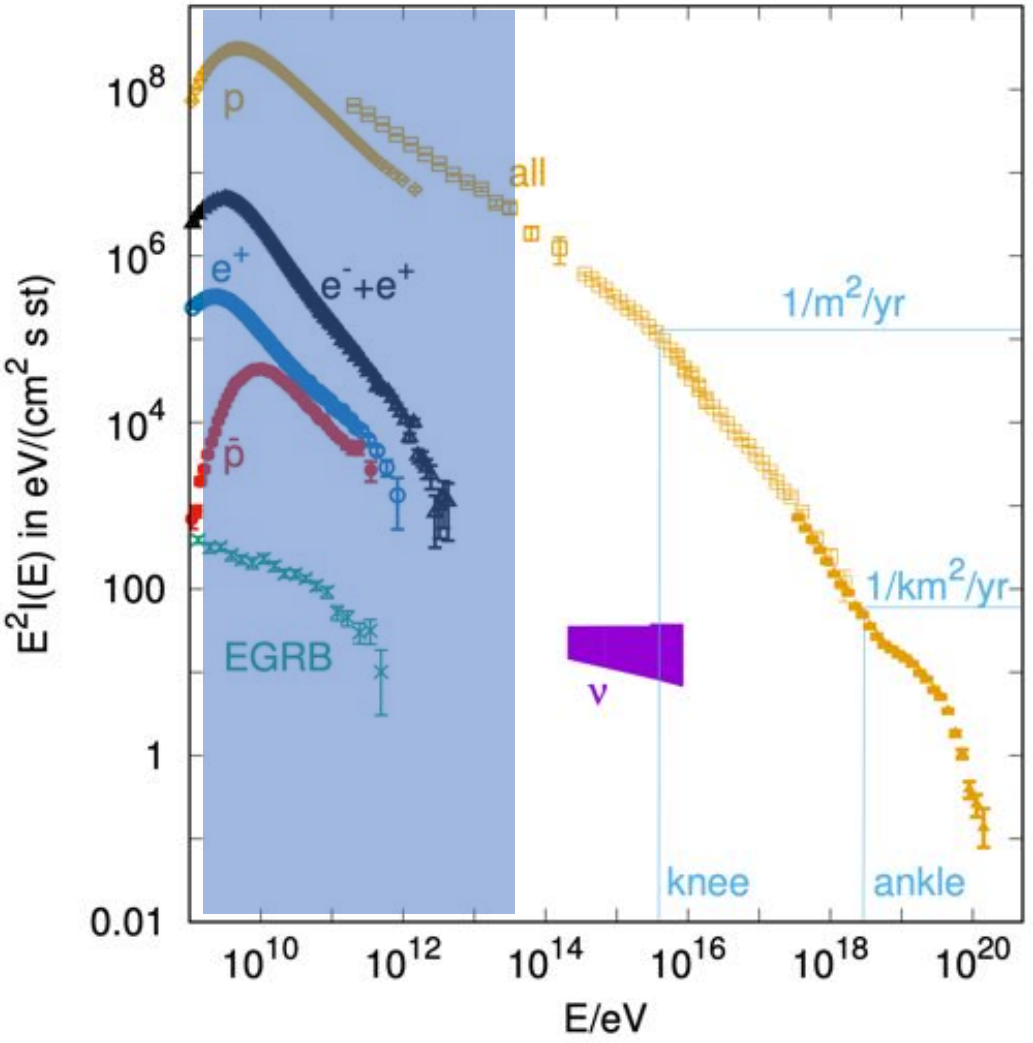

Cosmic ray detection

CR with energies much below the knee can be detected ”directly” using particle detectors on spacecrafts or high-altitude balloons .

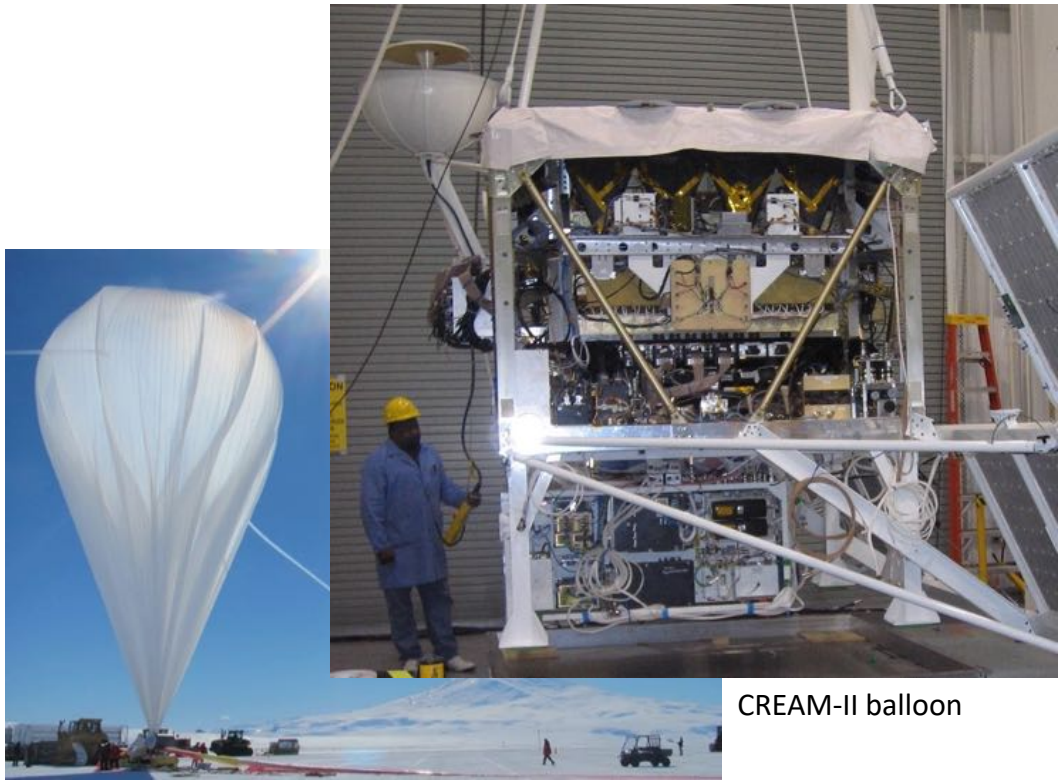

CREAM-II balloon

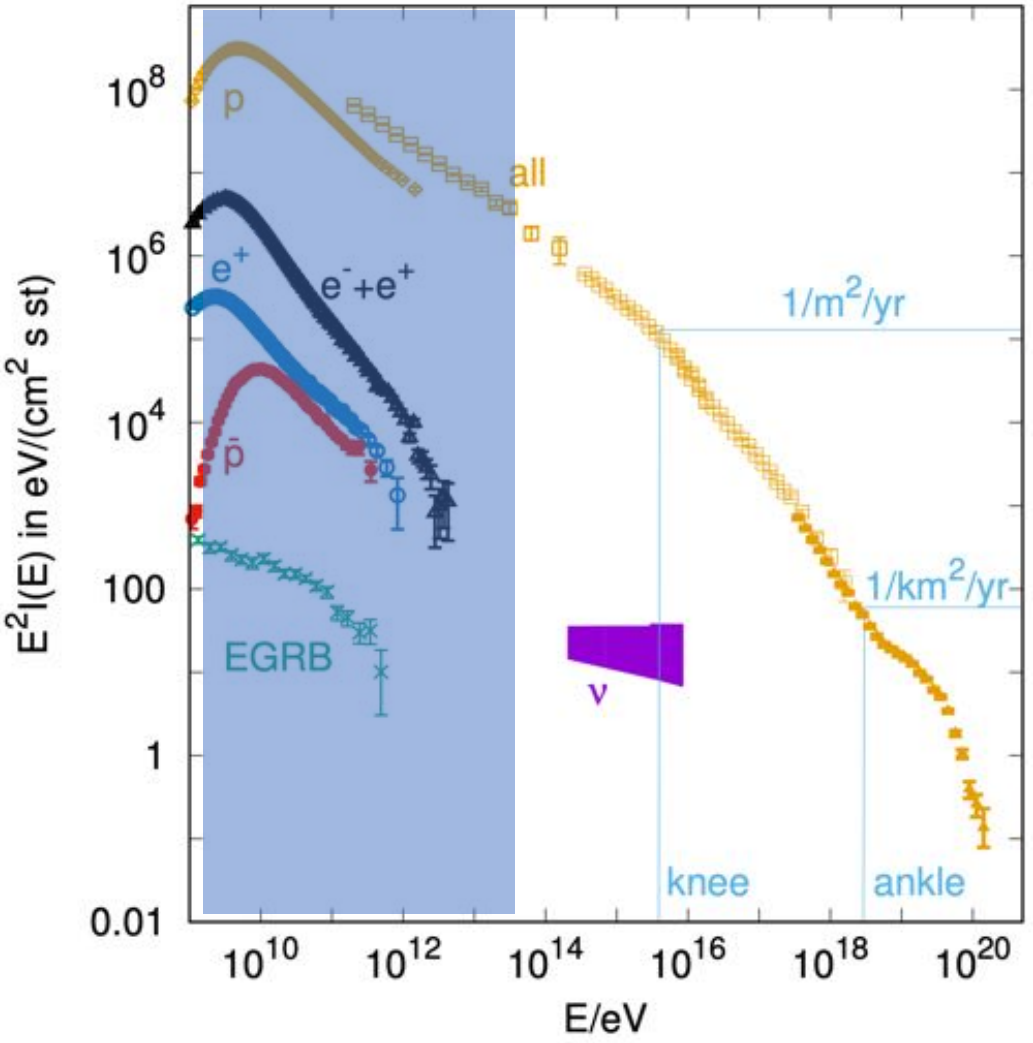

Cosmic ray detection

CR with energies much below the knee can be detected ”directly” using particle detectors on spacecrafts or high-altitude balloons .

Higher energy CRs are detected by Extensive Air Shower (EAS) arrays.

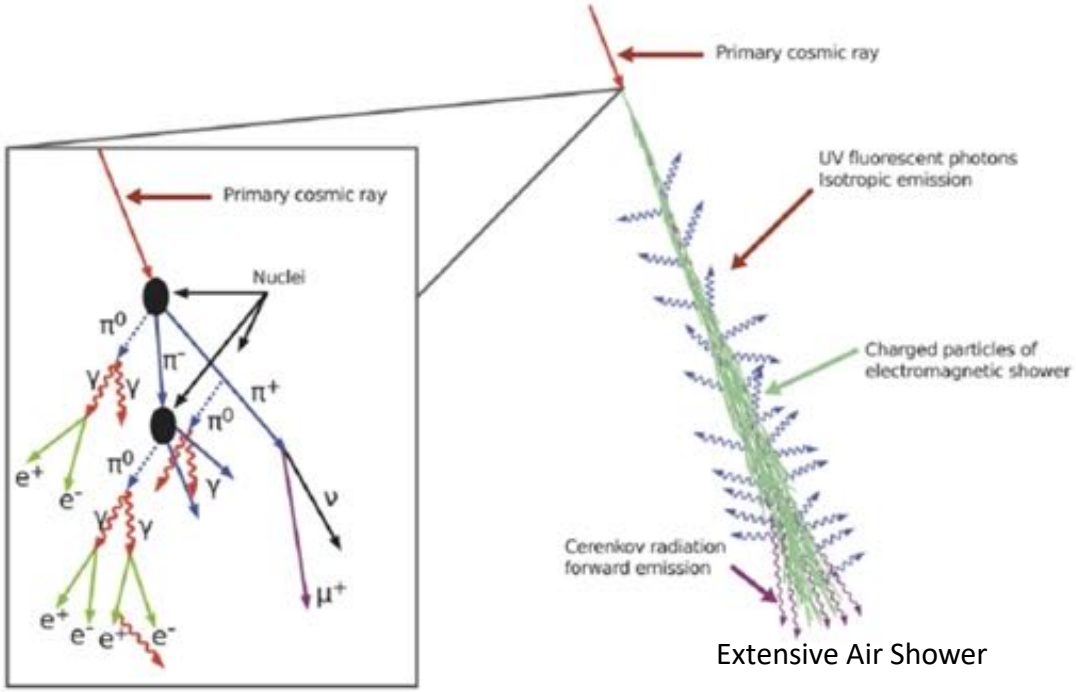

Extensive Air Shower

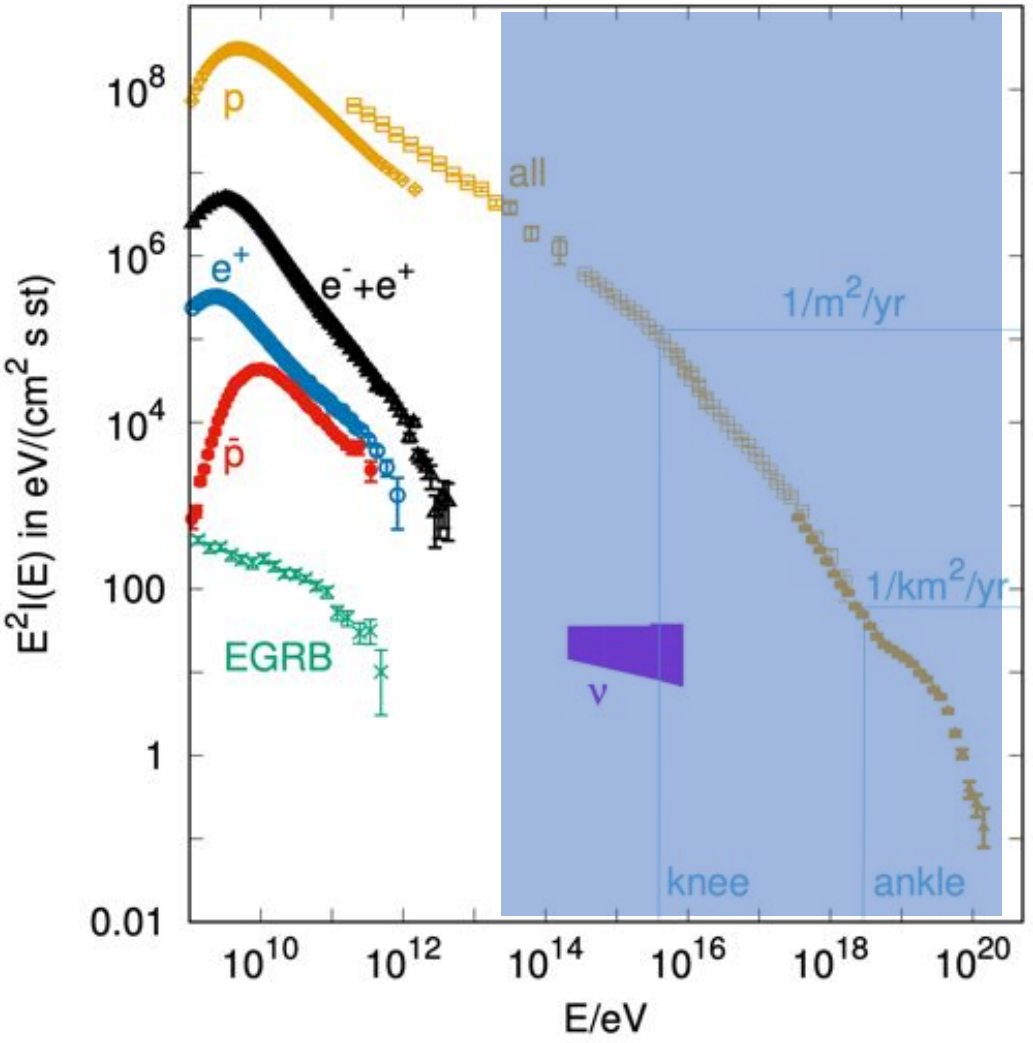

Cosmic ray detection

CR with energies much below the knee can be detected ”directly” using particle detectors on spacecrafts or high-altitude balloons .

Higher energy CRs are detected by Extensive Air Shower (EAS) arrays.

Pierre Auger

MEASURING COSMIC RAYS IN THE SWISS ALPS

The author (*left*) and his collaborator, P. Ehrenfest, set up their apparatus in the Jungfraujoch.

EAS phenomenon was discovery has Swiss connection ☺

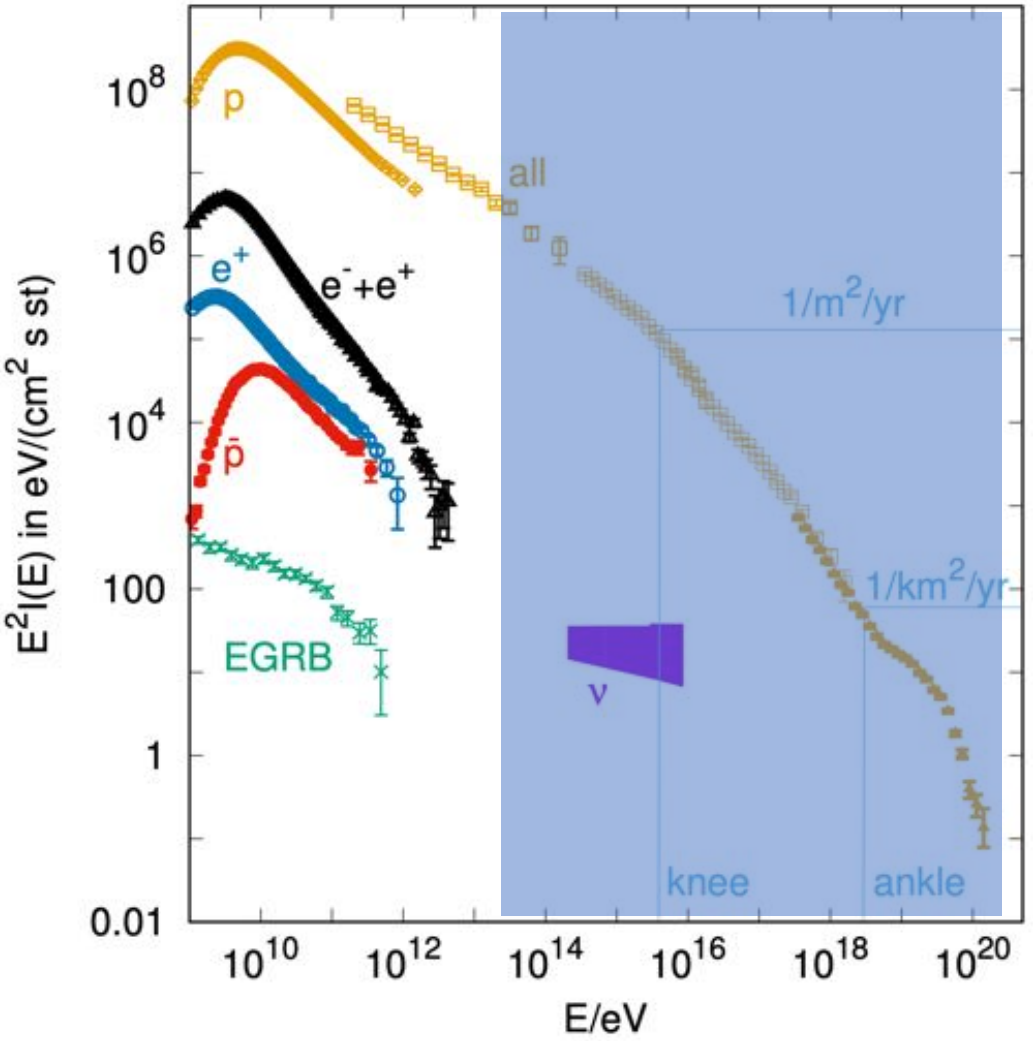

Cosmic ray detection

CR with energies much below the knee can be detected ”directly” using particle detectors on spacecrafts or high-altitude balloons .

Higher energy CRs are detected by Extensive Air Shower (EAS) arrays.

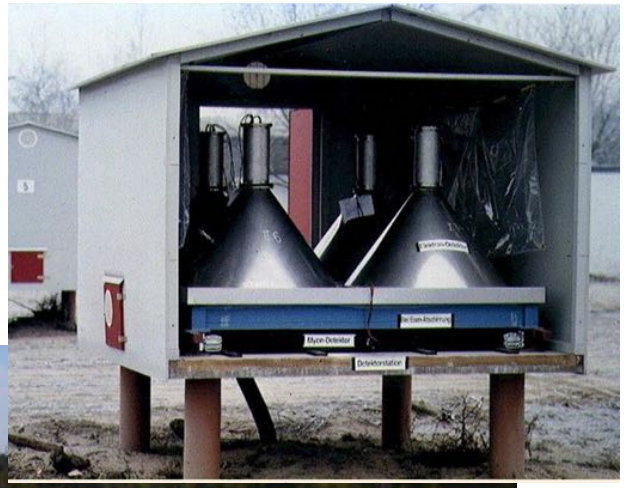

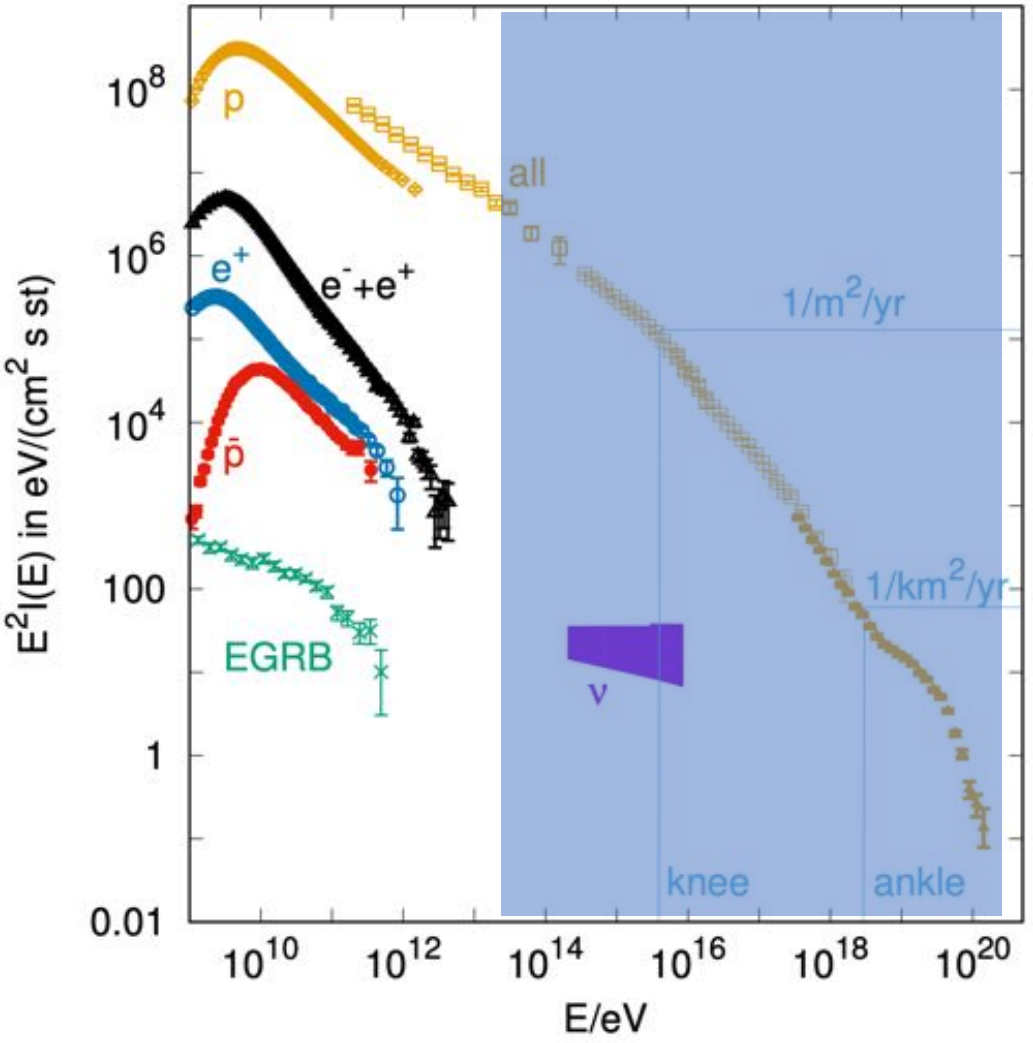

Cosmic ray detection

CR with energies much below the knee can be detected ”directly” using particle detectors on spacecrafts or high-altitude balloons .

Higher energy CRs are detected by Extensive Air Shower (EAS) arrays.

Pierre Auger Observatory

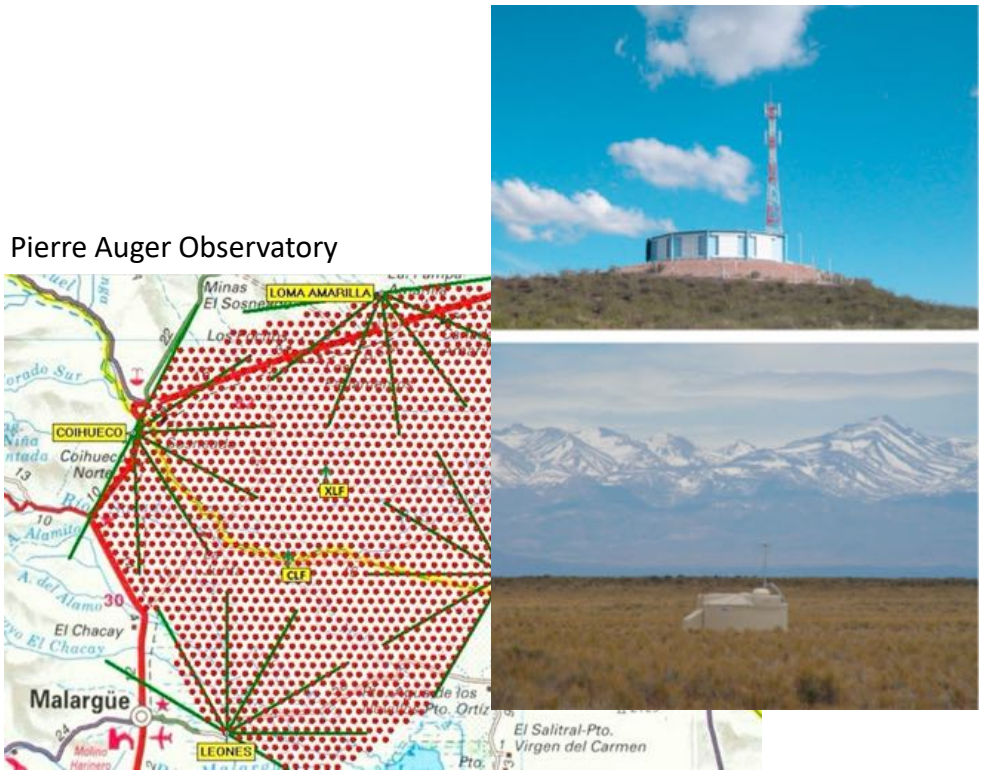

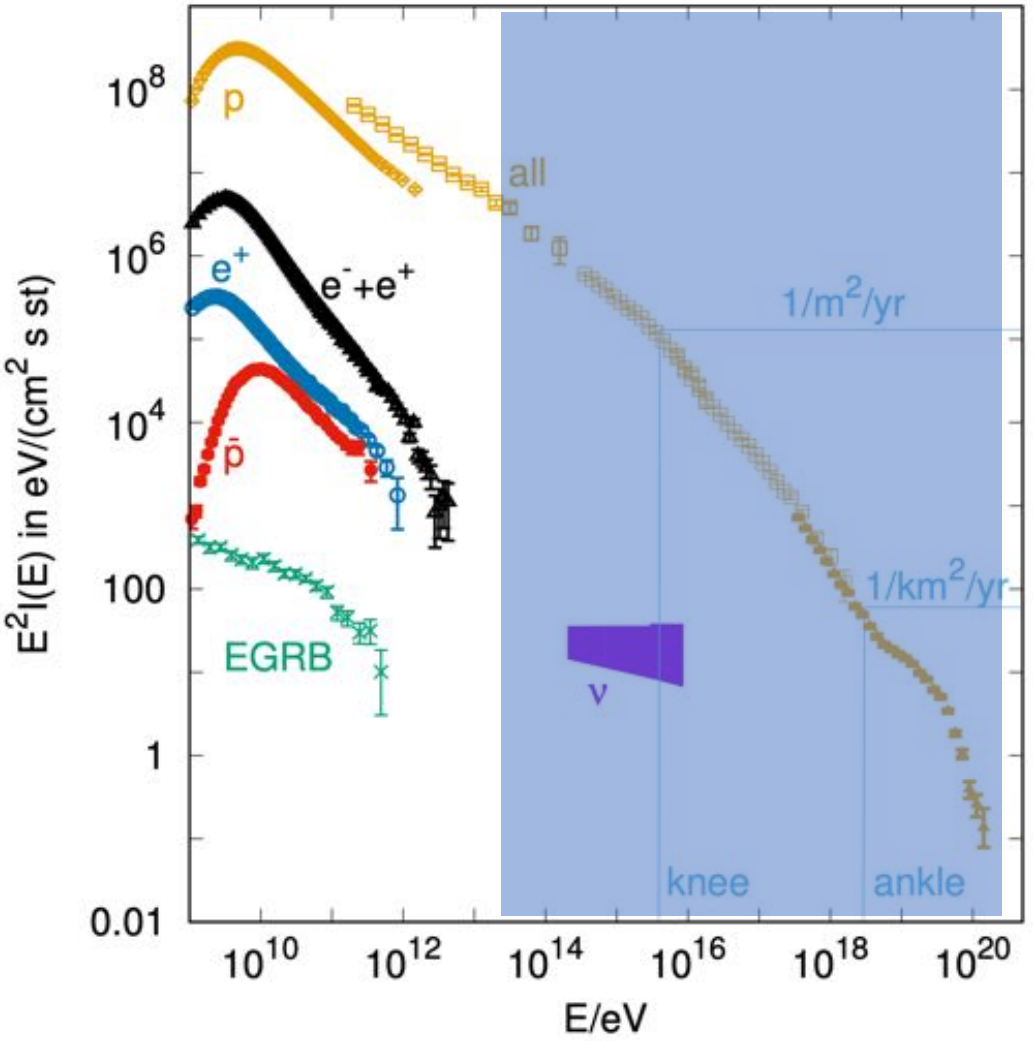

Cosmic ray propagation

Cosmic rays gyrate in Galactic magnetic field:

$$R_L = \frac{E}{eB} \simeq 10^{12} \left[\frac{E}{10^9\ \mathrm{eV}}\right]\left[\frac{B}{3\ \mu\mathrm{G}}\right]^{-1}\ \mathrm{cm}$$

(* natural system of units: $1\ \mathrm{G} \simeq 0.1\ \mathrm{eV}^2$; $e \simeq 0.1$; $\hbar c \simeq 2{\times}10^{-5}\ \mathrm{eV\ cm}$).

R_L is much smaller than the characteristic scale of the pattern of the ordered magnetic field (uncertain, but of the scale comparable to the size of the Galactic disk, $\sim 10\ \mathrm{kpc} = 3{\times}10^{22}\ \mathrm{cm}$). CR trajectories follow the ordered field lines.

R_L is also much smaller than the scale of variations of the random component of the Galactic magnetic field (yet more uncertain, in the $10 - 100\ \mathrm{pc}$ range). CRs scatter on magnetic field inhomogeneities.

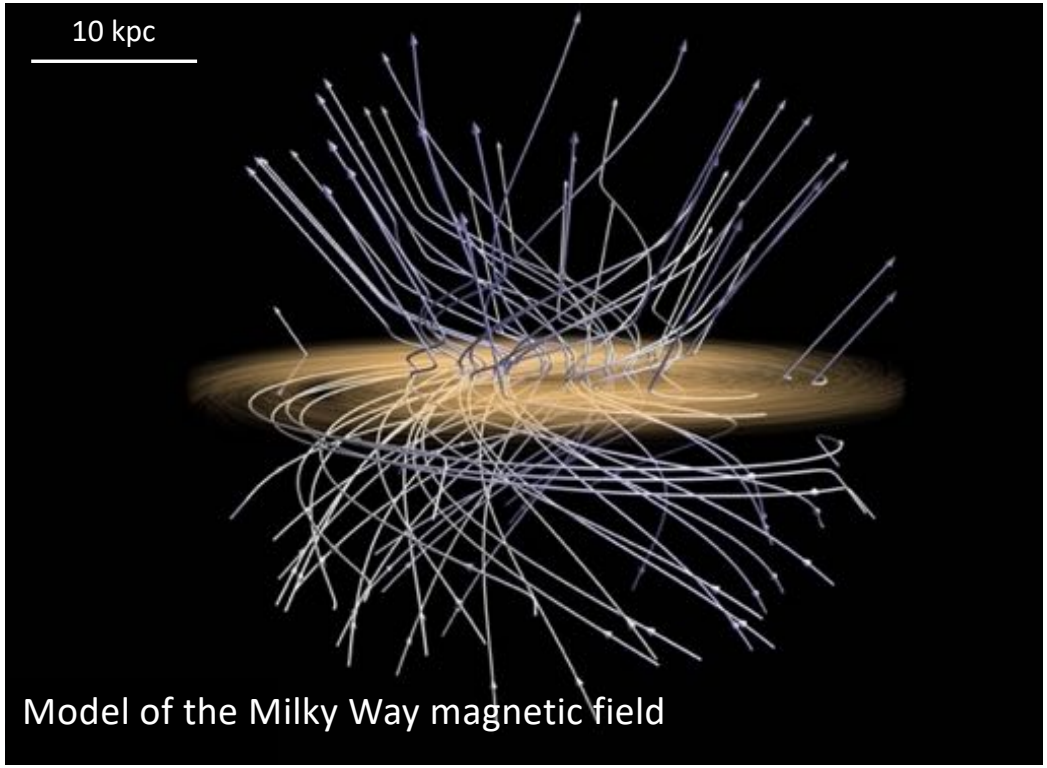

Model of the Milky Way magnetic field

Cosmic ray propagation

Cosmic rays gyrate in Galactic magnetic field:

$$R_L = \frac{E}{eB} \simeq 10^{12} \left[\frac{E}{10^9\ \mathrm{eV}}\right]\left[\frac{B}{3\ \mu\mathrm{G}}\right]^{-1}\ \mathrm{cm}$$

(* natural system of units: $1\ \mathrm{G} \simeq 0.1\ \mathrm{eV}^2$; $e \simeq 0.1$; $\hbar c \simeq 2{\times}10^{-5}\ \mathrm{eV\ cm}$).

R_L is much smaller than the characteristic scale of the pattern of the ordered magnetic field (uncertain, but of the scale comparable to the size of the Galactic disk, $\sim 10\ \mathrm{kpc} = 3{\times}10^{22}\ \mathrm{cm}$). CR trajectories follow the ordered field lines.

R_L is also much smaller than the scale of variations of the random component of the Galactic magnetic field (yet more uncertain, in the $10 - 100\ \mathrm{pc}$ range). CRs scatter on magnetic field inhomogeneities.

A "toy model" of cosmic ray propagation is diffusion out of the "cylindric box" of radius R_d and height H:

$$-\frac{\partial}{\partial z}\left[D\frac{\partial f}{\partial z}\right] = Q(p,z);\ \ f(z = H, E) = 0$$

$$Q(E,z) = \frac{Q_0(E)}{\pi R_d^2}\,\delta(z)$$

Here D is the diffusion coefficient and Q is the injection spectrum, as a function of momentum E. CRs are supposedly injected by sources in the Galactic Disk at $z \simeq 0$.

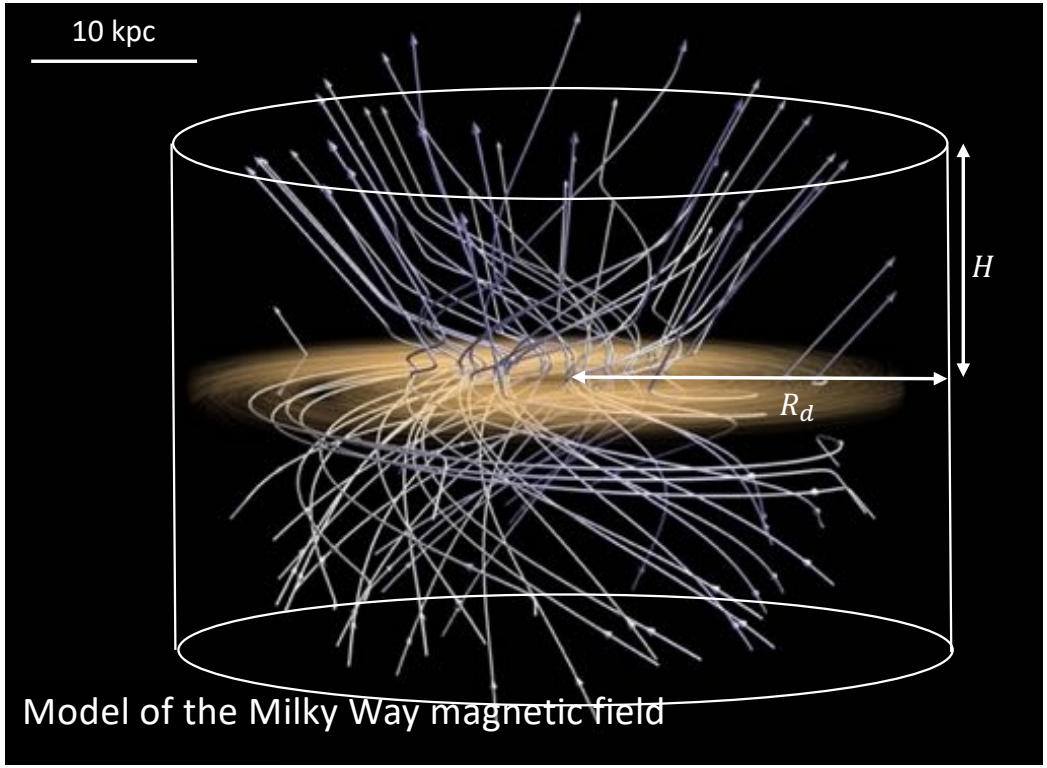

Model of the Milky Way magnetic field

Cosmic ray propagation

Cosmic rays gyrate in Galactic magnetic field:

$$R_L = \frac{E}{eB} \simeq 10^{12} \left[\frac{E}{10^9\ \mathrm{eV}}\right]\left[\frac{B}{3\ \mu\mathrm{G}}\right]^{-1}\ \mathrm{cm}$$

(* natural system of units: $1\ \mathrm{G} \simeq 0.1\ \mathrm{eV}^2$; $e \simeq 0.1$; $\hbar c \simeq 2{\times}10^{-5}\ \mathrm{eV\ cm}$).

R_L is much smaller than the characteristic scale of the pattern of the ordered magnetic field (uncertain, but of the scale comparable to the size of the Galactic disk, $\sim 10\ \mathrm{kpc} = 3{\times}10^{22}\ \mathrm{cm}$). CR trajectories follow the ordered field lines.

R_L is also much smaller than the scale of variations of the random component of the Galactic magnetic field (yet more uncertain, in the $10 - 100\ \mathrm{pc}$ range). CRs scatter on magnetic field inhomogeneities.

A "toy model" of cosmic ray (proton) propagation is diffusion out of the "cylindric box" of radius R_d and height H:

$$-\frac{\partial}{\partial z}\left[D\frac{\partial f}{\partial z}\right] = Q(E,z);\ \ f(z=H,E) = 0$$

$$Q(p,z) = \frac{Q_0(E)}{\pi R_d^2}\,\delta(z)$$

Here D is the diffusion coefficient and Q is the injection spectrum, as a function of momentum p. CRs are supposedly injected by sources in the Galactic Disk at $z \simeq 0$.

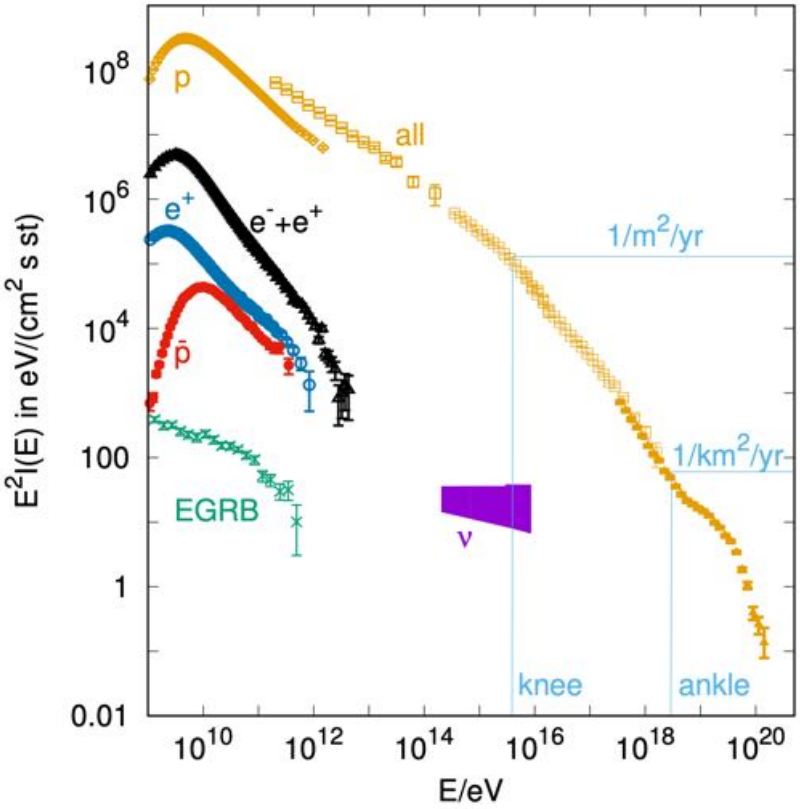

Solution:

Volume injection rate | Diffusion time

$$f = f_0\left(1 - \frac{|z|}{H}\right);\ \ f_0 = \boxed{\frac{Q_0(E)}{2\pi R_d^2 H}}\,\boxed{\frac{H^2}{D}}$$

If $Q_0(E) \propto E^{-\gamma}$ and $D(E) \propto E^{\delta}$, $f(E) \propto E^{-\gamma-\delta}$. This "explains" the powerlaw nature of the CR spectrum.

Cosmic ray propagation

Cosmic rays gyrate in Galactic magnetic field:

$$R_L = \frac{E}{eB} \simeq 10^{12} \left[\frac{E}{10^9 \text{ eV}}\right] \left[\frac{B}{3\ \mu\text{G}}\right]^{-1} \text{ cm}$$

(* natural system of units: $1 \text{ G} \simeq 0.1 \text{ eV}^2$; $e \simeq 0.1$; $\hbar c \simeq 2{\times}10^{-5}$ eV cm).

R_L is much smaller than the characteristic scale of the pattern of the ordered magnetic field (uncertain, but of the scale comparable to the size of the Galactic disk, ~ 10 kpc $= 3{\times}10^{22}$ cm). CR trajectories follow the ordered field lines.

R_L is also much smaller than the scale of variations of the random component of the Galactic magnetic field (yet more uncertain, in the $10 - 100$ pc range). CRs scatter on magnetic field inhomogeneities.

A "toy model" of cosmic ray (nuclei) propagation is diffusion out of the "cylindric box" of radius R_d and height H:

$$-\frac{\partial}{\partial z}\left[D\frac{\partial f_\alpha}{\partial z}\right] = Q(E,z) - \kappa\delta(z)\sigma_\alpha f_\alpha + \kappa\delta(z)\sum_{\alpha'>\alpha}\sigma'_{\alpha\to\alpha} f_{\alpha'} - \frac{f_\alpha}{\tau_\alpha}$$

Spallation with cross-section σ_α

Decay on time scale τ_α

There is a source term for nuclei that are not initially injected by cosmic ray sources. This explains higher abundance of "secondary" nuclei produced in spallation of the primary nuclei (e.g. B from spallation of C).

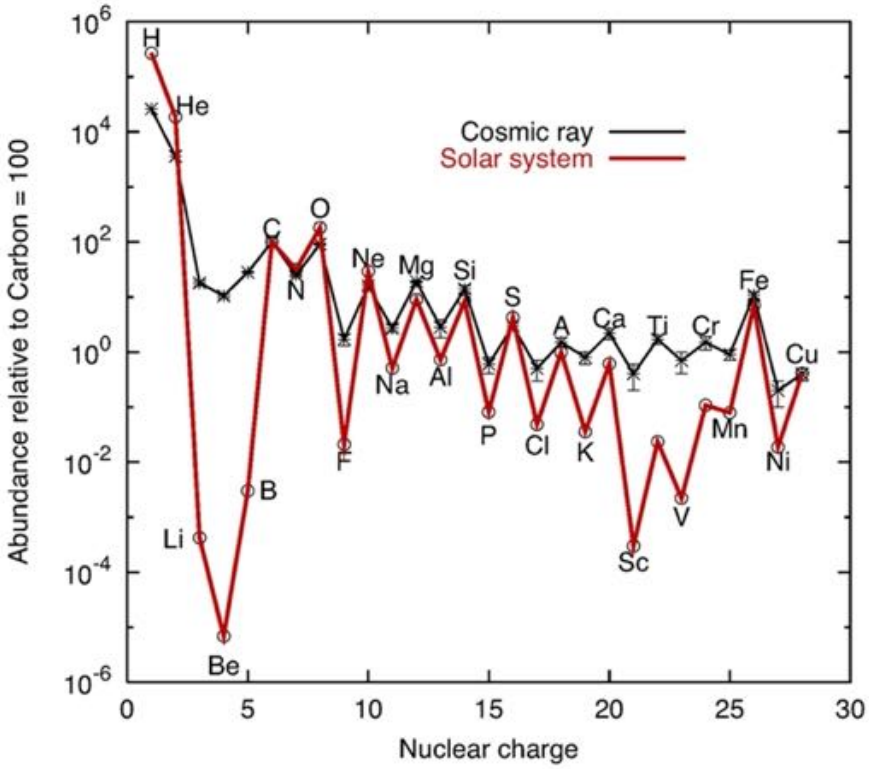

Cosmic ray propagation

Cosmic rays gyrate in Galactic magnetic field:

$$R_L = \frac{E}{eB} \simeq 10^{12} \left[\frac{E}{10^9\ \mathrm{eV}}\right]\left[\frac{B}{3\ \mu\mathrm{G}}\right]^{-1}\ \mathrm{cm}$$

(* natural system of units: $1\ \mathrm{G} \simeq 0.1\ \mathrm{eV}^2$; $e \simeq 0.1$; $\hbar c \simeq 2\times10^{-5}\ \mathrm{eV\ cm}$).

R_L is much smaller than the characteristic scale of the pattern of the ordered magnetic field (uncertain, but of the scale comparable to the size of the Galactic disk, $\sim 10\ \mathrm{kpc} = 3\times10^{22}\ \mathrm{cm}$). CR trajectories follow the ordered field lines.

R_L is also much smaller than the scale of variations of the random component of the Galactic magnetic field (yet more uncertain, in the $10 - 100\ \mathrm{pc}$ range). CRs scatter on magnetic field inhomogeneities.

A "toy model" of cosmic ray (nuclei) propagation is diffusion out of the "cylindric box" of radius R_d and height H:

$$-\frac{\partial}{\partial z}\left[D\frac{\partial f_\alpha}{\partial z}\right] = Q(E,z) - \kappa\delta(z)\sigma_\alpha f_\alpha + \kappa\delta(z)\sum_{\alpha'>\alpha}\sigma'_{\alpha\to\alpha}f_{\alpha'} - \frac{f_\alpha}{\tau_\alpha}$$

Spallation with cross-section σ_α

Decay on time scale τ_α

There is a source term for nuclei that are not initially injected by cosmic ray sources. This explains higher abundance of "secondary" nuclei produced in spallation of the primary nuclei (e.g. B from spallation of C).

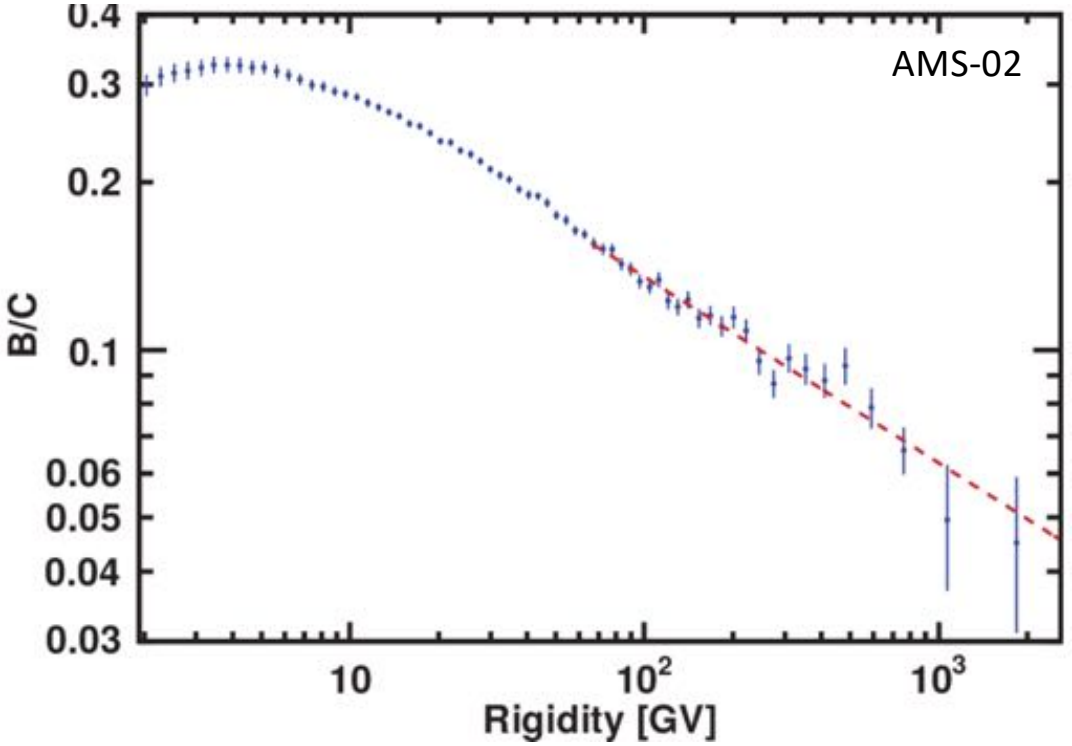

Solutions for "primary" and "secondary" nuclei differ in energy dependence: the injection spectrum of secondary nuclei is $\propto E^{-\gamma-\delta}$, their propagated spectrum is $\propto E^{-\gamma-\delta-\delta}$:

$$\frac{f_B}{f_C} \propto E^{-\delta} \propto \frac{1}{D}$$

Secondary-to-primary nuclei ratio spectrum provides a measurement of energy dependence of the diffusion coefficient.

Cosmic ray propagation

Cosmic rays gyrate in Galactic magnetic field:

$$R_L = \frac{E}{eB} \simeq 10^{12} \left[\frac{E}{10^9\ \mathrm{eV}}\right]\left[\frac{B}{3\ \mu\mathrm{G}}\right]^{-1}\ \mathrm{cm}$$

(* natural system of units: $1\ \mathrm{G} \simeq 0.1\ \mathrm{eV}^2$; $e \simeq 0.1$; $\hbar c \simeq 2\times10^{-5}\ \mathrm{eV\ cm}$).

R_L is much smaller than the characteristic scale of the pattern of the ordered magnetic field (uncertain, but of the scale comparable to the size of the Galactic disk, $\sim 10\ \mathrm{kpc} = 3\times10^{22}\ \mathrm{cm}$). CR trajectories follow the ordered field lines.

R_L is also much smaller than the scale of variations of the random component of the Galactic magnetic field (yet more uncertain, in the $10 - 100\ \mathrm{pc}$ range). CRs scatter on magnetic field inhomogeneities.

A "toy model" of cosmic ray (nuclei) propagation is diffusion out of the "cylindric box" of radius R_d and height H:

$$-\frac{\partial}{\partial z}\left[D\frac{\partial f_\alpha}{\partial z}\right] = Q(E,z) - \kappa\delta(z)\sigma_\alpha f_\alpha + \kappa\delta(z)\sum_{\alpha'>\alpha}\sigma'_{\alpha\to\alpha}f_{\alpha'} - \frac{f_\alpha}{\tau_\alpha}$$

Spallation with cross-section σ_α

Decay on time scale τ_α

There is a source term for nuclei that are not initially injected by cosmic ray sources. This explains higher abundance of "secondary" nuclei produced in spallation of the primary nuclei (e.g. B from spallation of C).

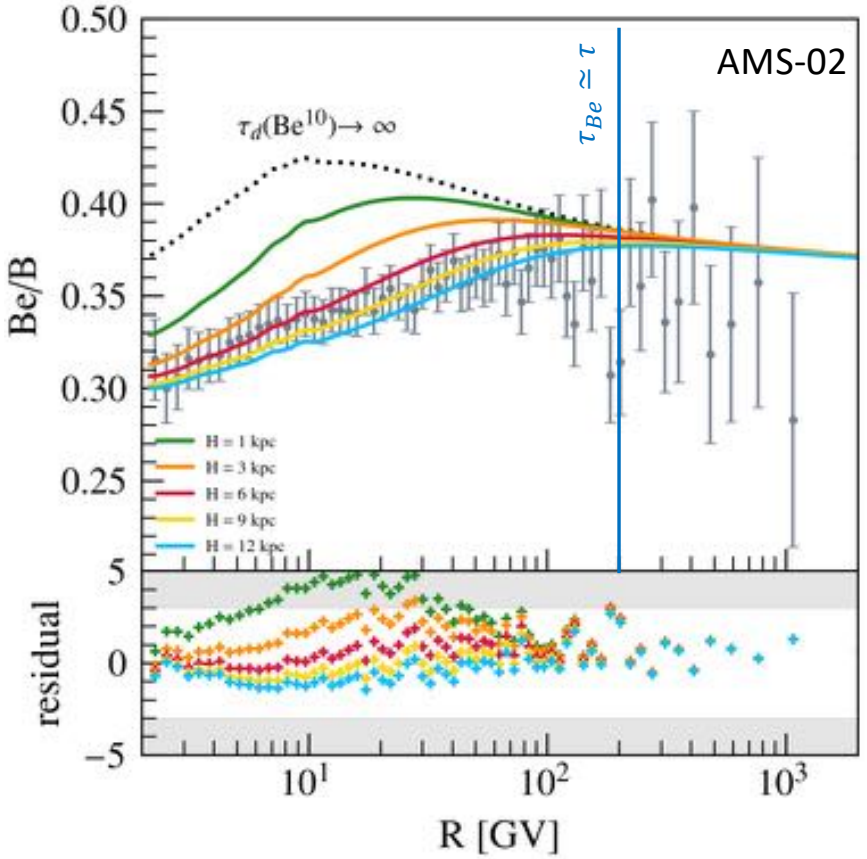

Flux of unstable particles is suppressed by decays, especially at lower energies. This suppression can be measured (e.g. both B and ^{10}Be are "secondaries" produced in similar reactions, but Be is unstable). This gives constraint on the escape time $\tau = H^2/2D$, $\sim 10 - 100$ Myr at 100 GeV energy.

Ultra-high-energy cosmic rays (UHECR)

Cosmic rays gyrate in Galactic magnetic field:

$$R_L = \frac{E}{eB} \simeq 10^{20} \left[\frac{E}{10^{17}\ \mathrm{eV}}\right]\left[\frac{B}{3\ \mu\mathrm{G}}\right]^{-1}\ \mathrm{cm}$$

(* natural system of units: $1\ \mathrm{G} \simeq 0.1\ \mathrm{eV}^2$; $e \simeq 0.1$; $\hbar c \simeq 2{\times}10^{-5}$ eV cm).

R_L is also much **larger** than the scale of variations of the random component of the Galactic magnetic field (yet more uncertain, in the $10 - 100$ pc range) for CRs with energies above $10^{16}..10^{17}$ eV. Such cosmic rays free-stream through the Galactic magnetic field. They would quickly escape from the Galaxy, if injected by Galactic sources. → Perhaps the highest energy cosmic rays come from extragalactic sources (potentially at cosmological distances).

$$R_L = \frac{E}{eB} \simeq 3{\times}10^{26} \left[\frac{E}{10^{20}\ \mathrm{eV}}\right]\left[\frac{B}{1\ \mathrm{nG}}\right]^{-1}\ \mathrm{cm}$$

R_L can be much **larger** than the distance to the nearest extragalactic sources for CR s with energies in the 10^{20} eV range, the Ultra-High-Energy Cosmic Rays (UHECR).

Greizen-Zatsepin-Kuzmin effect: UHECR loose energy on the distance $D \sim 10 - 100$ Mpc because of pion production in interactions of with Cosmic Microwave Background photons ($\epsilon_{ph} \sim 10^{-3}$ eV). The threshold is

$$E = \frac{2m_p m_\pi + m_\pi^2}{4\epsilon_{ph}} \simeq 6{\times}10^{19}\ \mathrm{eV}$$

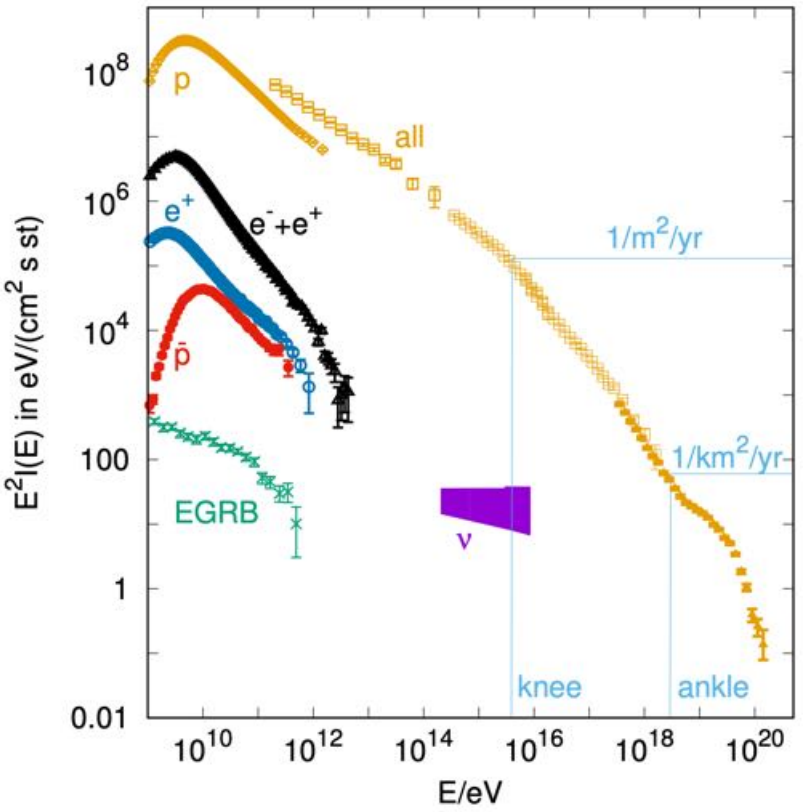

UHECR sources may be identifiable via direct back-tracing of UHECR arrival directions on the sky…..

Ultra-high-energy cosmic rays (UHECR)

Cosmic rays gyrate in Galactic magnetic field:

$$R_L = \frac{E}{eB} \simeq 10^{20} \left[\frac{E}{10^{17}\ \mathrm{eV}}\right]\left[\frac{B}{3\ \mu\mathrm{G}}\right]^{-1}\ \mathrm{cm}$$

(* natural system of units: $1\ \mathrm{G} \simeq 0.1\ \mathrm{eV}^2$; $e \simeq 0.1$; $\hbar c \simeq 2{\times}10^{-5}\ \mathrm{eV\ cm}$).

R_L is also much **larger** than the scale of variations of the random component of the Galactic magnetic field (yet more uncertain, in the $10 - 100$ pc range) for CRs with energies above $10^{16}..10^{17}$ eV. Such cosmic rays free-stream through the Galactic magnetic field. They would quickly escape from the Galaxy, if injected by Galactic sources. → Perhaps the highest energy cosmic rays come from extragalactic sources (potentially at cosmological distances).

$$R_L = \frac{E}{eB} \simeq 3{\times}10^{26} \left[\frac{E}{10^{20}\ \mathrm{eV}}\right]\left[\frac{B}{1\ \mathrm{nG}}\right]^{-1}\ \mathrm{cm}$$

R_L can be much **larger** than the distance to the nearest extragalactic sources for CR s with energies in the 10^{20} eV range, the Ultra-High-Energy Cosmic Rays (UHECR).

Greizen-Zatsepin-Kuzmin effect: UHECR loose energy on the distance $D \sim 10 - 100$ Mpc because of pion production in interactions of with Cosmic Microwave Background photons ($\epsilon_{ph} \sim 10^{-3}$ eV). The threshold is

$$E = \frac{2m_p m_\pi + m_\pi^2}{4\epsilon_{ph}} \simeq 6{\times}10^{19}\ \mathrm{eV}$$

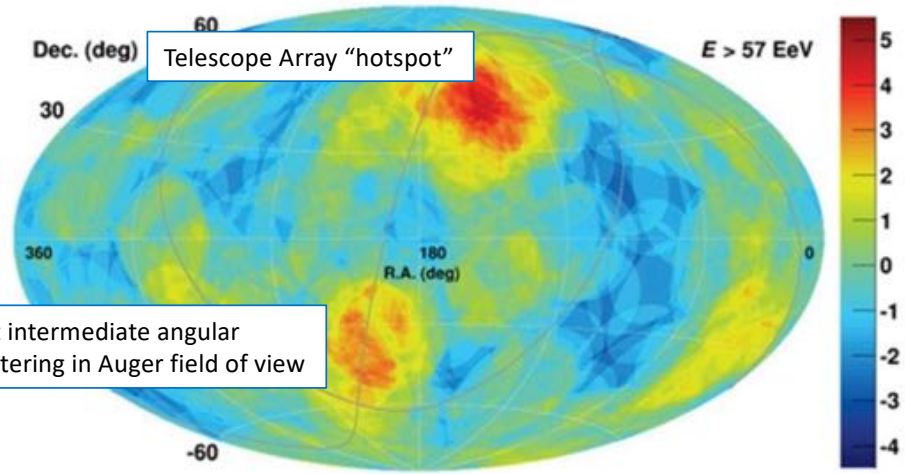

UHECR sources may be identifiable via direct back-tracing of UHECR arrival directions on the sky…..

Ultra-high-energy cosmic rays (UHECR)

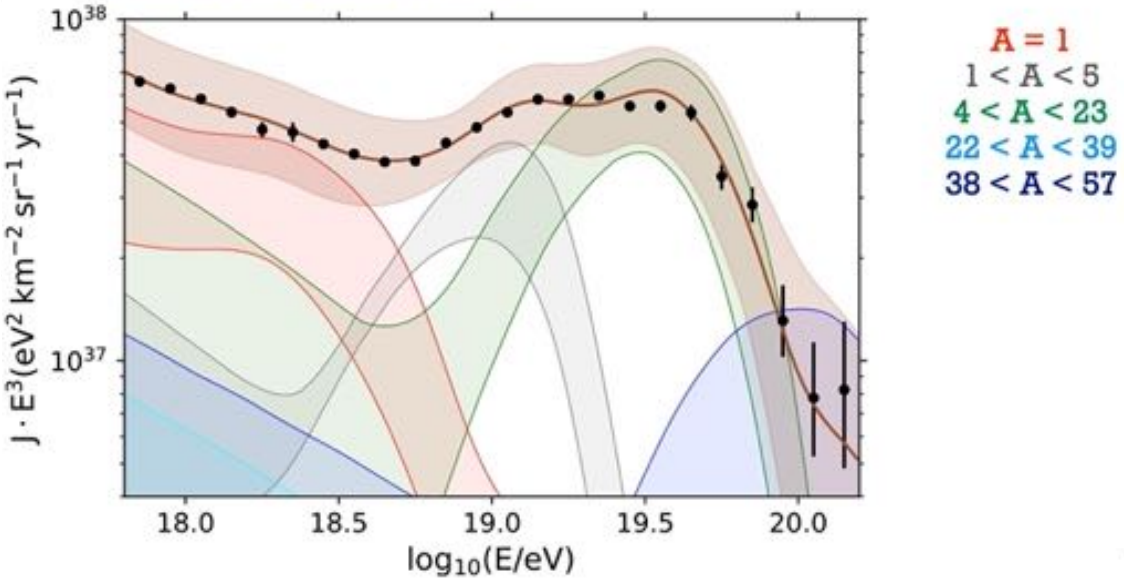

Auger and Telescope array measurements indicate that Northern and Southern sky spectra differ at the highest energy end. The spectra are consistent in the part of the sky visible to both experiments, if cross-calibration is performed (10% level correction of energy scale).

Analysis of composition of UHECR flux by Auger indicates that the highest energy flux is dominated by heavy nuclei

$$R_L = \frac{E}{ZeB} \simeq 3\times10^{26} Z^{-1} \left[\frac{E}{10^{20}\ \text{eV}}\right]\left[\frac{B}{1\ \text{nG}}\right]^{-1}\ \text{cm}$$

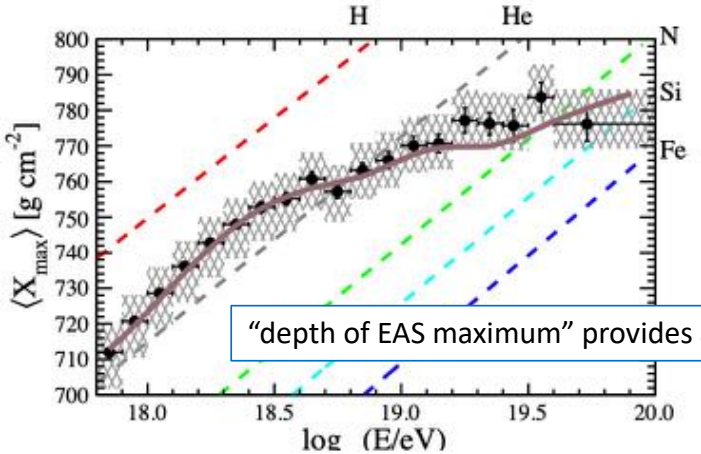

"depth of EAS maximum" provides an estimate for A

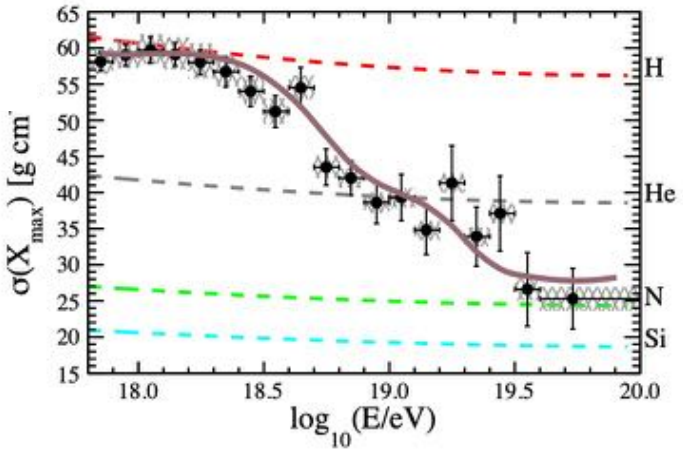

Heavy nuclei composition of UHECR flux complicates clustering analysis aimed at the search of UHECR sources via backtracing of their UHECR arrival directions. Uncertainties of knowledge of Galactic magnetic field strongly affect precision of the analysis.

Cosmic ray sources

Cosmic rays are injected with the spectrum $Q \propto E^{-\gamma} \sim E^{-2.7+\delta} \sim E^{-2.2..2.4}$ (within the toy model of propagation).

This powerlaw spectrum is either “average over source population” or “characteristic for the entire source population”.

It may be “characteristic for the entire galactic source population” or be “peculiar for the specific location of the Solar system in the Milky Way”.

Astronomical objects accelerating particles to cosmic ray energies should be able to “retain” the particles on the acceleration time scale. This suggests that the source size should be larger than the gyro-radius, $R > R_L$. This limits the maximal attainable energy to

$$E < eBR \sim 10^{20} \left[\frac{B}{10^4\ G}\right]\left[\frac{R}{10^{14}\ \mathrm{cm}}\right]\ \mathrm{eV}$$

Estimates of particle acceleration capabilities of different object types are conventionally presented in the form of a “Hillas plot”.

Cosmic rays with energies up to the “knee” can be accelerated by sources in the Milky Way, such as supernova remnants. Higher energy cosmic rays possibly come from extragalactic sources, Active Galactic Nuclei (AGN) are most commonly considered candidate source class.

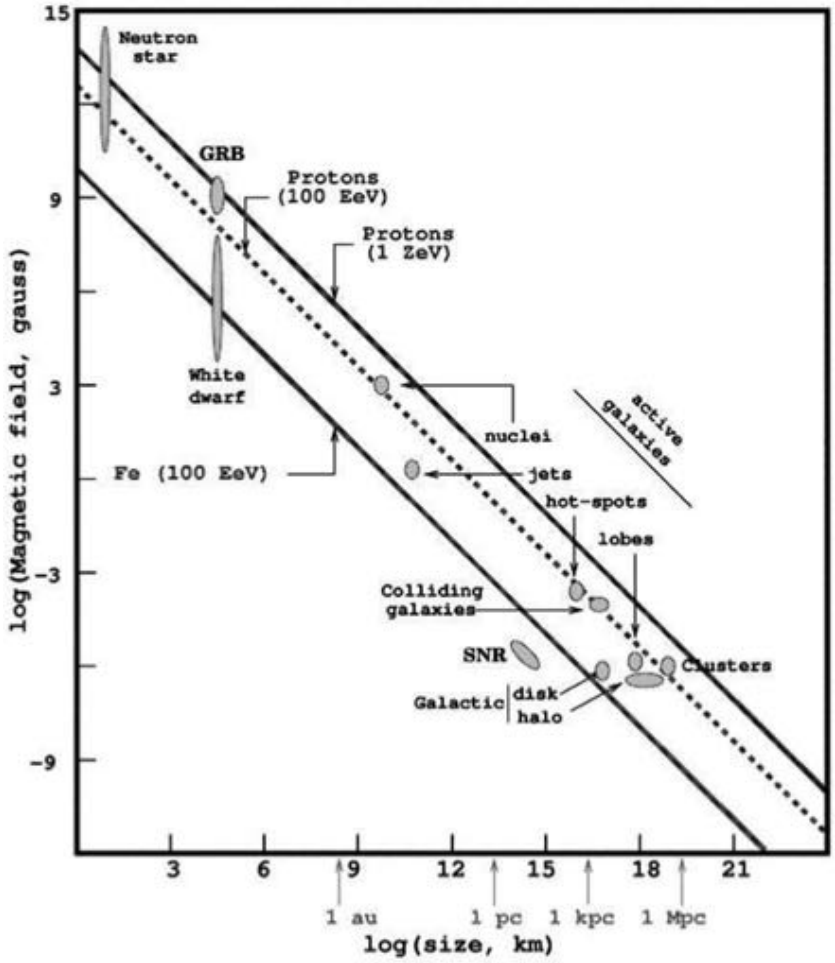

Cosmic ray acceleration mechanisms: large scale electric field

Charged particles are accelerated by electric field. Strong ordered electric field can exist e.g. near magnetized neutron stars (working as "pulsars"), of the size $R \sim 10$ km, with dipole magnetic field reaching $B \sim 10^{12}..10^{15}$ G. Magnetic dipole rotating with angular velocity $\Omega = 2\pi/T$ generates potential difference $U \sim \Omega B R^2$, potentially providing possibility to accelerate particles up to the energy

$$E \sim e\Omega B R^2$$

(note that the Hillas formula would be recovered for "millisecond" pulsars rotating with the periods close to $T \sim 2\pi R/c$).

This, however, does not happen because large scale electric fields are difficult to maintain in the presence of charged particle plasma: charge redistribution creates electrostatic field that "neutralizes" the rotation-induced electric field in pulsar "magnetosphere".

Nevertheless, charged particle plasma is continuously washed out of the magnetosphere (because of rotation), creating "vacuum gaps" close to the neutron star surface. Particles are accelerated in the vacuum gaps.

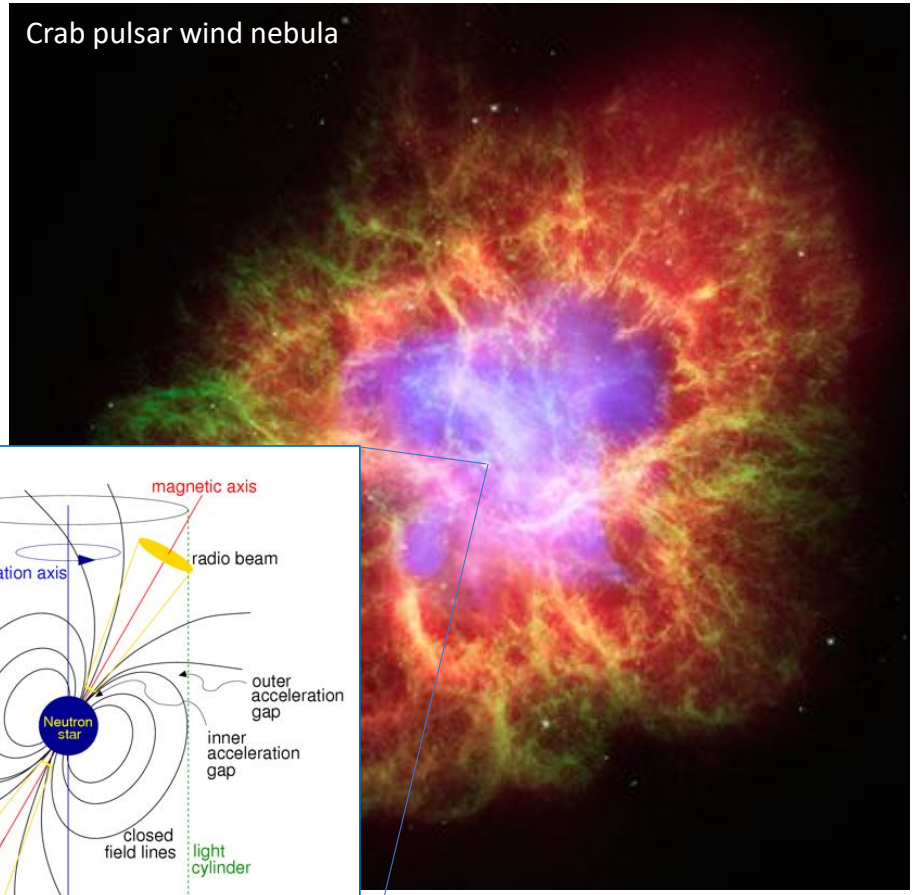

Cosmic ray acceleration mechanisms: large scale electric fields

Charged particles are accelerated by electric field. Strong ordered electric field can exist e.g. near magnetized neutron stars (working as "pulsars"), of the size $R \sim 10$ km, with dipole magnetic field reaching $B \sim 10^{12}..10^{15}$ G. Magnetic dipole rotating with angular velocity $\Omega = 2\pi/T$ generates potential difference $U \sim \Omega B R^2$, potentially providing possibility to accelerate particles up to the energy

$$E \sim e\Omega B R^2$$

(note that the Hillas formula would be recovered for "millisecond" pulsars rotating with the periods close to $T \sim 2\pi R/c$).

This, however, does not happen because large scale electric fields are difficult to maintain in the presence of charged particle plasma: charge redistribution creates electrostatic field that "neutralizes" the rotation-induced electric field in pulsar "magnetosphere".

Nevertheless, charged particle plasma is continuously washed out of the magnetosphere (because of rotation), creating "vacuum gaps" close to the neutron star surface. Particles are accelerated in the vacuum gaps.

The accelerated particles loose energy on electromagnetic emission, and are responsible for the pulsed signal from the magnetosphere (synchrotron, curvature, inverse Compton).

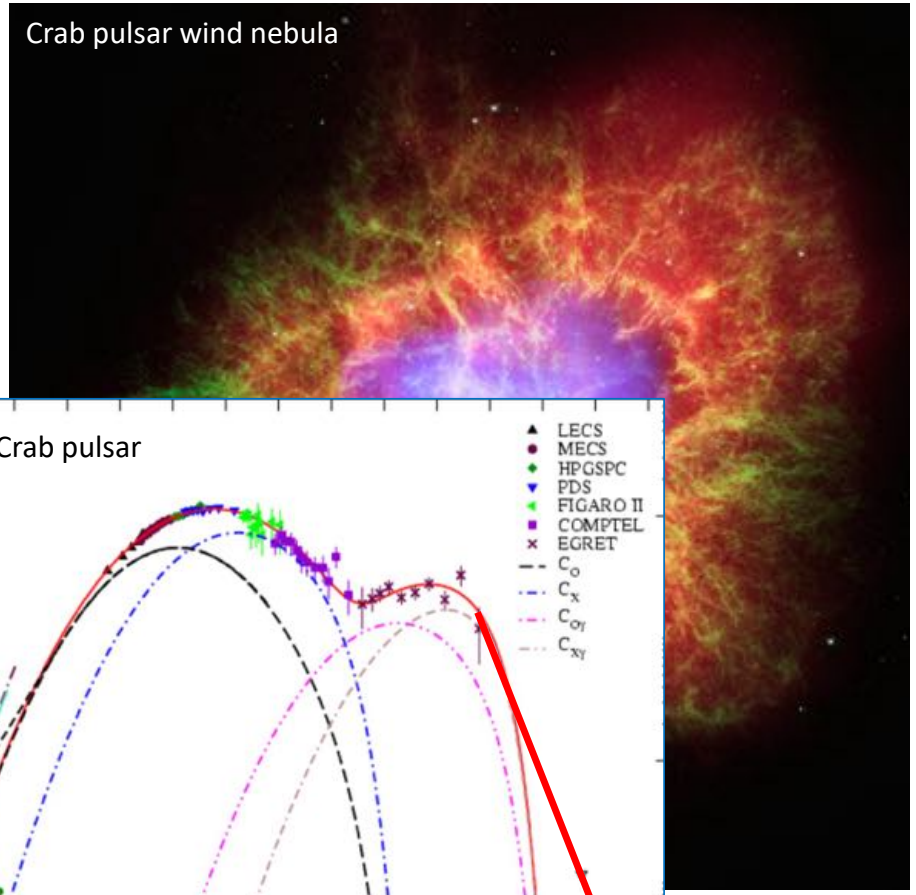

Cosmic ray acceleration mechanisms: Fermi (2nd order)

Alternative to acceleration by large scale electric fields is Fermi acceleration mechanism(s). A particle of energy E incident of a "cloud" moving with velocity V at an angle $\cos\ \alpha = \mu$ to the particle velocity has energy and momentum along the cloud motion direction

$$E' = \gamma E + V\gamma p\mu$$
$$p'_x = V\gamma E + \gamma p\mu$$

In the cloud comoving frame. Bouncing off the cloud changes $p''_x = -p'_x$. Its energy in the lab frame after the bounce is

$$E'' = \gamma E' + V\gamma p'_x = \gamma^2 E\left(1 + \frac{2Vp\mu}{E} + V^2\right)$$

Particles can gain or loose energy depending on the sign of μ (gain in head-on collisions, loose in tail-in).

If the clouds are moving randomly, the the probability of head-on collisions is higher than that of the tail-in:

$$P \propto (relative\ velocity) \simeq (1 + V\mu)$$

$$\left\langle \frac{\Delta E}{E} \right\rangle = \left\langle \frac{(E'' - E)}{E} \right\rangle = \int d\mu P(\mu) \frac{\Delta E}{E} \simeq \frac{8}{3} V^2$$

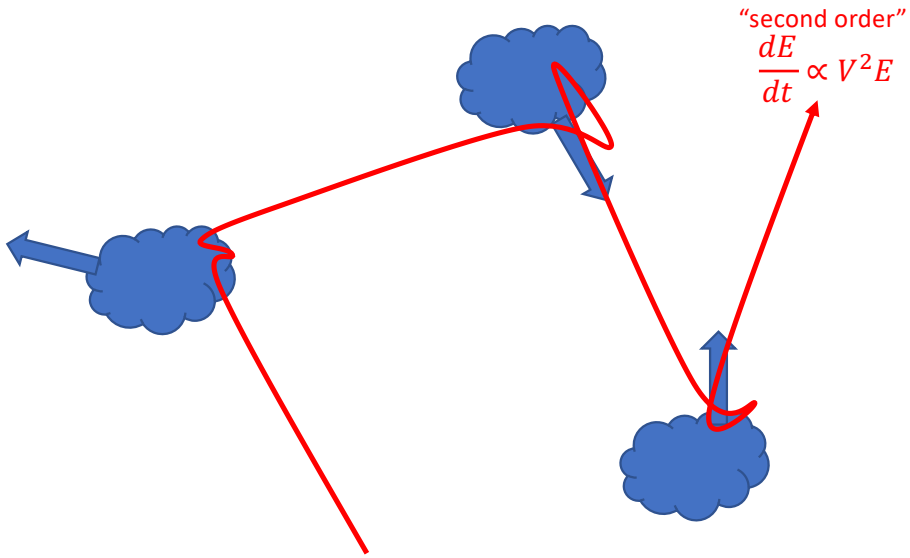

Cosmic ray acceleration mechanisms: Fermi (1st order)

Alternative to acceleration by large scale electric fields is Fermi acceleration mechanism(s). A particle of energy E incident of a "cloud" moving with velocity V at an angle $\cos\ \alpha = \mu$ to the particle velocity has energy and momentum along the cloud motion direction

$$E' = \gamma E + V\gamma p\mu$$
$$p'_x = V\gamma E + \gamma p\mu$$

In the cloud comoving frame. Bouncing off the cloud changes $p''_x = -p'_x$. Its energy in the lab frame after the bounce is

$$E'' = \gamma E' + V\gamma p'_x = \gamma^2 E\left(1 + \frac{2Vp\mu}{E} + V^2\right)$$

Particles can gain or loose energy depending on the sign of μ (gain in head-on collisions, loose in tail-in).

If the clouds are moving randomly, the the probability of head-on collisions is higher than that of the tail-in:

$$P \propto (relative\ velocity) \simeq (1 + V\mu)$$

$$\left\langle \frac{\Delta E}{E} \right\rangle = \left\langle \frac{(E''-E)}{E} \right\rangle = \int d\mu P(\mu) \frac{\Delta E}{E} \simeq \frac{8}{3} V^2$$

Otherwise, if clouds are always approaching, particles always gain energy and

$$\left\langle \frac{\Delta E}{E} \right\rangle = \left\langle \frac{(E''-E)}{E} \right\rangle = \int d\mu P(\mu) \frac{\Delta E}{E} \simeq \frac{4}{3} V$$

Such situation is encountered when particles are bouncing across a shock front, e.g. in supernova remnants expanding in interstellar medium.

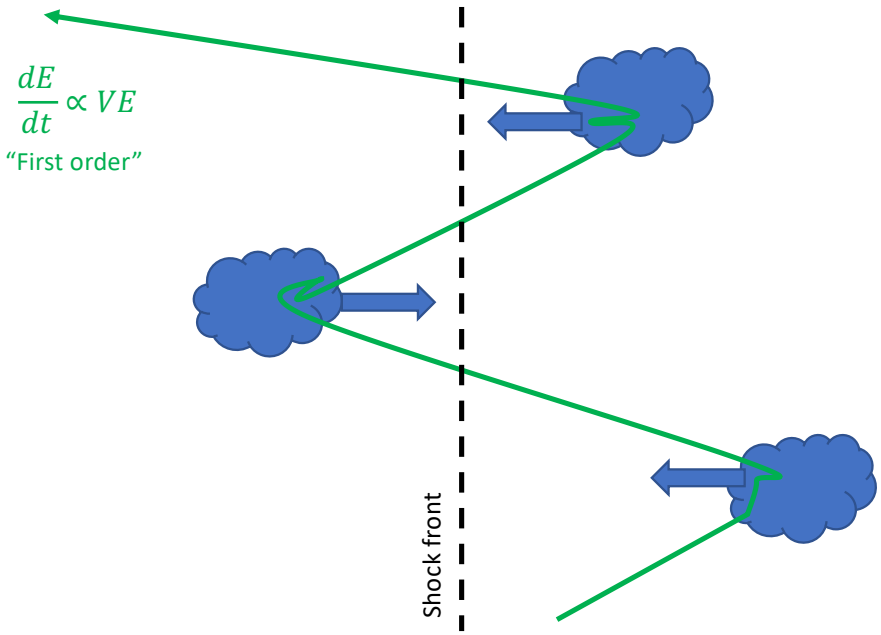

Cosmic ray acceleration mechanisms: Fermi (1st order)

Alternative to acceleration by large scale electric fields is Fermi acceleration mechanism(s). A particle of energy E incident of a "cloud" moving with velocity V at an angle $\cos\ \alpha = \mu$ to the particle velocity has energy and momentum along the cloud motion direction

$$E' = \gamma E + V\gamma p\mu$$
$$p'_x = V\gamma E + \gamma p\mu$$

In the cloud comoving frame. Bouncing off the cloud changes $p''_x = -p'_x$. Its energy in the lab frame after the bounce is

$$E'' = \gamma E' + V\gamma p'_x = \gamma^2 E\left(1 + \frac{2Vp\mu}{E} + V^2\right)$$

Particles can gain or loose energy depending on the sign of μ (gain in head-on collisions, loose in tail-in).

If the clouds are moving randomly, the the probability of head-on collisions is higher than that of the tail-in:

$$P \propto (relative\ velocity) \simeq (1 + V\mu)$$

$$\left\langle \frac{\Delta E}{E} \right\rangle = \left\langle \frac{(E''-E)}{E} \right\rangle = \int d\mu P(\mu) \frac{\Delta E}{E} \simeq \frac{8}{3} V^2$$

Otherwise, if clouds are always approaching, particles always gain energy and

$$\left\langle \frac{\Delta E}{E} \right\rangle = \left\langle \frac{(E''-E)}{E} \right\rangle = \int d\mu P(\mu) \frac{\Delta E}{E} \simeq \frac{4}{3} V$$

Such situation is encountered when particles are bouncing across a shock front, e.g. in supernova remnants expanding in interstellar medium.

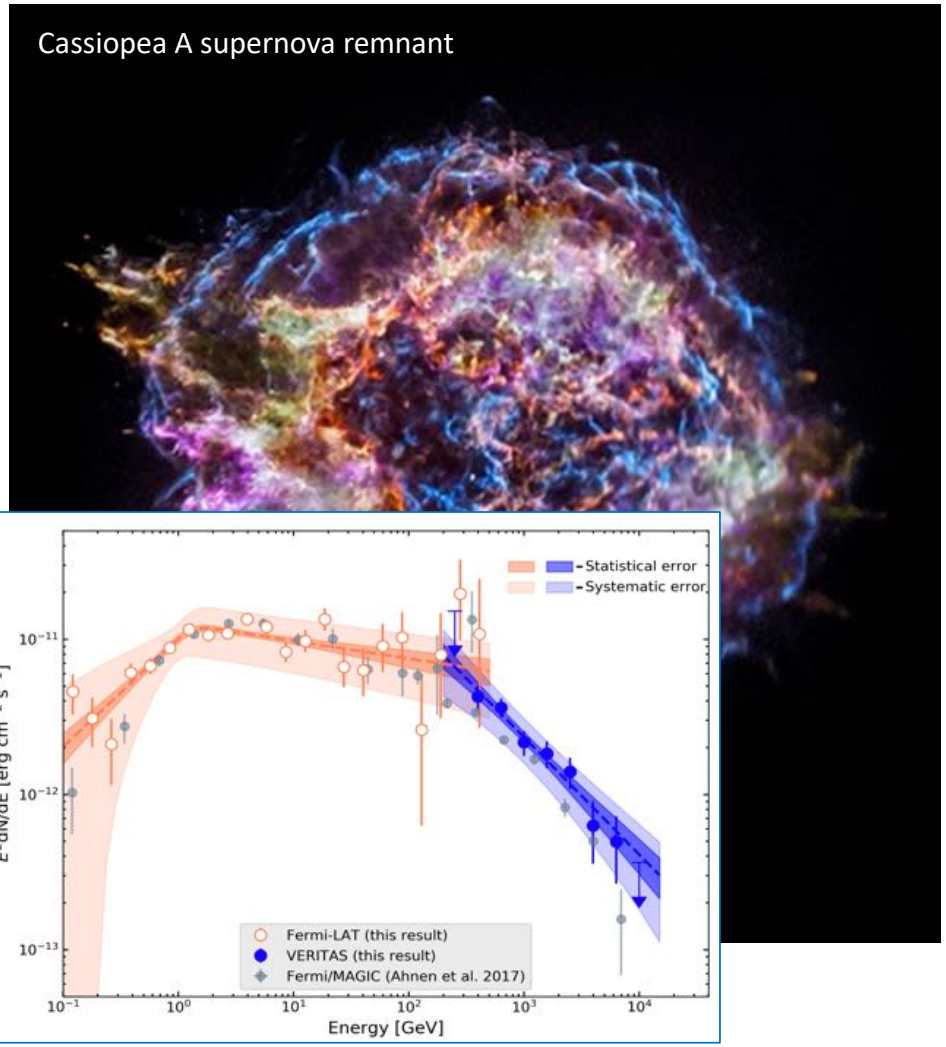

Cosmic ray acceleration mechanisms: Fermi (1st order)

Alternative to acceleration by large scale electric fields is Fermi acceleration mechanism(s). A particle of energy E incident of a "cloud" moving with velocity V at an angle $\cos\ \alpha = \mu$ to the particle velocity has energy and momentum along the cloud motion direction

$$E' = \gamma E + V\gamma p\mu$$
$$p'_x = V\gamma E + \gamma p\mu$$

In the cloud comoving frame. Bouncing off the cloud changes $p''_x = -p'_x$. Its energy in the lab frame after the bounce is

$$E'' = \gamma E' + V\gamma p'_x = \gamma^2 E\left(1 + \frac{2Vp\mu}{E} + V^2\right)$$

Particles can gain or loose energy depending on the sign of μ (gain in head-on collisions, loose in tail-in).

If the clouds are moving randomly, the the probability of head-on collisions is higher than that of the tail-in:

$$P \propto (relative\ velocity) \simeq (1 + V\mu)$$

$$\left\langle \frac{\Delta E}{E} \right\rangle = \left\langle \frac{(E''-E)}{E} \right\rangle = \int d\mu P(\mu) \frac{\Delta E}{E} \simeq \frac{8}{3} V^2$$

Otherwise, if clouds are always approaching, particles always gain energy and

$$\left\langle \frac{\Delta E}{E} \right\rangle = \left\langle \frac{(E''-E)}{E} \right\rangle = \int d\mu P(\mu) \frac{\Delta E}{E} \simeq \frac{4}{3} V$$

Such situation is encountered when particles are bouncing across a shock front, e.g. in supernova remnants expanding in interstellar medium.

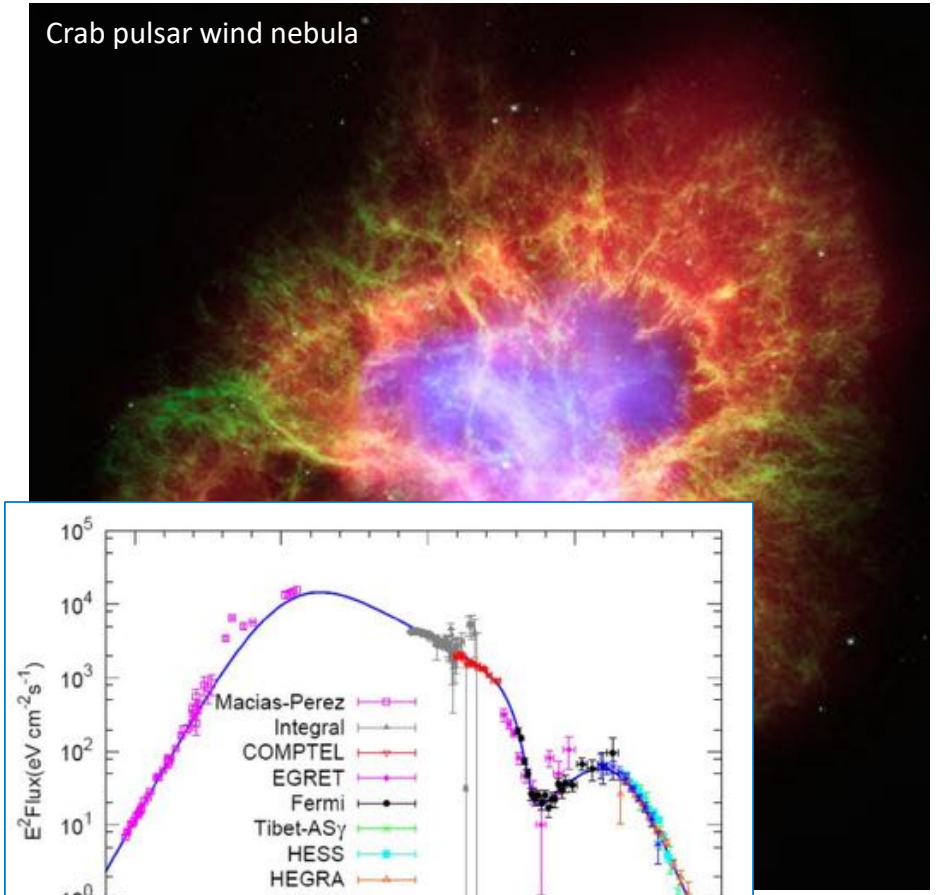

Cosmic rays and fundamental physics

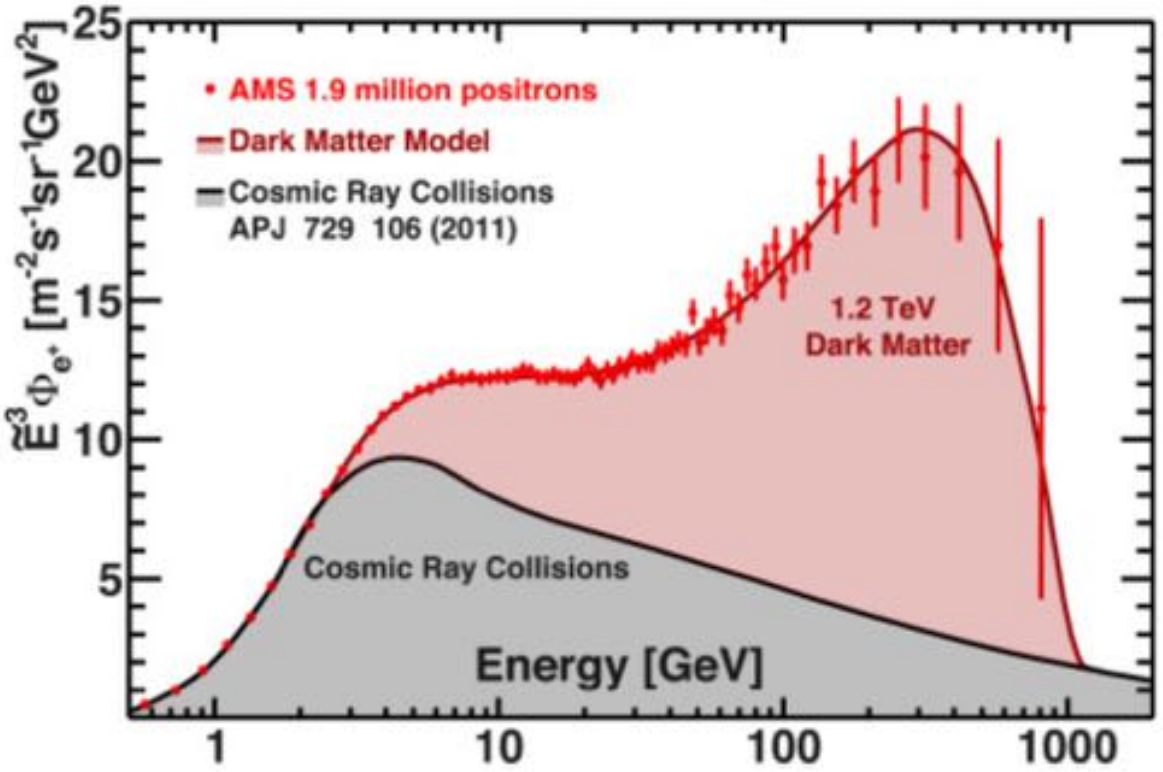

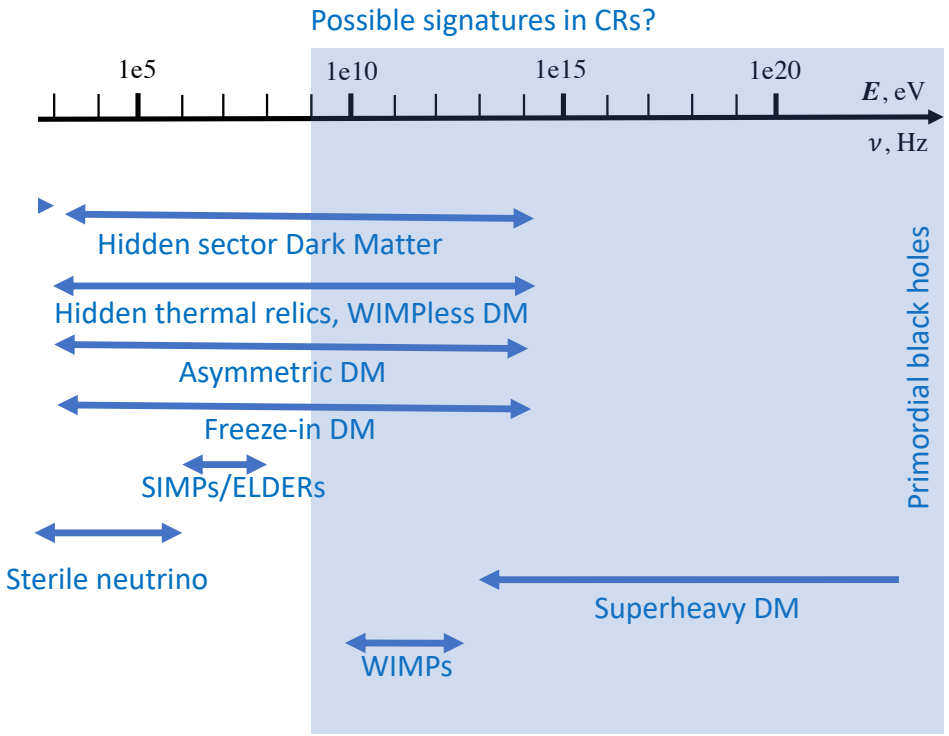

Interactions of dark matter particles (annihilation, decays) in the halo of the Milky Way can provide an additional source term for the cosmic rays particles. This should generate an unmodelled “feature” in spectrum and anisotropy of cosmic rays…. More readily observable in the “secondary” cosmic ray components, such as positrons, or anti-protons.

Gamma-ray astronomy

EM: electromagnetic

GW: gravitational wave

NU: neutrino

CR: cosmic ray

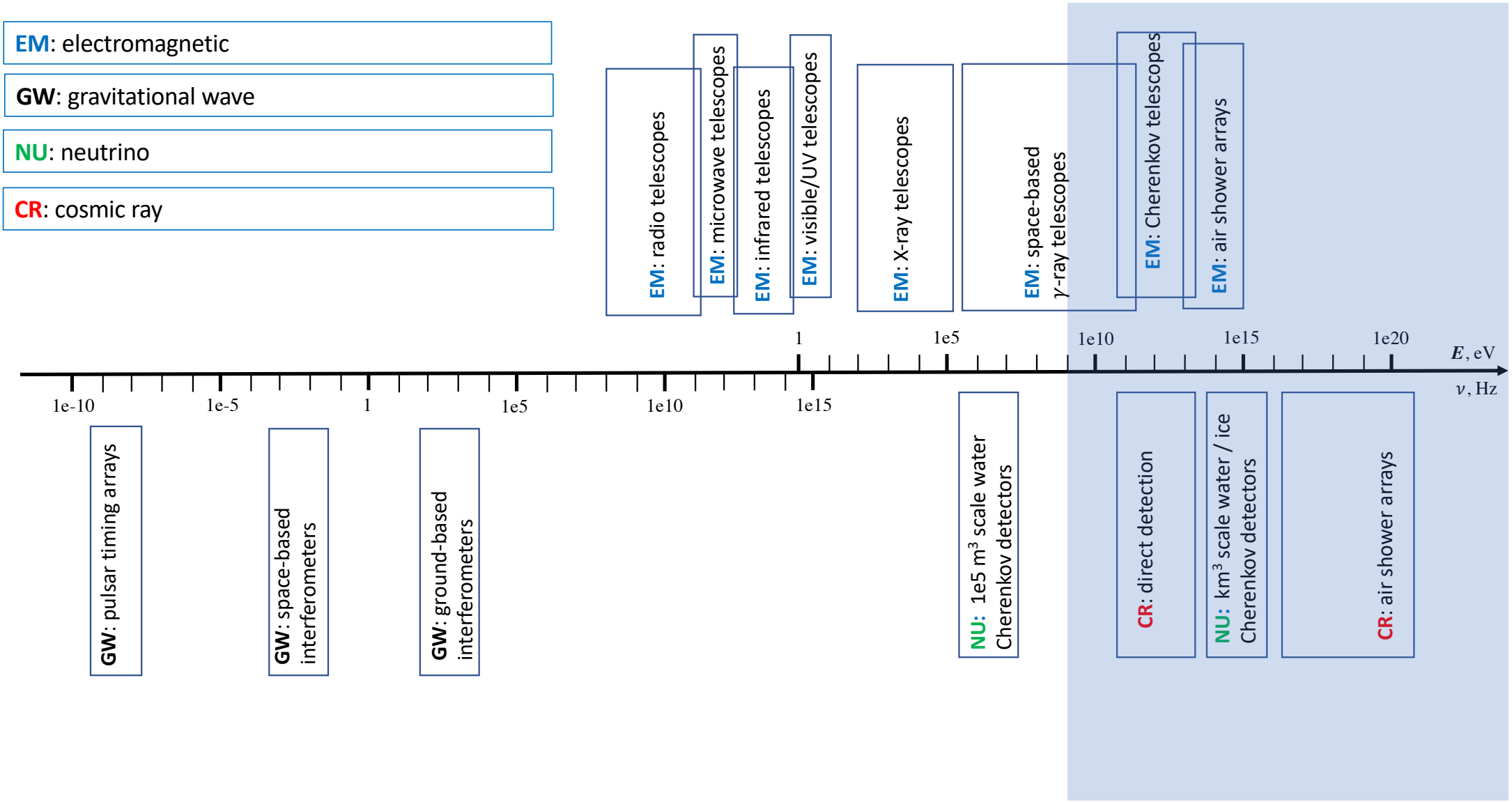

Gamma-ray astronomy

Cassiopea A supernova remnant

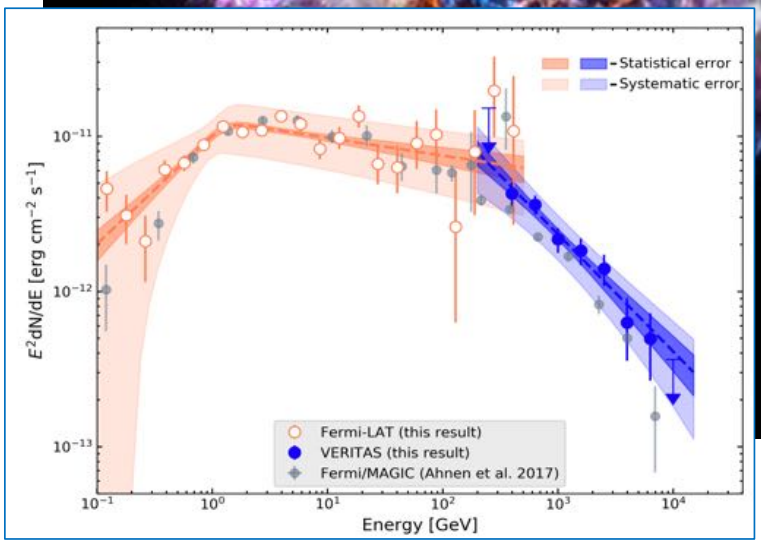

Crab pulsar wind nebula

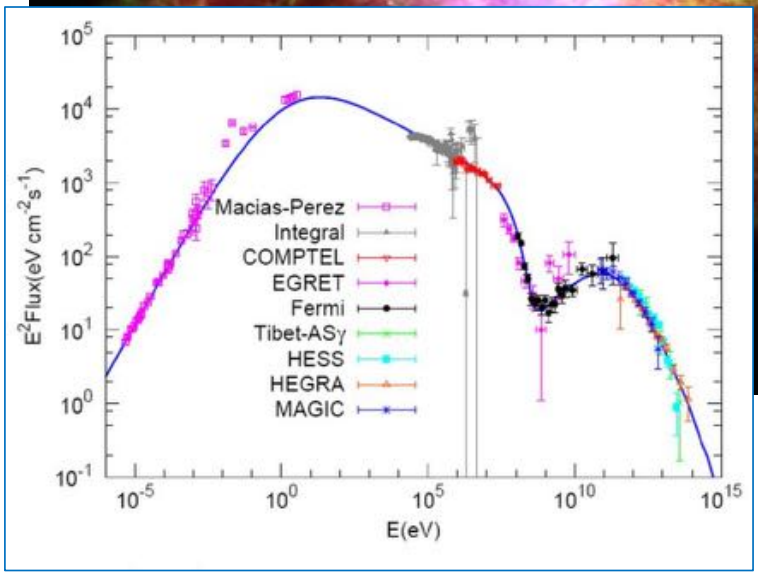

Gamma-ray telescopes

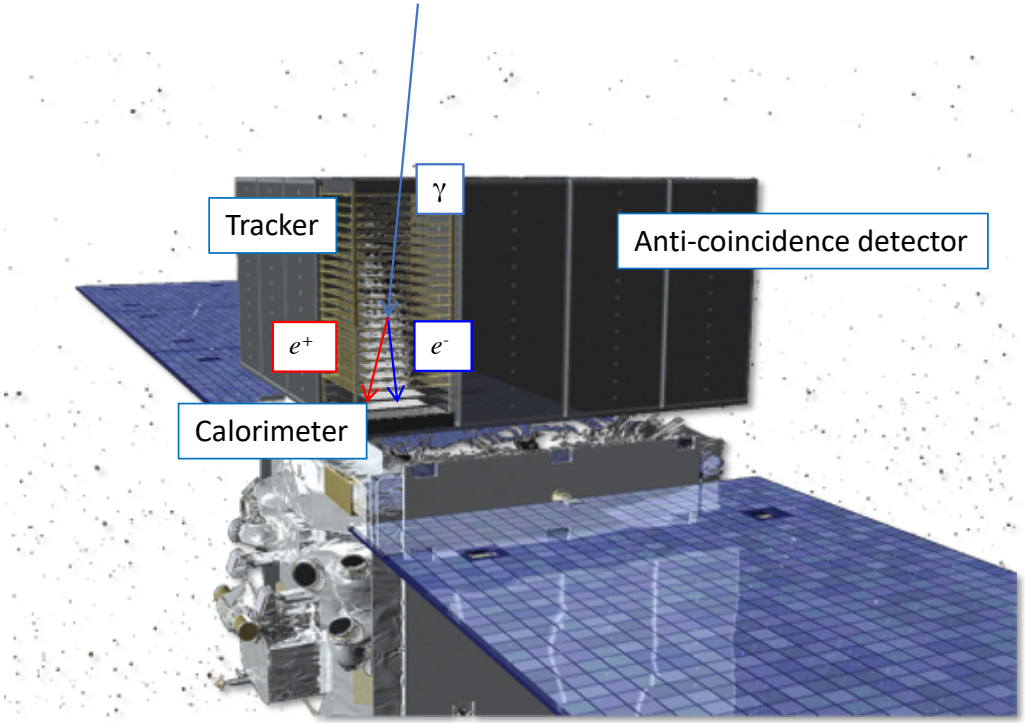

Pair conversion telescope (Fermi-LAT).

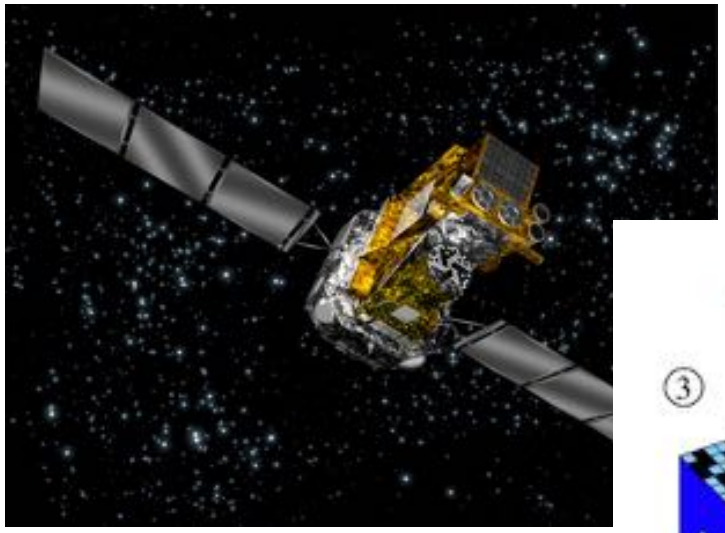

Coded mask telescope (INTEGRAL).

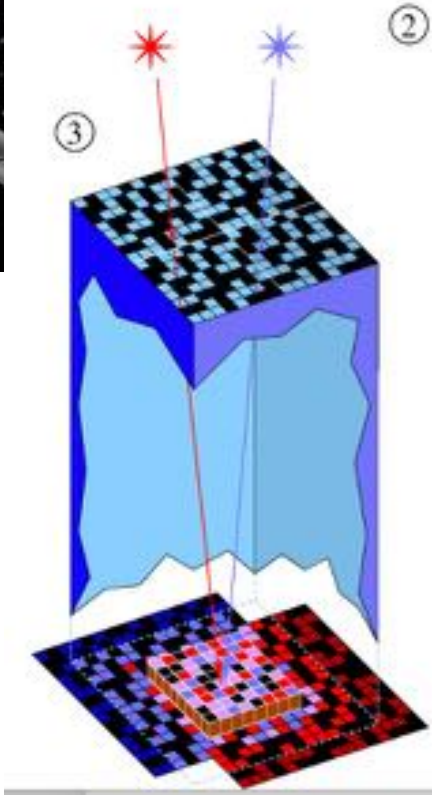

Gamma-ray telescopes

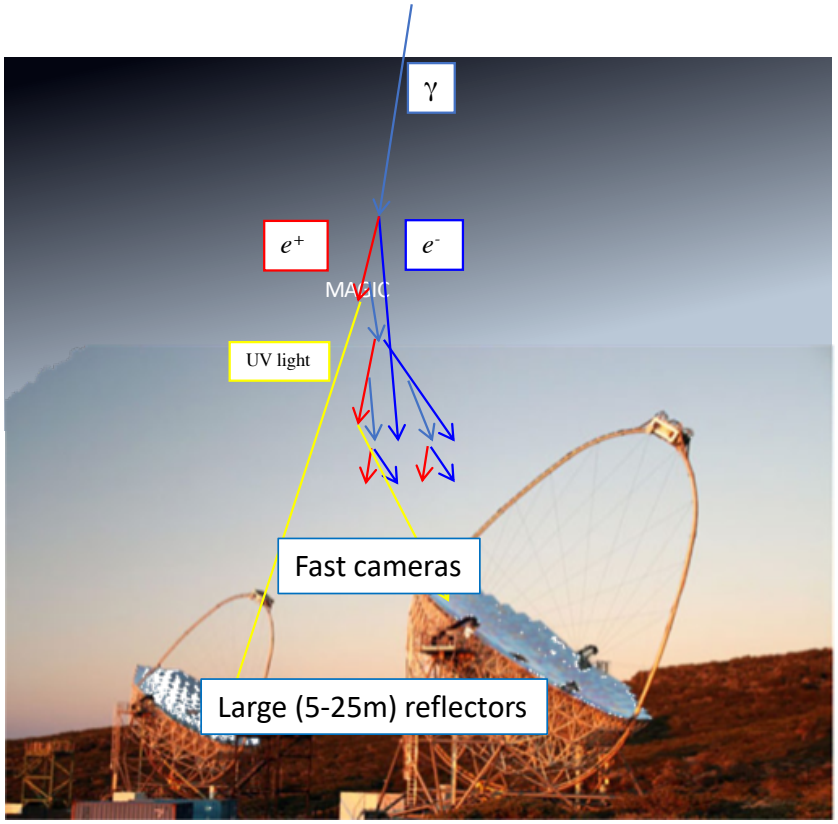

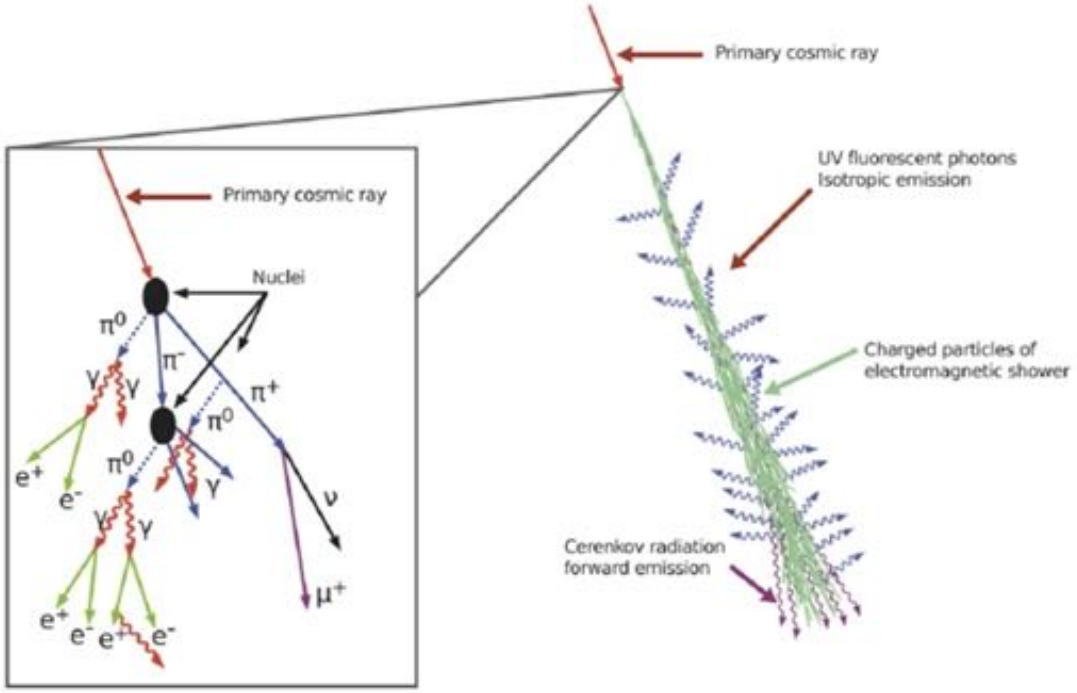

Ground-based Imaging Atmospheric Cherenkov (IACT) arrays (HESS, MAGIC, VERITAS, in the near future: CTA).

Gamma-ray sky

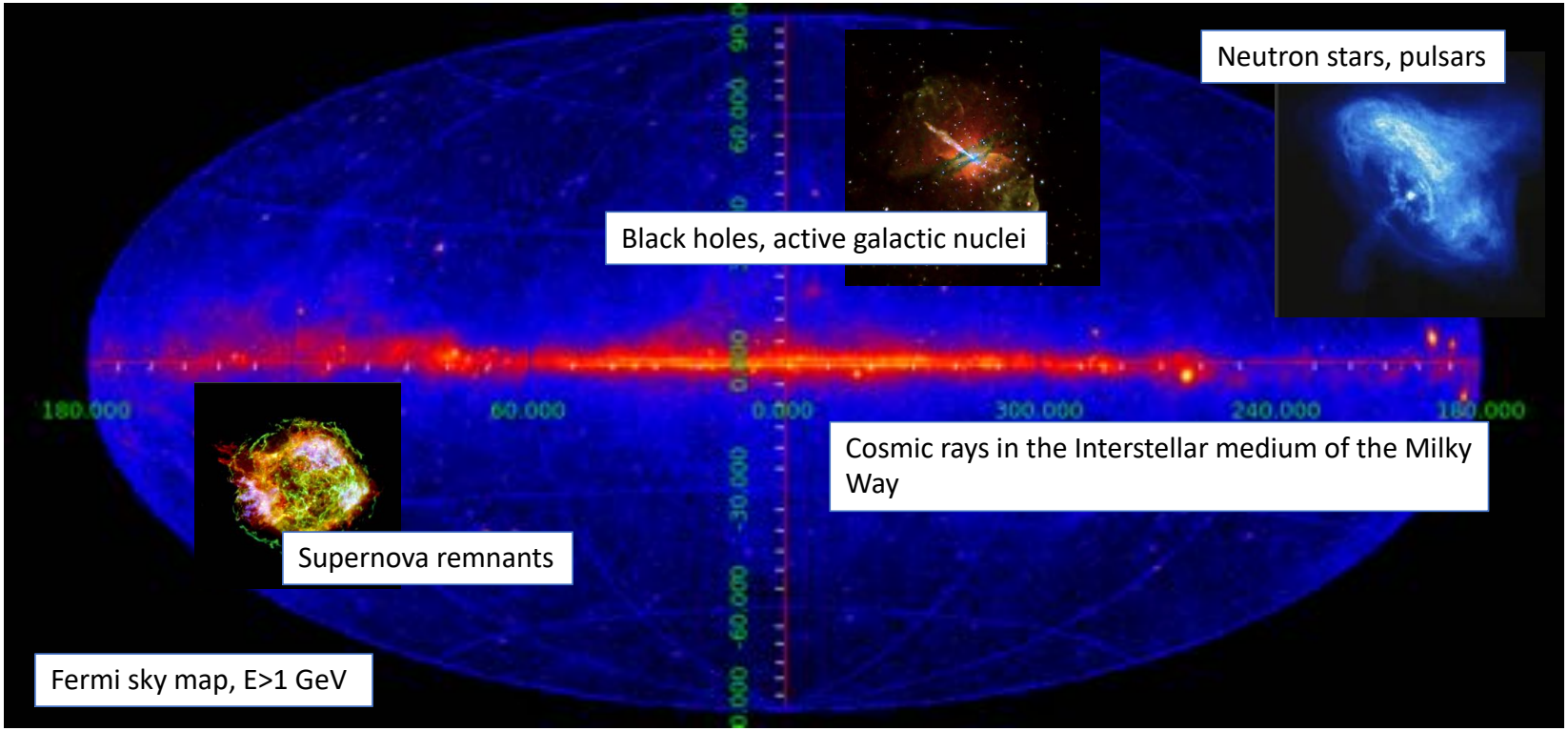

Gamma-ray sky

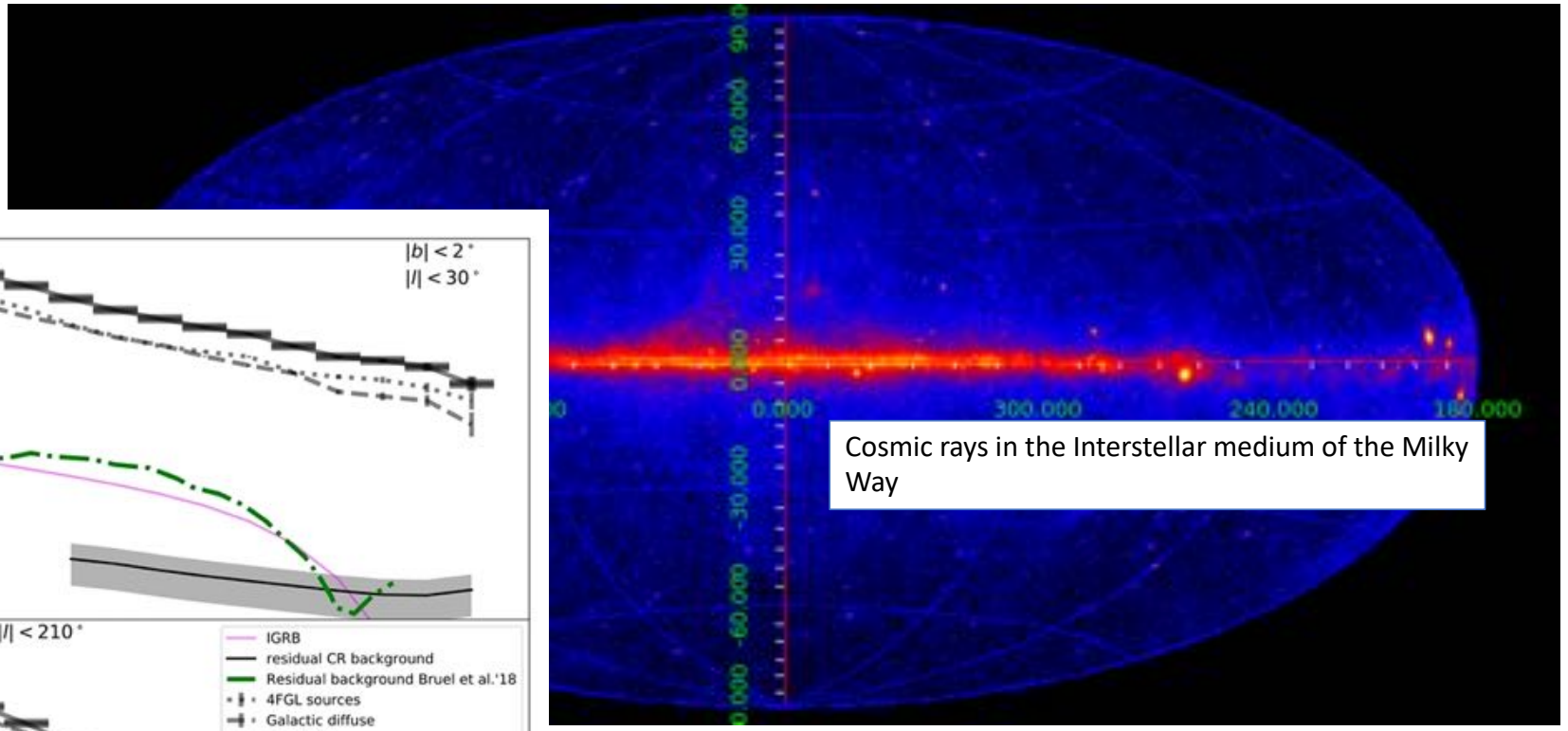

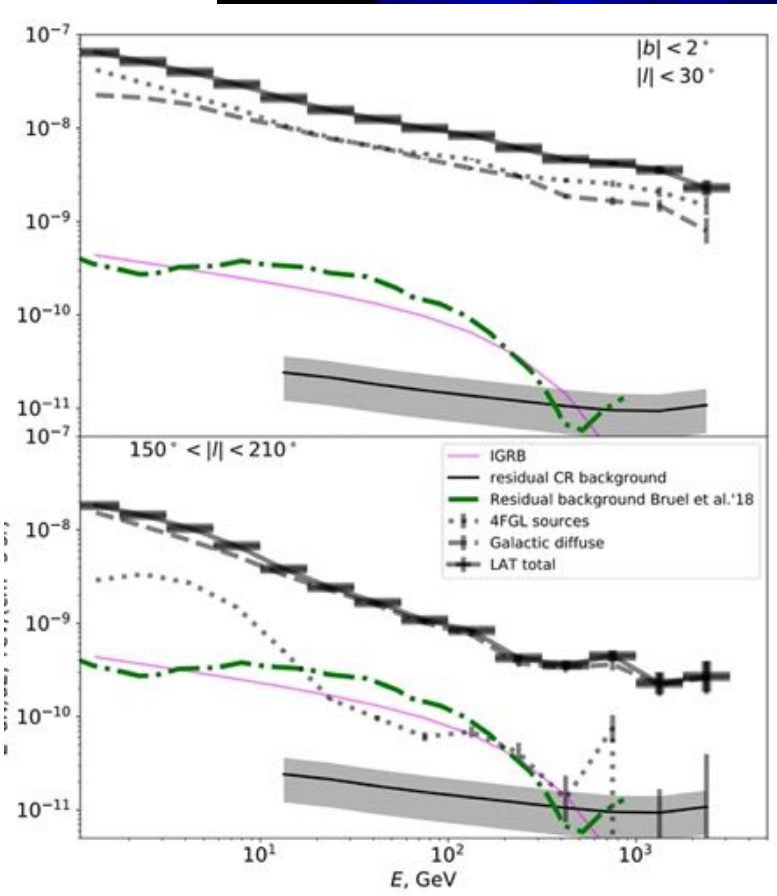

Dominant gamma-ray flux from the sky is from interactions of cosmic rays with low-energy protons in the Galactic Disk. The main process is production and decays of neutral pions in proton-proton interactions.

Imaging and spectroscopy of the diffuse emission allows to measure the spectrum of cosmic rays across the Galaxy (not only at the location of the Solar system).

Gamma-ray sky up to 1 PeV

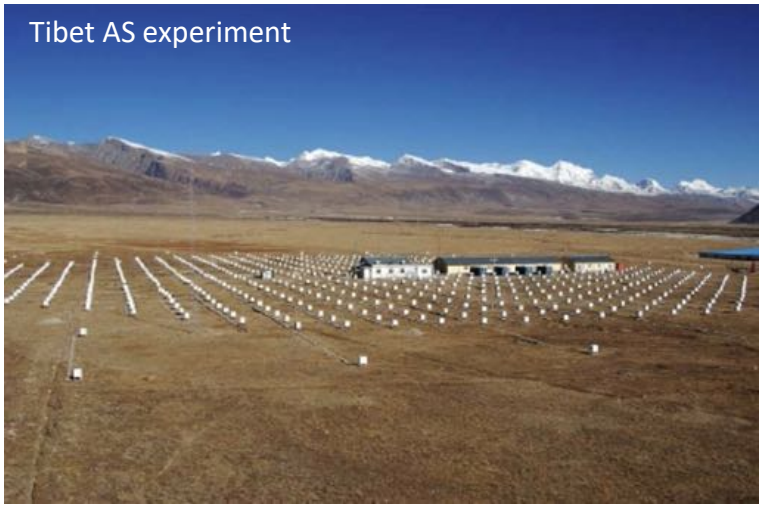

Tibet AS γ-ray map E>398 TeV

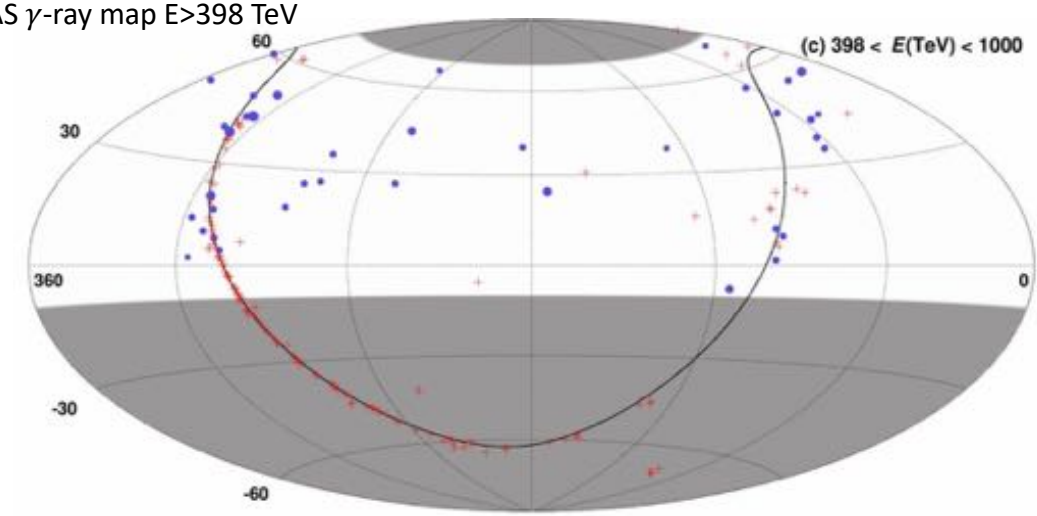

The energy frontier of astronomy is currently at PeV: first (low statistics). Galactic sources or diffuse emission from the Galactic plane has been detected. Highest energy photons from Crab nebula are also in the PeV range.

Gamma-ray sky

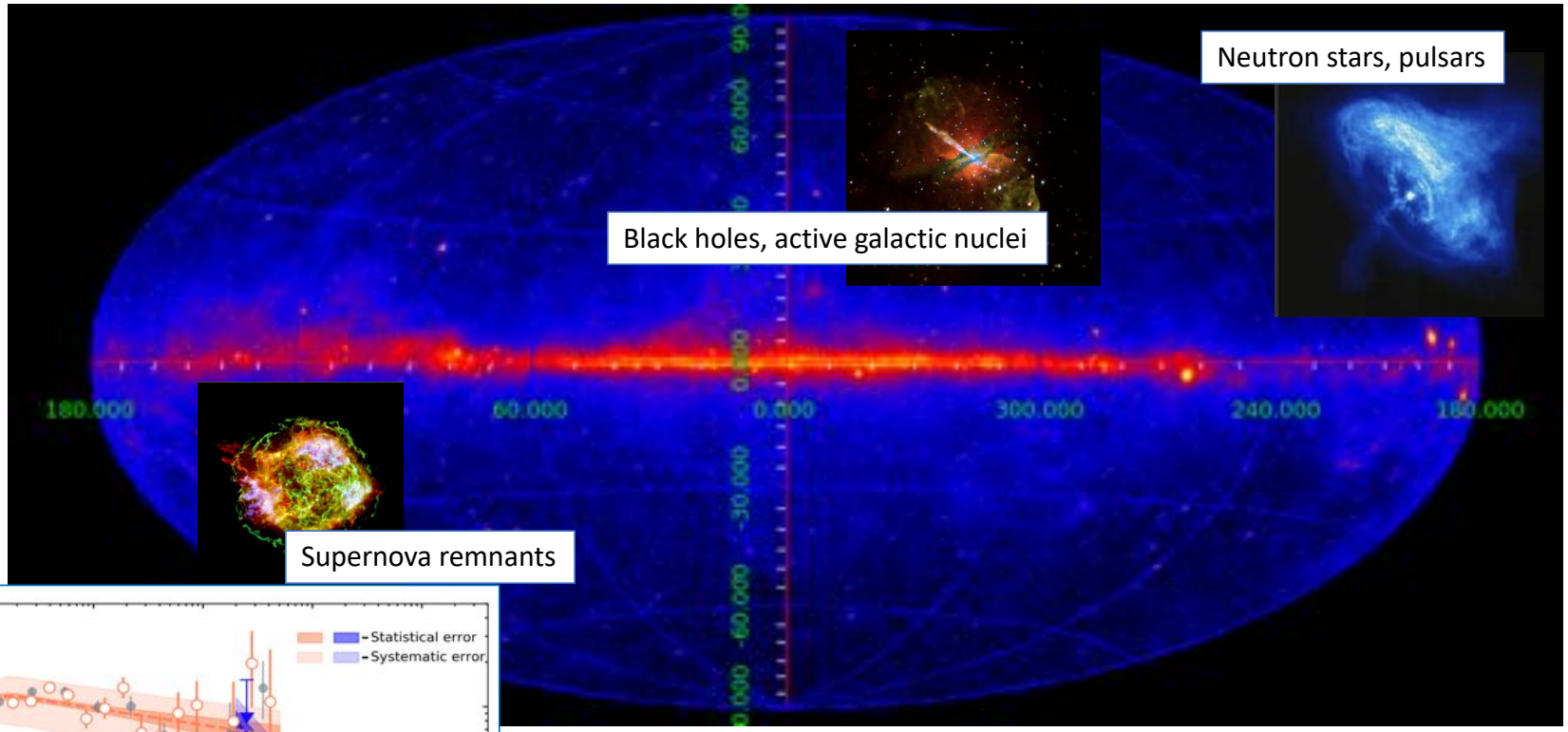

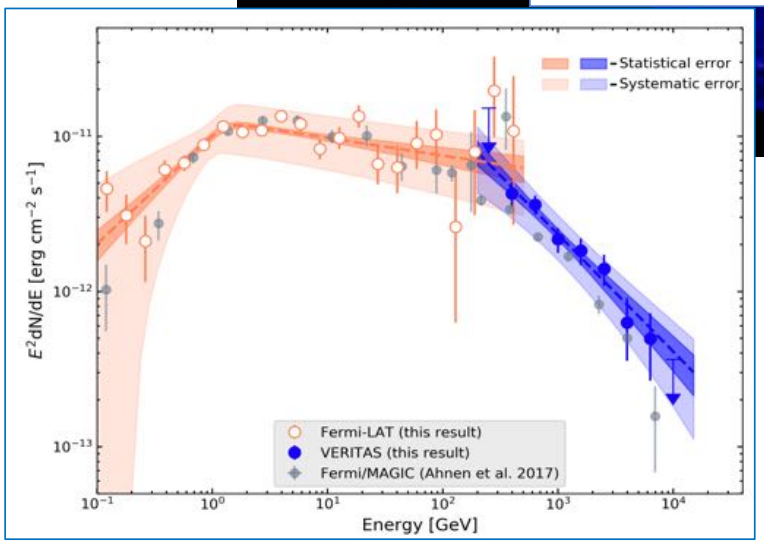

Gamma-rays coming from isolated sources can also be produced through pion production and decays in interactions of protons accelerated in the sources.

Alternatively (and perhaps more commonly), Gamma-rays are emitted through inverse Compton scattering of low-energy photons by electrons accelerated in the sources.

In both cases, gamma-ray observations allow to identify (potential) sources of cosmic rays (both Galactic and extragalactic).

Active Galactic Nuclei

The most powerful (persistent) extragalactic gamma-ray sources are Active Galactic Nuclei (AGN). Particle acceleration in AGN can operate via large scale electric field induced by black hole rotation (similar to particle acceleration in pulsar magnetosphere) or via Fermi acceleration process (shocks in relativistic outflows, jets, ejected by the black hole).

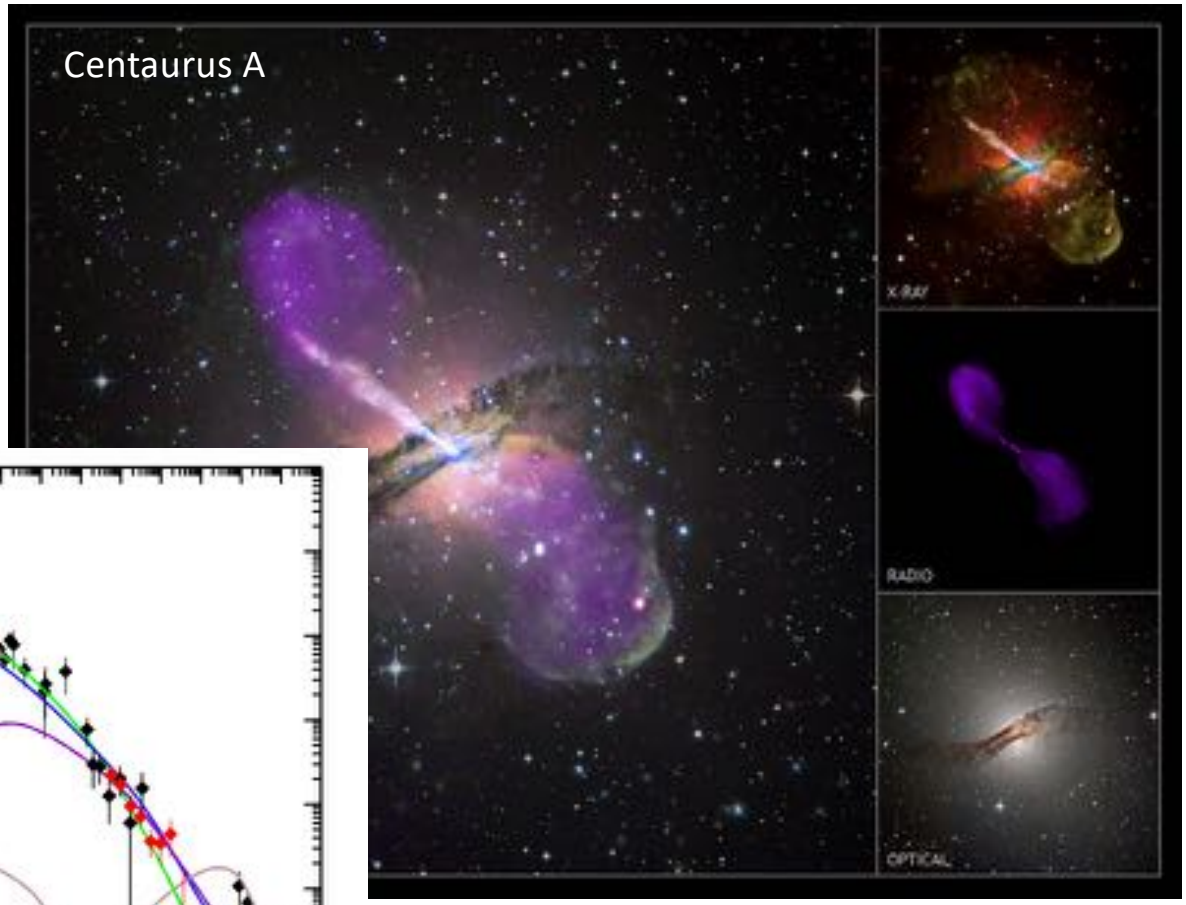

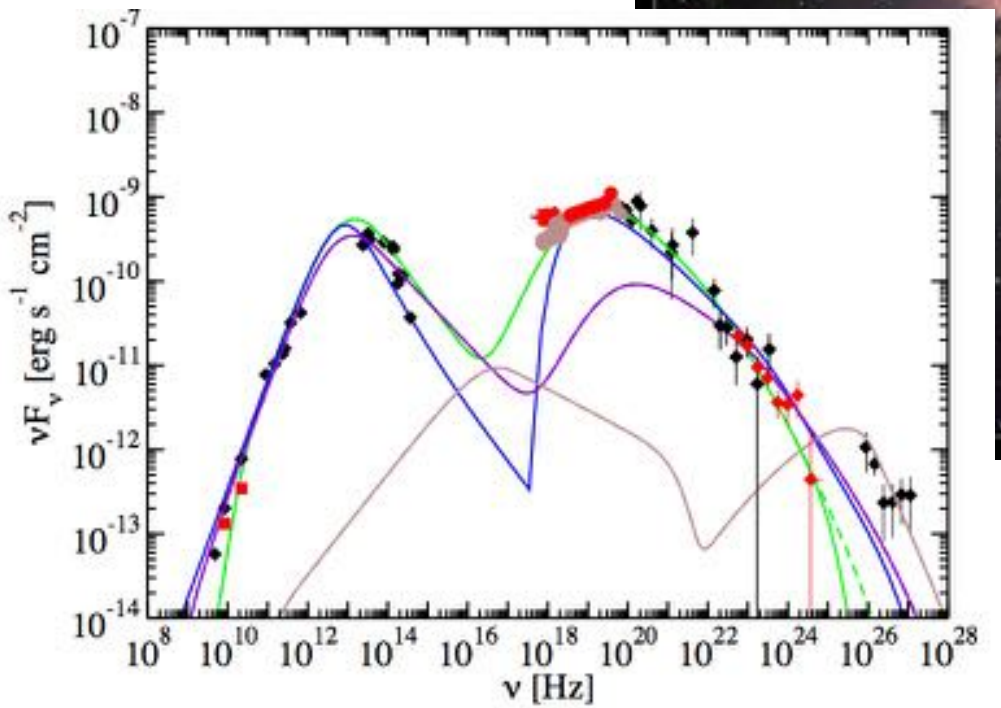

Active Galactic Nuclei

The most powerful (persistent) extragalactic gamma-ray sources are Active Galactic Nuclei (AGN). Particle acceleration in AGN can operate via large scale electric field induced by black hole rotation (similar to particle acceleration in pulsar magnetosphere) or via Fermi acceleration process (shocks in relativistic outflows, jets, ejected by the black hole).

AGN are considered as main candidates for UHECR sources.

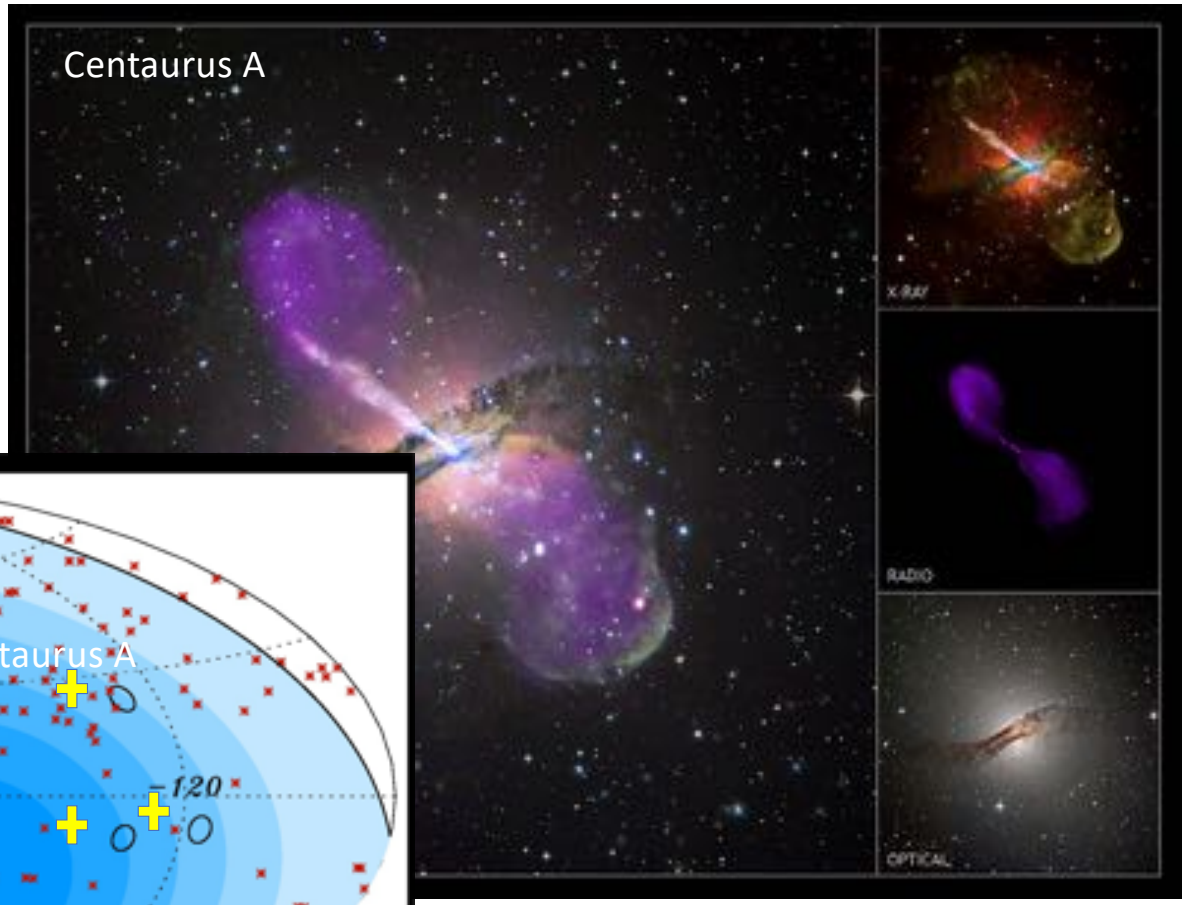

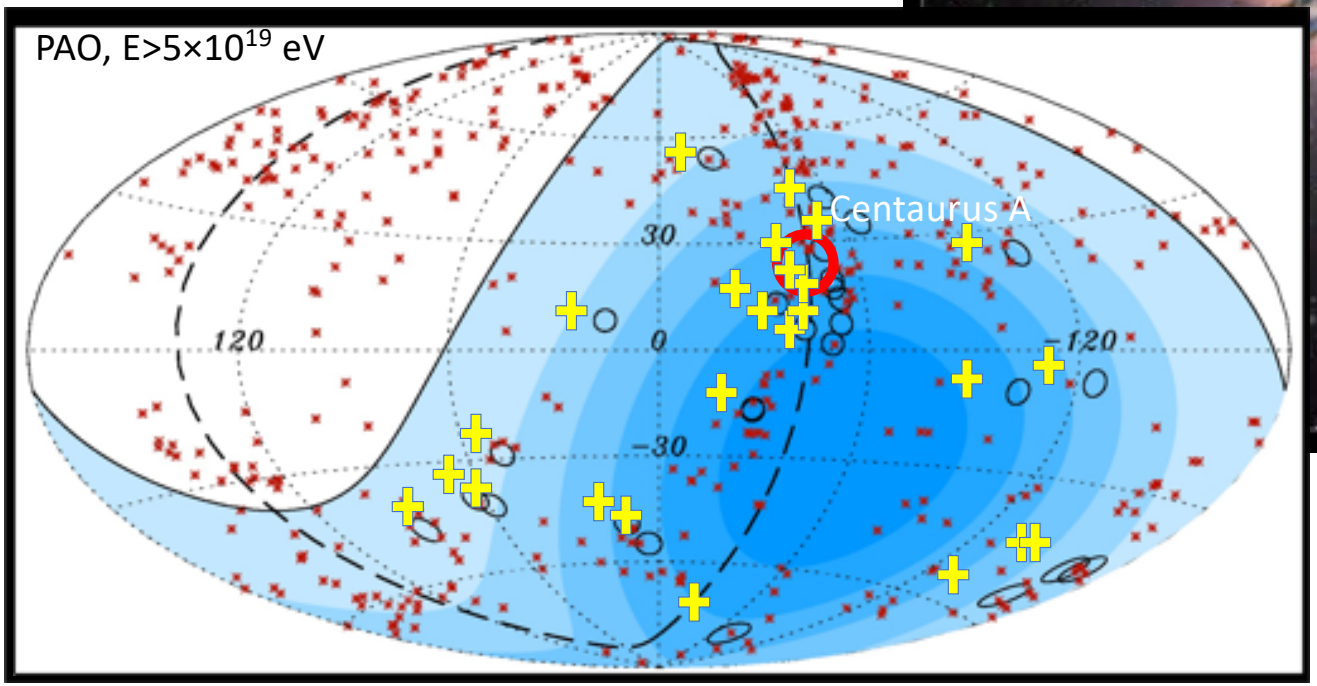

Only about 10% of AGN produce powerful jets. Most of the AGN, like Seyfert galaxies and radio quiet quasars emit thermal radiation and do not show signatures of particle acceleration.

Gamma-ray astronomy and fundamental physics

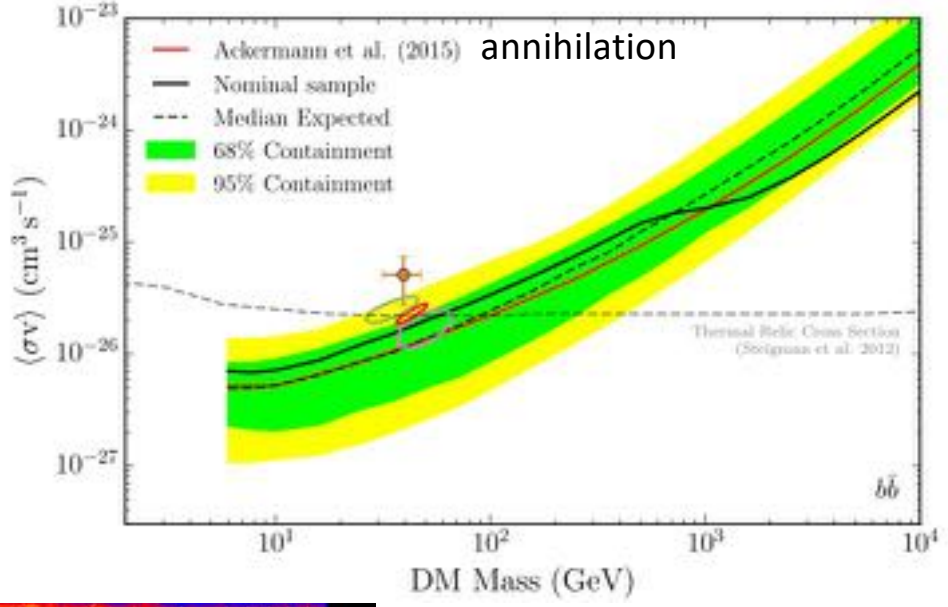

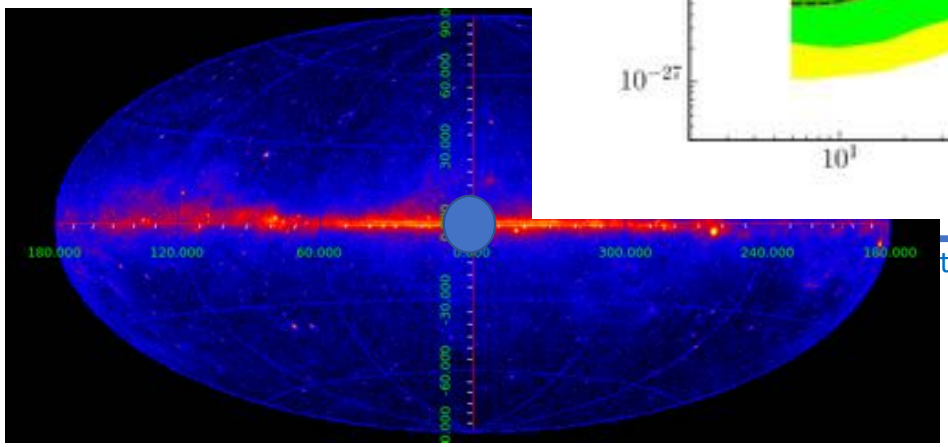

Possible signatures in gamma-rays ?

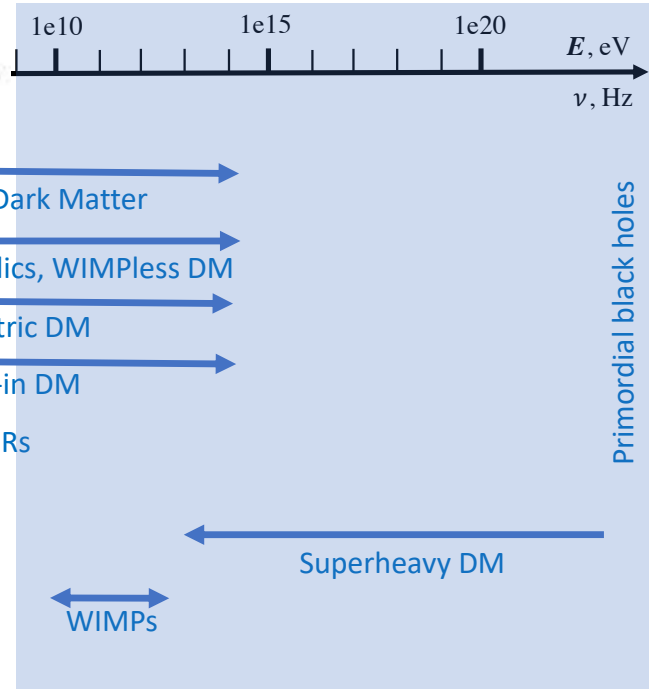

Interactions of dark matter particles (annihilation, decays) in the halo of the Milky Way can result in emission of gamma rays. This should generate an extended emission toward the inner Galaxy direction (highest concentration of dark matter particles).

An “unmodelled feature” of diffuse emission in the Galactic Center region exists in Fermi/LAT data. Consistent with the signal from WIMP annihilation….

Gamma-ray astronomy and fundamental physics

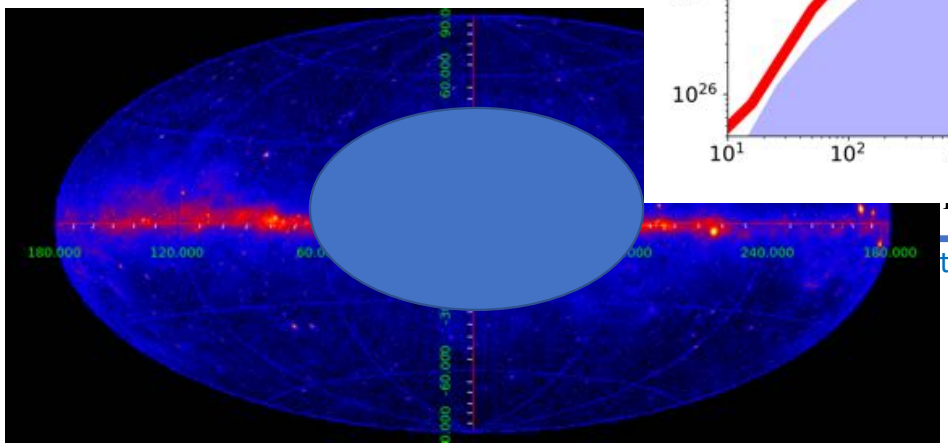

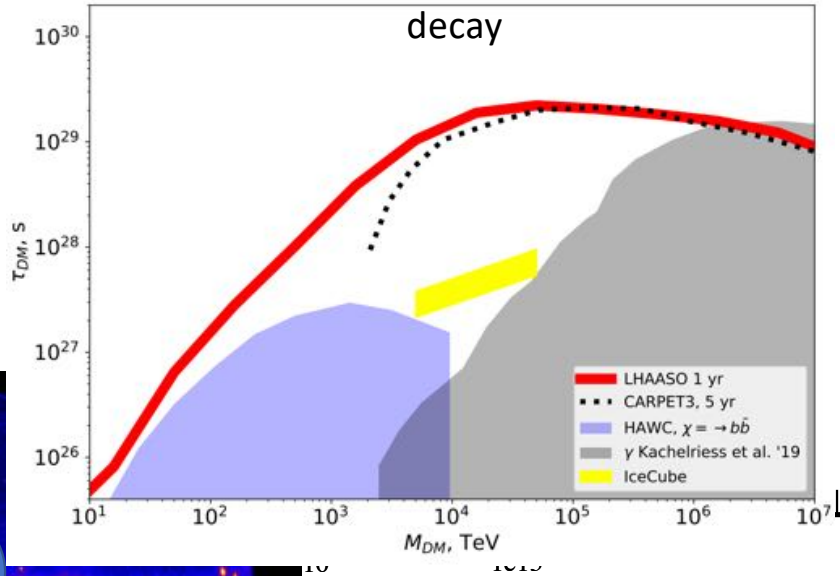

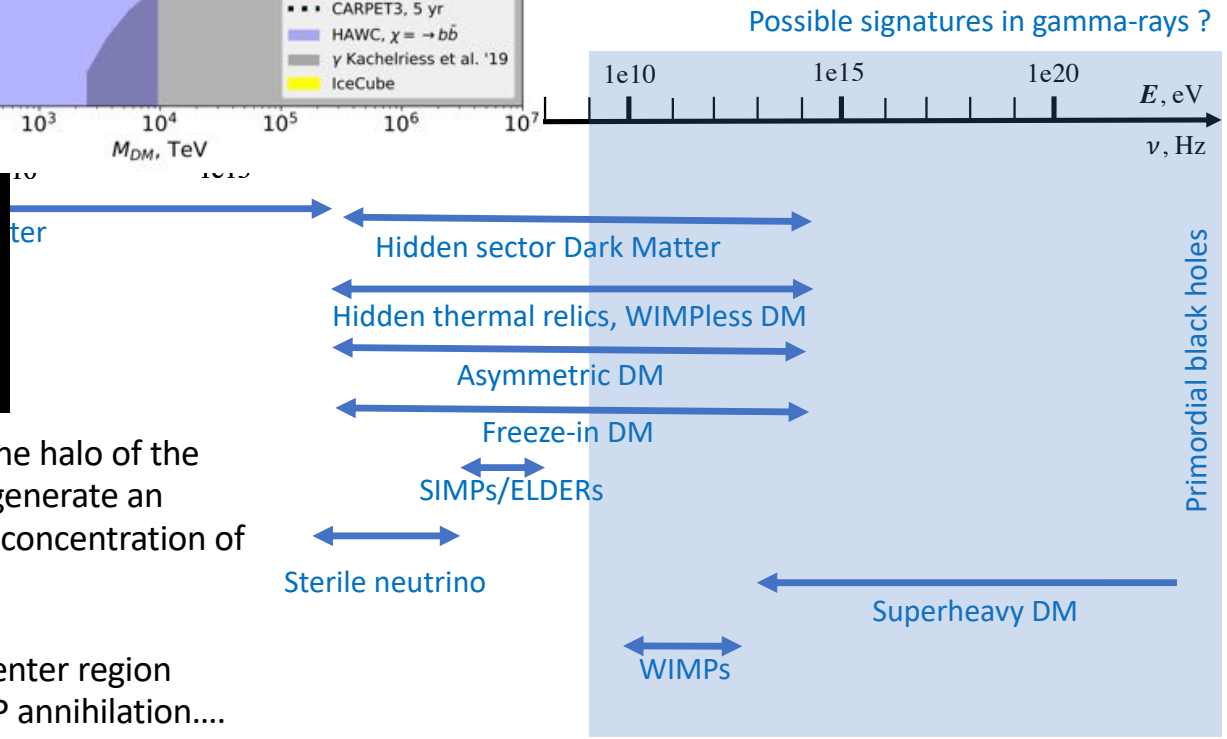

Interactions of dark matter particles (annihilation, decays) in the halo of the Milky Way can result in emission of gamma rays. This should generate an extended emission toward the inner Galaxy direction (highest concentration of dark matter particles).

An “unmodelled feature” of diffuse emission in the Galactic Center region exists in Fermi/LAT data. Consistent with the signal from WIMP annihilation….

Gamma-ray astronomy and fundamental physics

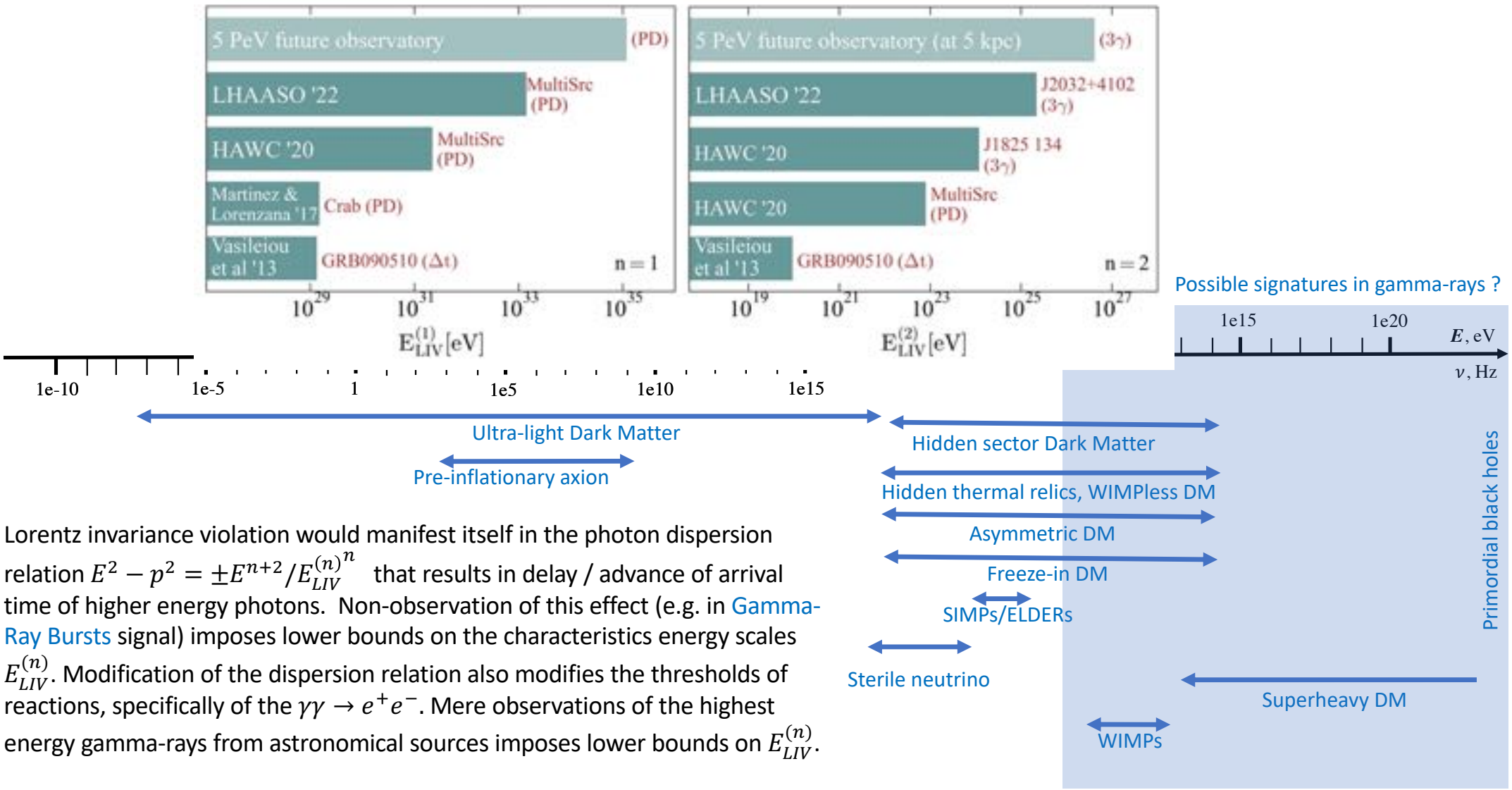

Lorentz invariance violation would manifest itself in the photon dispersion relation $E^2 - p^2 = \pm E^{n+2}/{E^{(n)}_{LIV}}^n$ that results in delay / advance of arrival time of higher energy photons. Non-observation of this effect (e.g. in Gamma-Ray Bursts signal) imposes lower bounds on the characteristics energy scales $E^{(n)}_{LIV}$. Modification of the dispersion relation also modifies the thresholds of reactions, specifically of the $\gamma\gamma \rightarrow e^+e^-$. Mere observations of the highest energy gamma-rays from astronomical sources imposes lower bounds on $E^{(n)}_{LIV}$.

Gamma-ray bursts

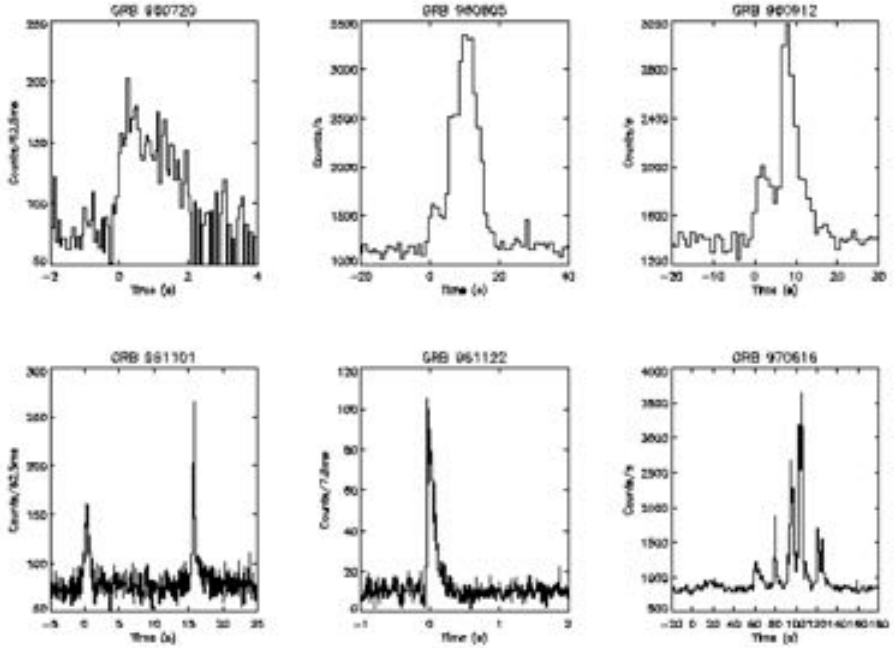

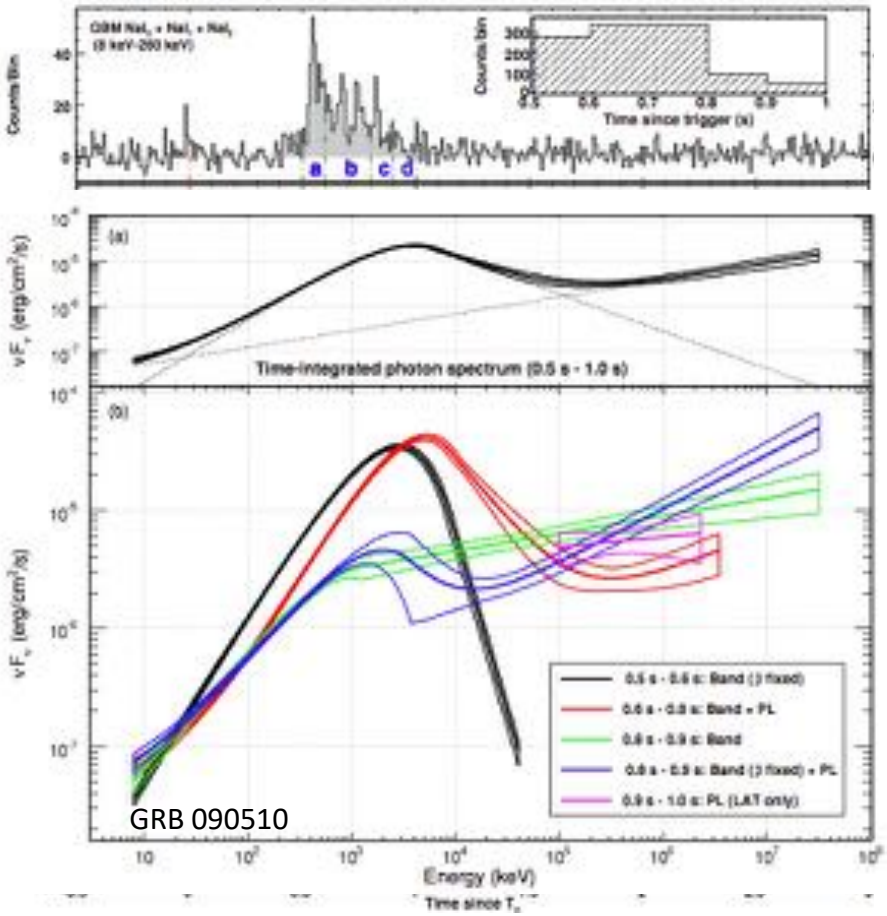

Second-scale transient sources of sub-MeV to TeV gamma-rays, mostly coming from cosmological (Giga-parsecs, $1\ \mathrm{Gpc} = 3{\times}10^{27}\ \mathrm{cm}$) distances.

Produced either in collapses of massive stars at the end of their life (sometimes explicitly associated to supernovae) or in mergers of components of neutron star binary systems or in giant flares of magnetars, highly magnetized neutron stars.

Gamma-ray bursts

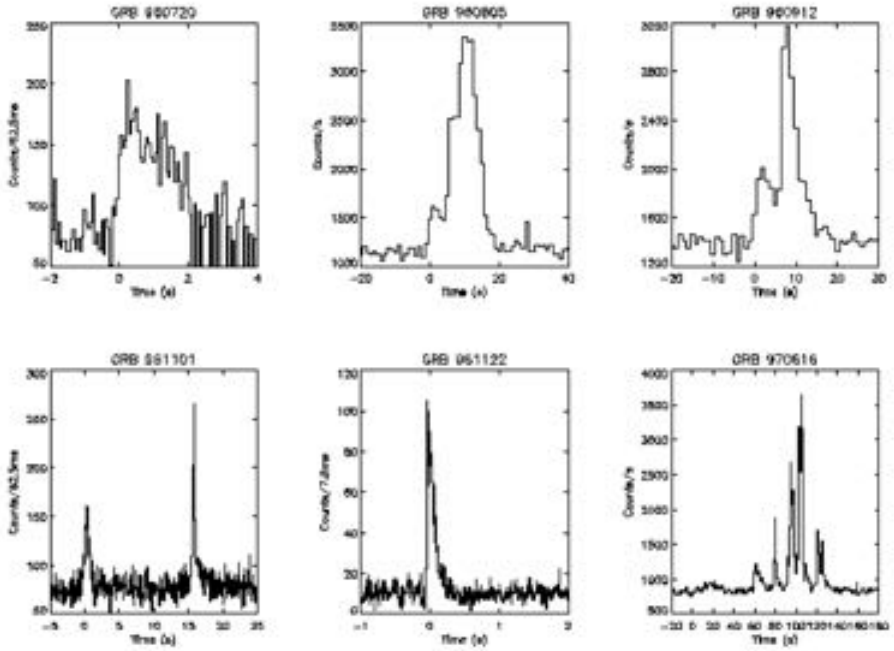

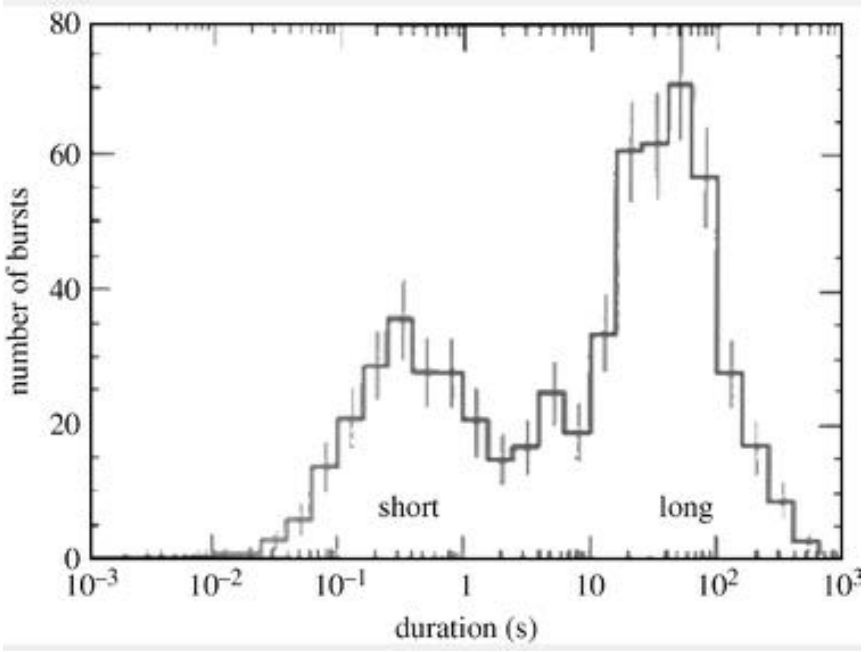

Second-scale transient sources of sub-MeV to TeV gamma-rays, mostly coming from cosmological (Giga-parsecs, $1\ \mathrm{Gpc} = 3{\times}10^{27}\ \mathrm{cm}$) distances. Historically divided onto “short” and “long” GRBs.

There is a range of transient phenomena associated to GRBs (and new phenomena keep being discovered).

“Short” gamma-ray bursts, Fast Radio Bursts, magnetars

Binary neutron star mergers is one of several possible mechanisms of short GRBs (<2 s spikes of gamma-ray flux). Such mergers produce multi-wavelength “afterglow” emission in radio-visible-X-ray bands due formation of a “kilonova”.

Another type of short GRBs is produced by soft gamma repeaters (magnetars, neutron stars with extremely strong magnetic field, $10^{14} - 10^{15}$G) are known to produce short GRB like giant flares. Flares of magnetars in other galaxies may account of a significant fraction of short GRBs.

Hurley et al. astro-ph/0502329

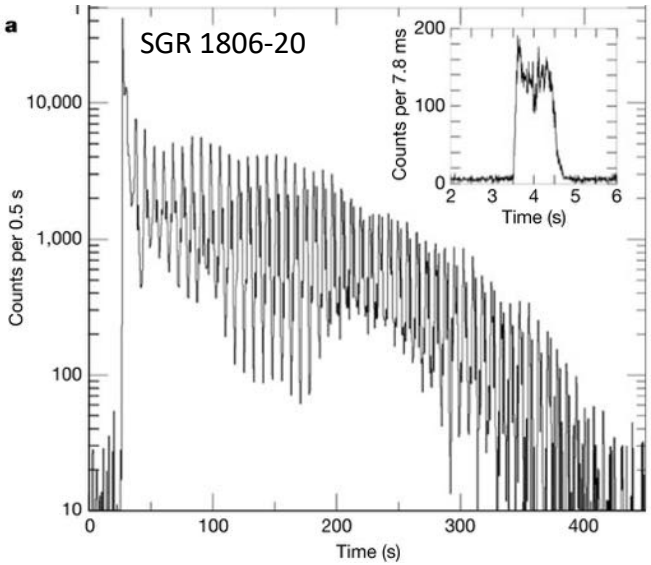

Soft gamma repeater SGR 1935+2154 flare has recently been associated also to another phenomenon: Fast Radio Burst (FRB), $\mu s - \mathrm{ms}$ long spikes of radio flux.

- Before this event only extragalactic FRBs have been detected, no evident counterparts, sometimes repeatedly from the same sky direction.
- Before this event, no magnetar bursts have been associated to radio counterparts…..

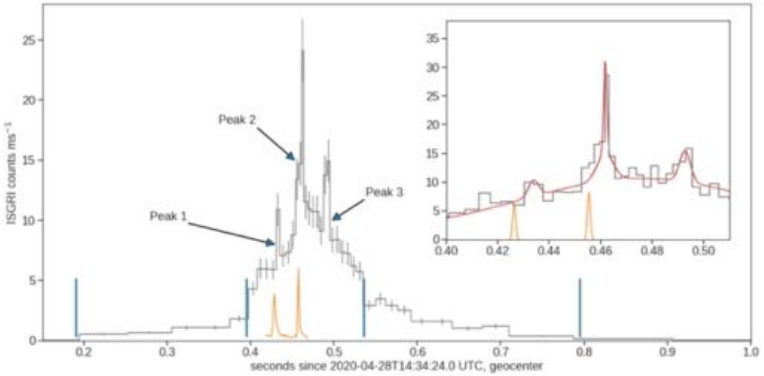

Mereghetti et al., 2005.06335

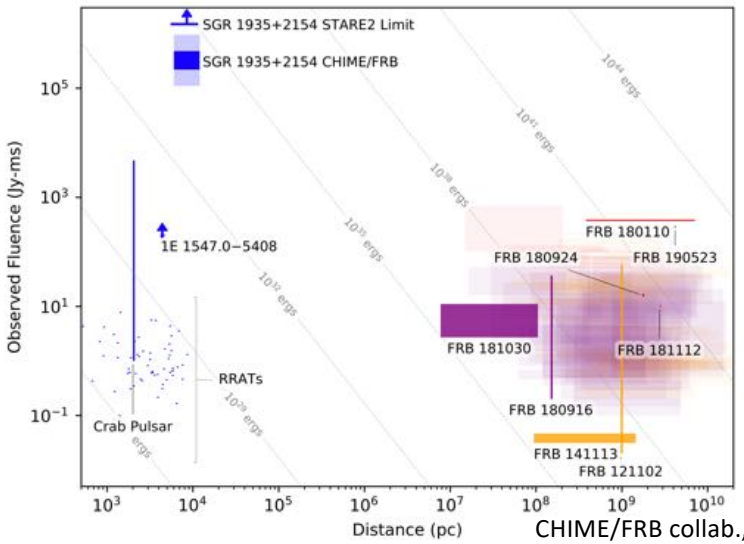

CHIME/FRB collab., 2005.10324.

”Long” GRBs, core collapse of massive stars, supernovae

Starting from SN 1998bw, Type Ibc supernovae (with progenitor stars stripped of their hydrogen and possibly helium envelope) are associated with long GRBs.

However, recently a long GRB211211A has been associated with a “kilonova”, i.e. the phenomenon produced by neutron star mergers. This is puzzling, because long/short GRB division was thought to be due to difference in physical mechanisms.

Long GRB afterglow emission is now detected at very-high energies, up to TeV (the record is GRB 221009A, claimed to be detected up to 18 TeV by LHAASO telescope). The emission properties are puzzling: hard spectrum up to several TeV energy, with no signature of cut-off and hard slope of the intrinsic spectra ($\frac{dN_\gamma}{dE} \propto E^{-2}$).

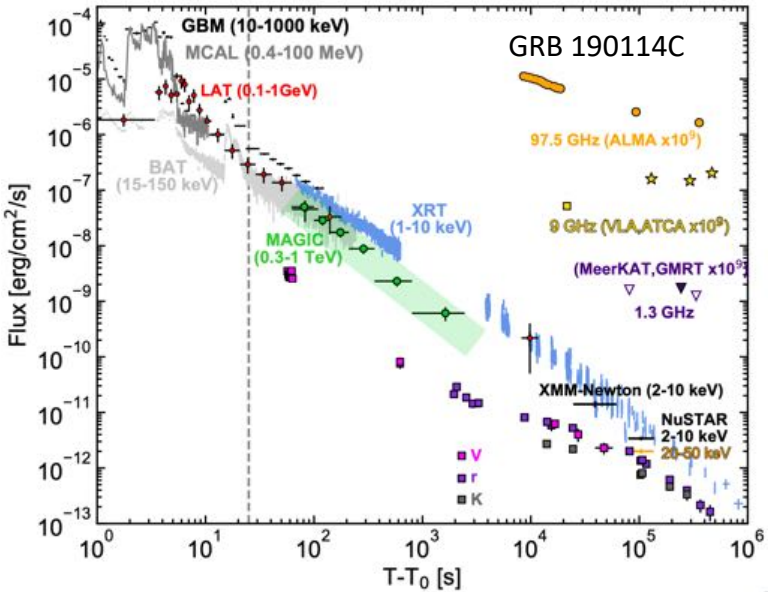

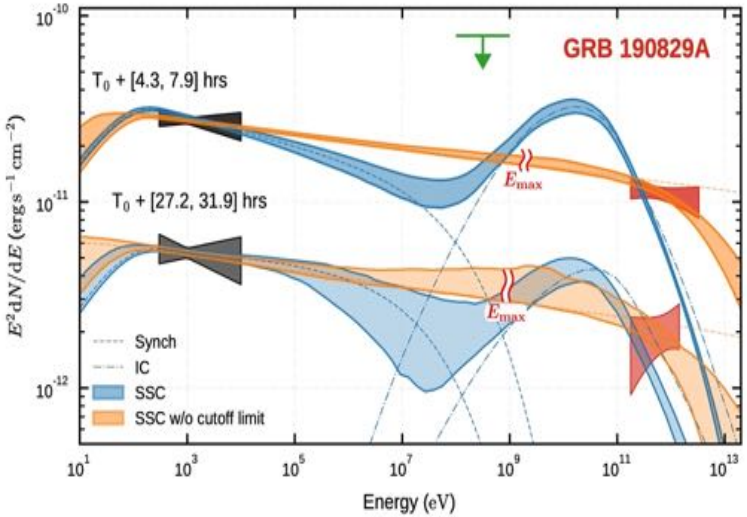

Multi-messenger transients

EM: electromagnetic

GW: gravitational wave

NU: neutrino

CR: cosmic ray

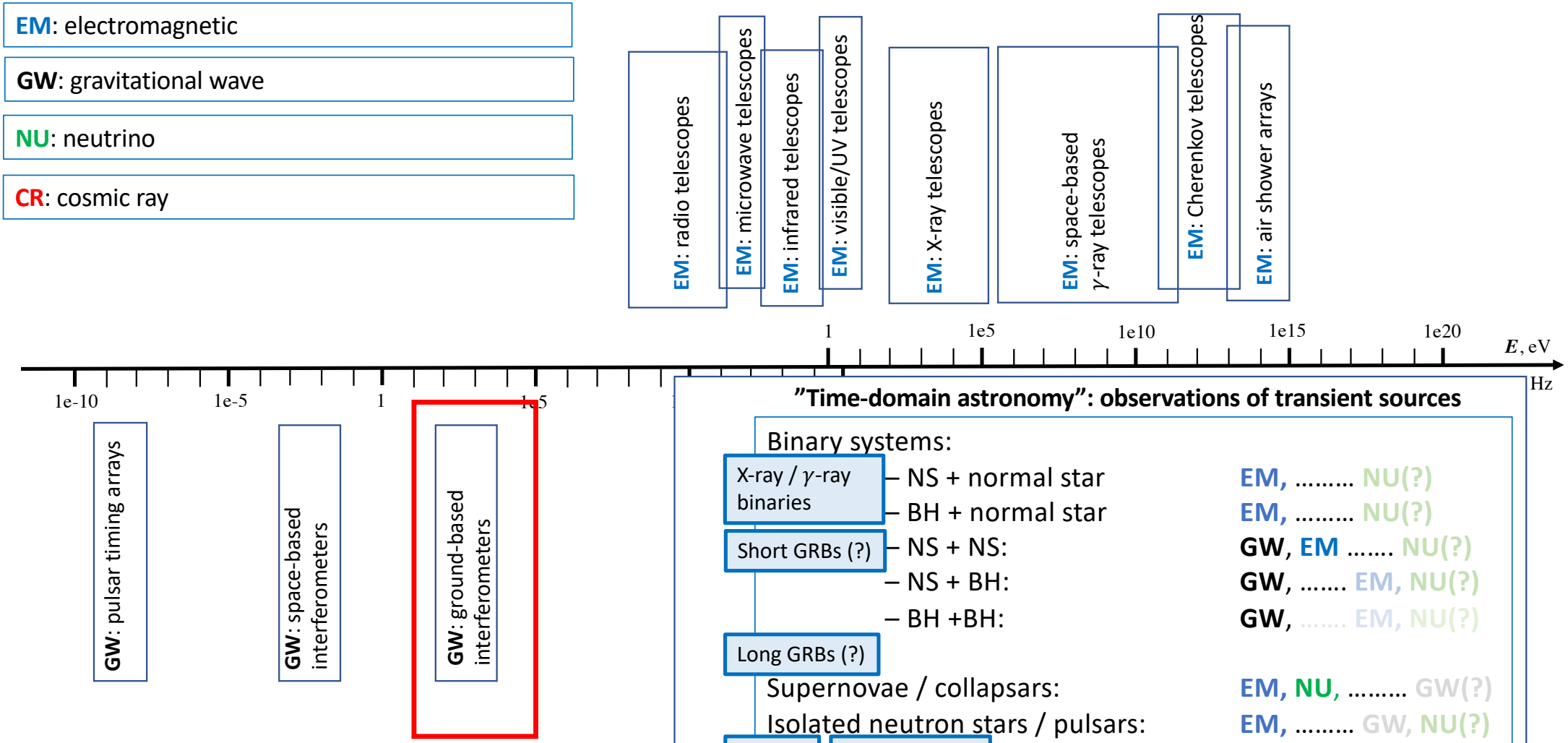

"Time-domain astronomy": observations of transient sources

Binary systems:

- X-ray / γ-ray binaries
  - NS + normal star — **EM,** …… NU(?)
  - BH + normal star — **EM,** …… NU(?)
- Short GRBs (?)
  - NS + NS: — **GW**, **EM** ……. NU(?)
  - NS + BH: — **GW**, ……. EM, NU(?)
  - BH +BH: — **GW**, ……. EM, NU(?)
- Long GRBs (?)

Supernovae / collapsars: — **EM, NU,** …… GW(?)

Isolated neutron stars / pulsars: — **EM,** …… GW, NU(?)

- FRBs(?)
- Short GRBs (?)

Gravitational wave detectors

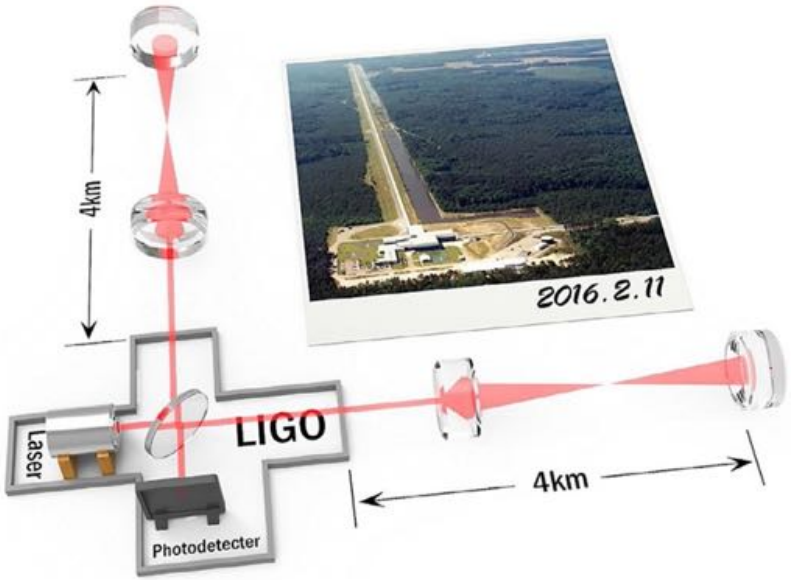

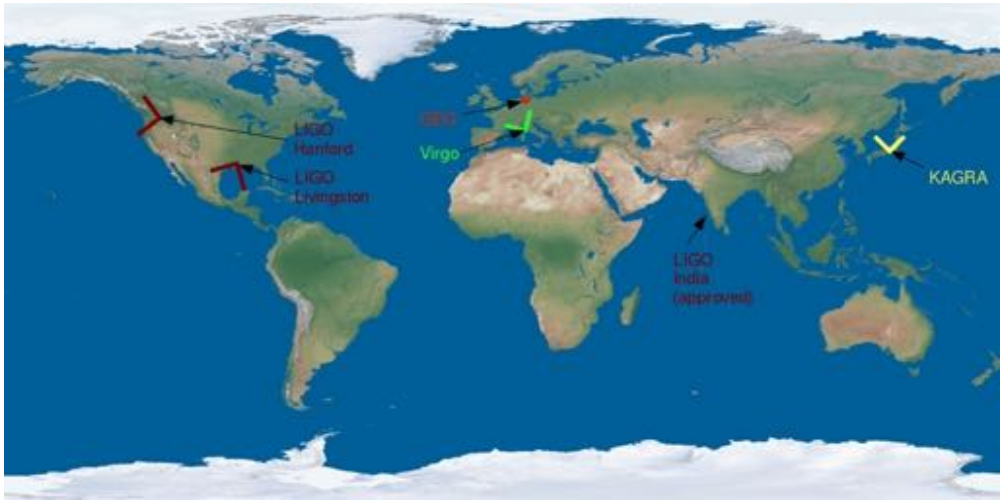

Passage of gravitational waves affects the propagation time of laser beam in the arms of an interferometer. Measurement of interference pattern variability allows to detect gravitational waves in the kHz range with km-scale interferometers and down to mHz with 10^9 cm long arms.

A network of kilo-Hertz gravitational wave detectors (LIGO, VIRGO, KAGRA) has been installed across the Globe over the last decade. Next generation project (Einstein Telescope) is planned for 2030th.

A space-based interferometer LISA is planned to be launched in 2030th.

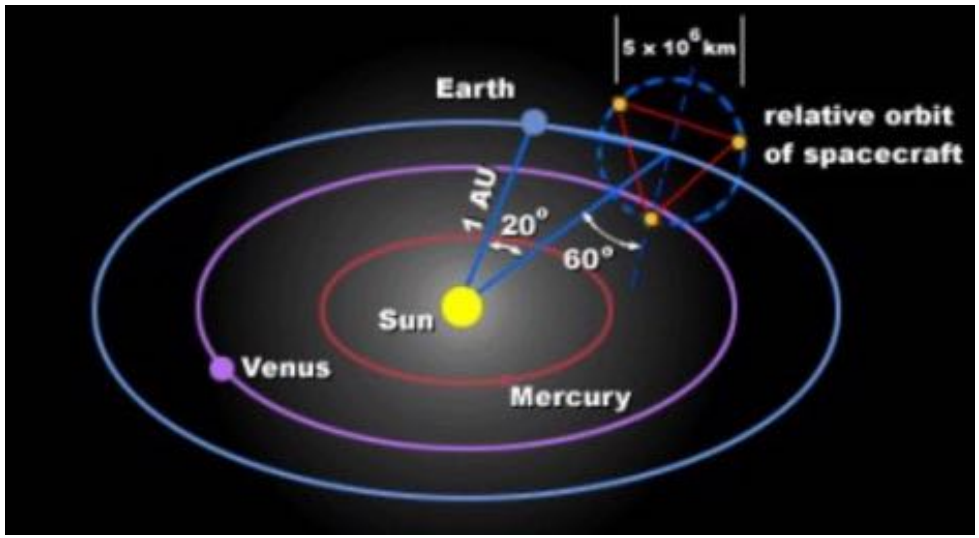

kHz gravitational wave sources

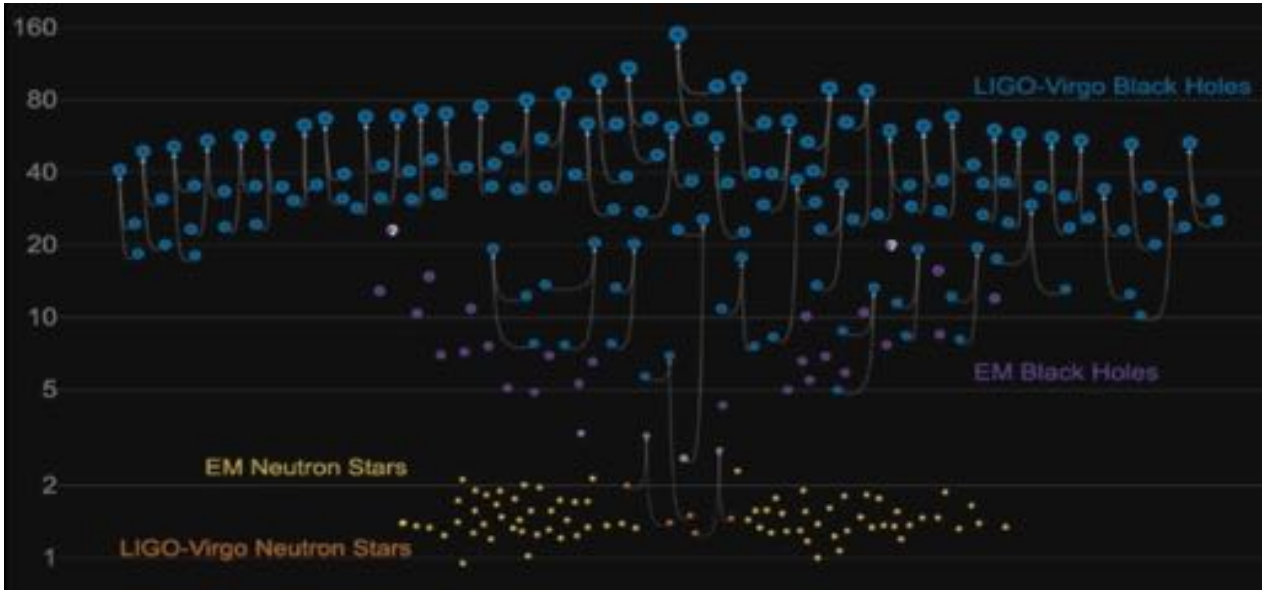

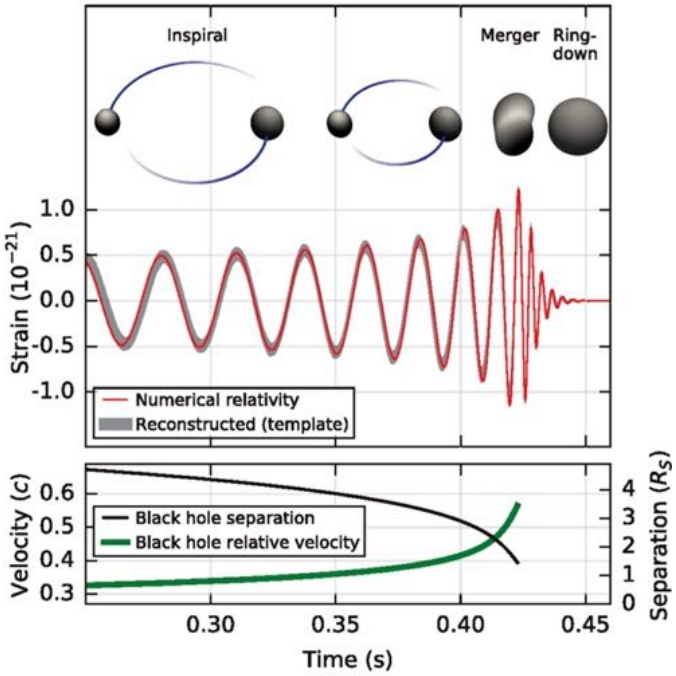

Period of rotation along an orbit at a distance R around a star of the mass M is

$$P = \sqrt{\frac{2\pi\, R^3}{G_N M}} \simeq 5 \left[\frac{M}{10^1 M_\odot}\right]^{-\frac{1}{2}} \left[\frac{R}{10^7\ \mathrm{cm}}\right]^{\frac{3}{2}}\ \mathrm{ms}$$

Binary systems with neutron stars or stellar mass black holes can have binary separation distances down to the size of the objects $R \sim 10\ \mathrm{km}$ and have binary rotation periods in the millisecond range.

Close binaries loose energy via gravitational radiation, in a catastrophic way for the close binary neutron stars and black holes.

A sample of $\sim 10^2$ compact object merger events has been detected in three runs (O1, O2, O3) of LIGO-VIRGO detectors. Most are binary black hole mergers, with black hole masses reaching 100 solar masses.

kHz gravitational wave sources

BH-NS mergers: GW200105 GW200115. Electromagnetic emission can arise because the neutron star can be tidally disrupted before merging with the black hole. This happens if the variation of black hole gravitational potential across the neutron star is larger than the gravitational potential of the neutron star itself:

$$\frac{\Delta U}{U} \sim \frac{G M_{BH} R_{NS}}{R_{BH}^2} \frac{R_{NS}}{G M_{NS}} \simeq 0.2 \left[\frac{M_{BH}}{5 M_{NS}}\right] \left[\frac{R_{NS}}{R_{BH}}\right]^2$$

This was not the case for the two mergers, no multi-messenger signal from them.

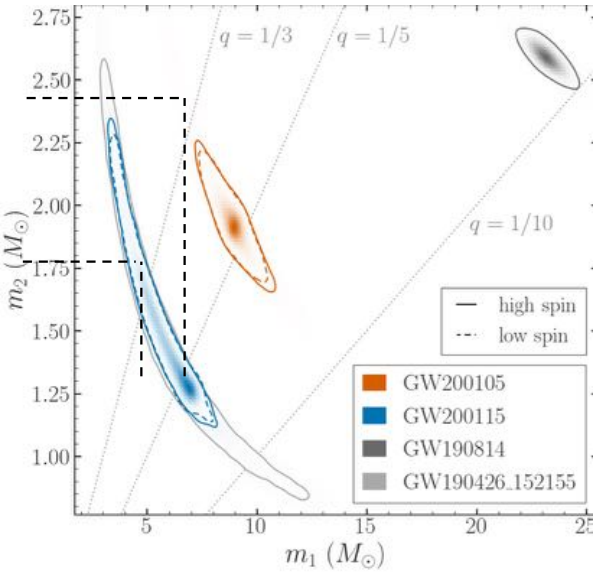

NS-NS mergers: GW170817 GW190425. Only GW170817 was detected in ”multi-messenger” mode. GW190425 has no detectable electromagnetic counterpart, as expected (distance 160 Mpc,4 times further than GW170817).

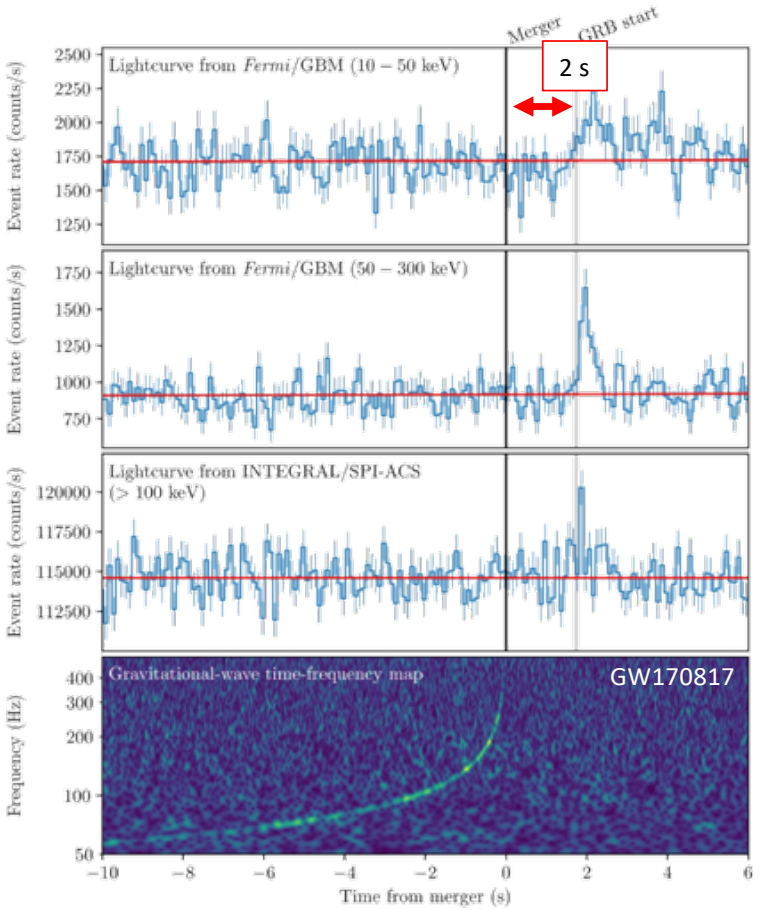

GW170817

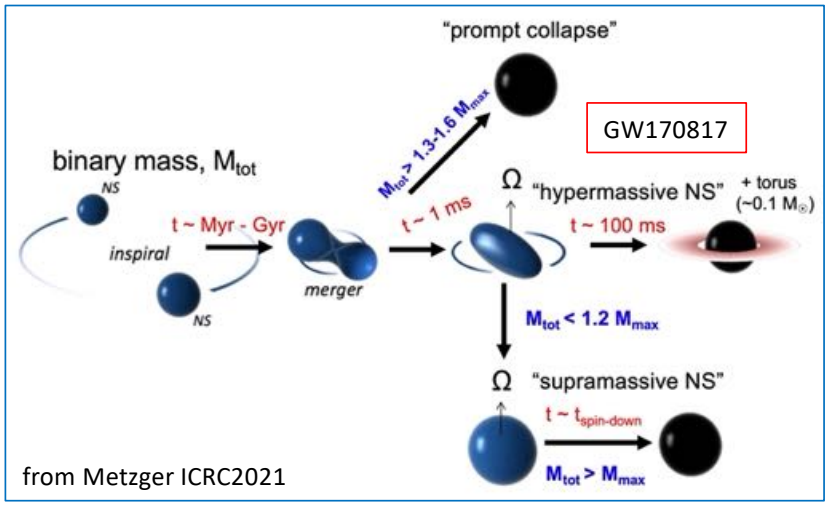

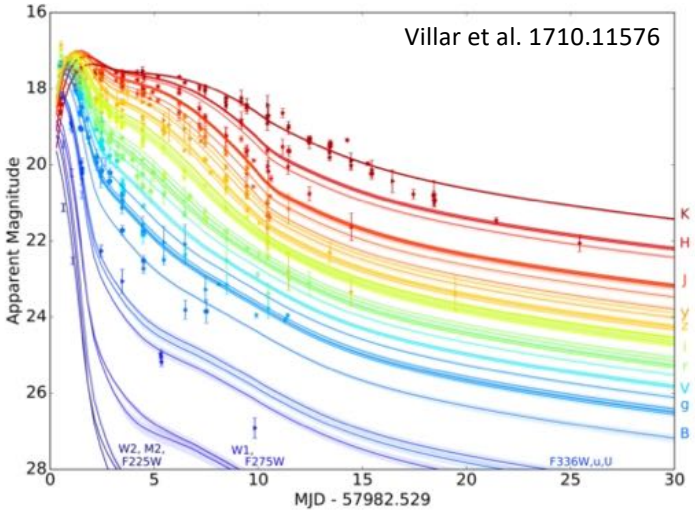

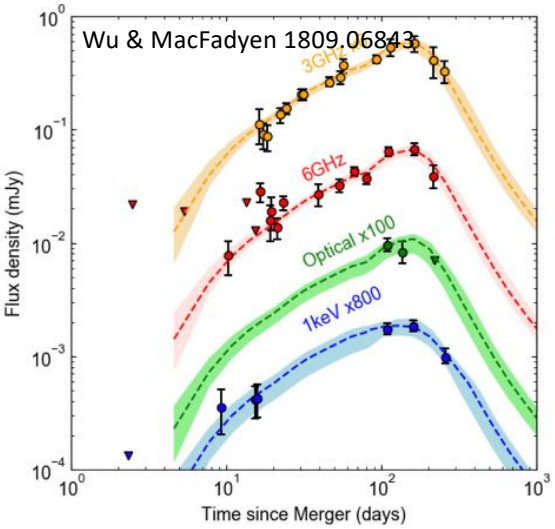

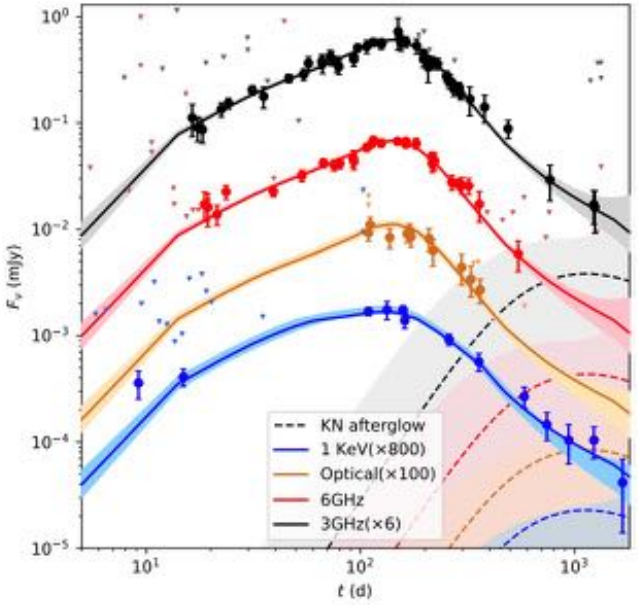

GW170817 neutron star merger event has

- produced short GRB like γ-ray emission
- X-ray and radio afterglow consistent with off-axis (20^o) GRB jet
- thermal optical emission consistent with models of kilonova powered by radioactive decays

5 years since the merger event, GW 170817 kilonova, AT2017gfo is still visible in X-rays and radio.

kHz gravitational wave astronomy and fundamental physics

Straightforward test of “speed of light vs. speed of gravity”: $\Delta v/c \leq 10^{-15}$

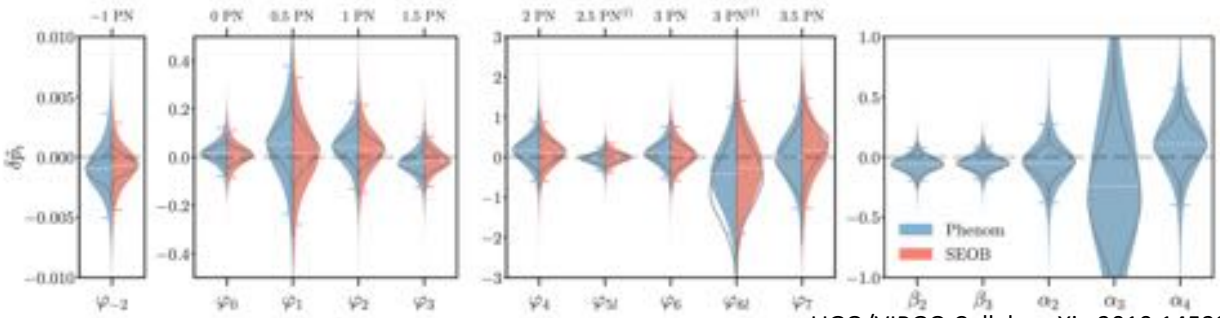

LIGO/VIRGO Collab. arXiv:2010.14529

Constraints on post-Newtonian parameters from O2 run

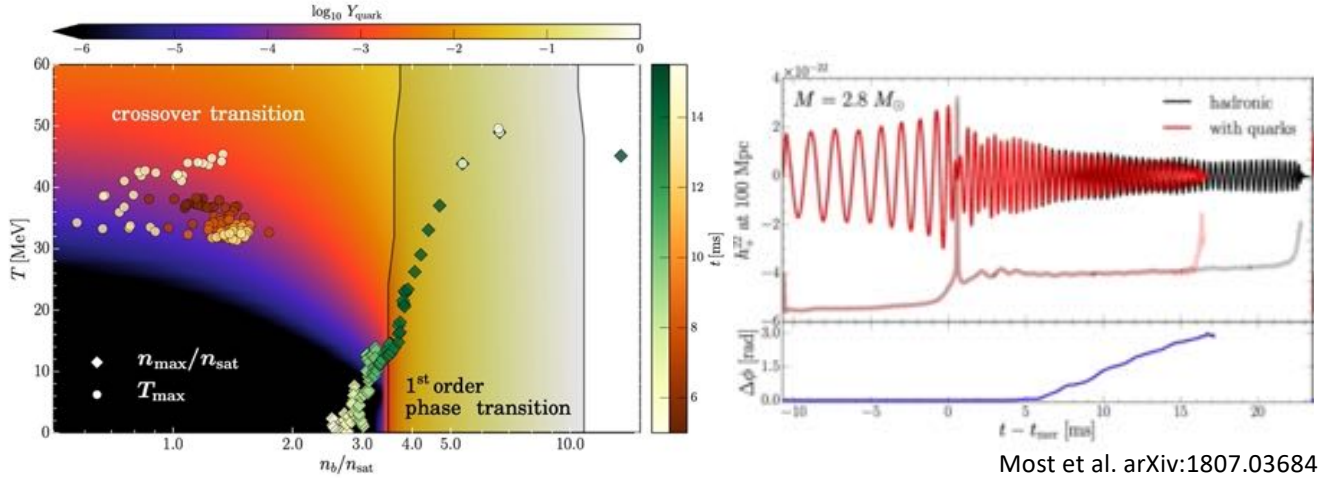

Most et al. arXiv:1807.03684

Post-merger “ring-down” phase waveform is sensitive to possible QCD phase transition that may occur in the collapsing merger object.

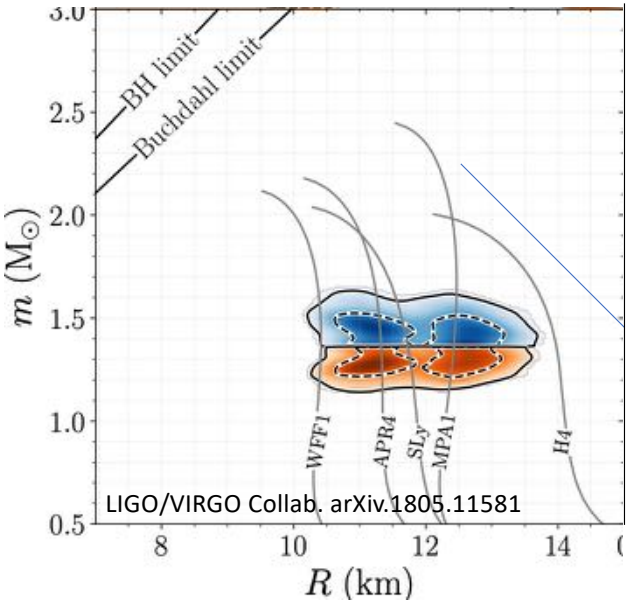

LIGO/VIRGO Collab. arXiv:1805.11581

Tidal deformation of the two inspiraling neutral stars influences the shape of the GW signal. This can be used to constrain the equation of state of nuclear matter inside the neutron stars.

Nano-Hz gravitational waves with Pular Timing Arrays (PTA)

Passage of gravitational waves distorts the pattern of arrival time of pulsars by changing the distance to the sources. Measurement of timing residuals allows to detect gravitational waves with extremely low frequency, down to nHz (low frequency end is determined by the duration of timing monitoring, currently ~ 10 yr scale).

Pulsar timing arrays can detect gravitational waves from binary supermassive black holes forming at galaxy mergers:

$$P = \sqrt{\frac{2\pi\, R^3}{G_N M}} \simeq 5 \left[\frac{M}{10^7 M_\odot}\right]^{-\frac{1}{2}} \left[\frac{R}{10^{16}\ \mathrm{cm}}\right]^{\frac{3}{2}} \mathrm{yr}; \quad \nu = P^{-1}$$

All PTA collaborations (NANOGrav, EPTA, PPTA, collaborating within “International” PTA, IPTA) have reported evidence for “common stochastic process” detectable in timing residuals of many pulsars. This is consistent with existence of stochastic gravitational wave background, but the definitive test, measurement of the angular dependence of cross-correlation power (Hellings-Downs) is not precise enough.

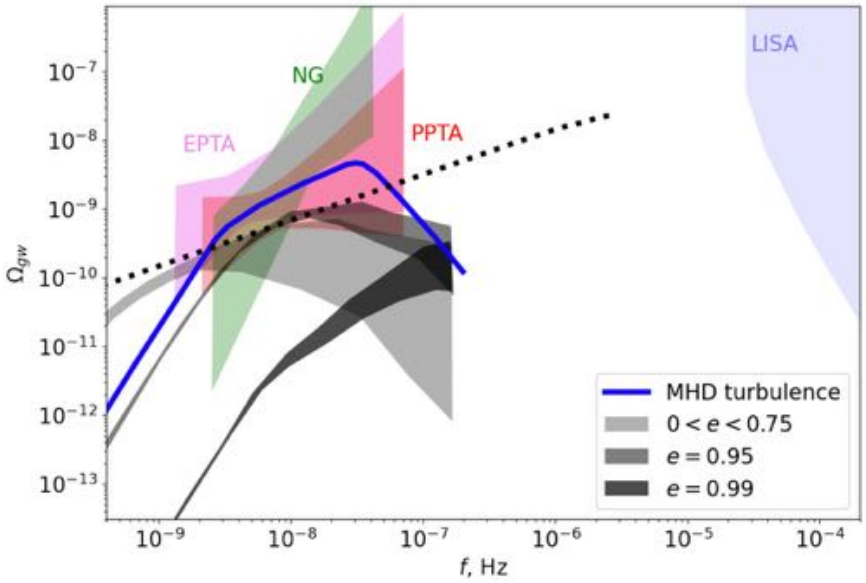

nHz gravitational waves and fundamental physics?

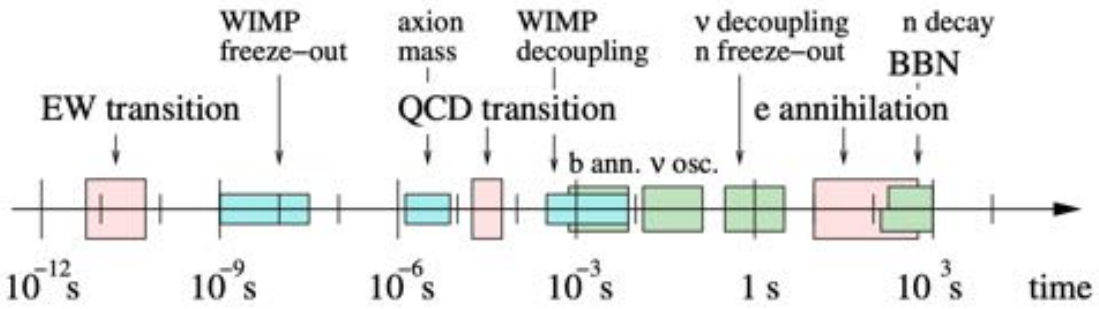

Within the Standard Model the Electroweak and QCD transitions are expected to cross-overs.

Detection of relic SGWB in nHz-mHz range would constitute an evidence for beyond-Standard-Model process.

1st-order phase transition also generates magnetic field that survives till present epoch as Intergalactic Magnetic Field (IGMF). This field can be measured in the near future via its effect on propagation of gamma-rays, and/or its effect on polarized radio signals and ultra-high-energy cosmic rays and/or its effect on Cosmic Microwave Background.

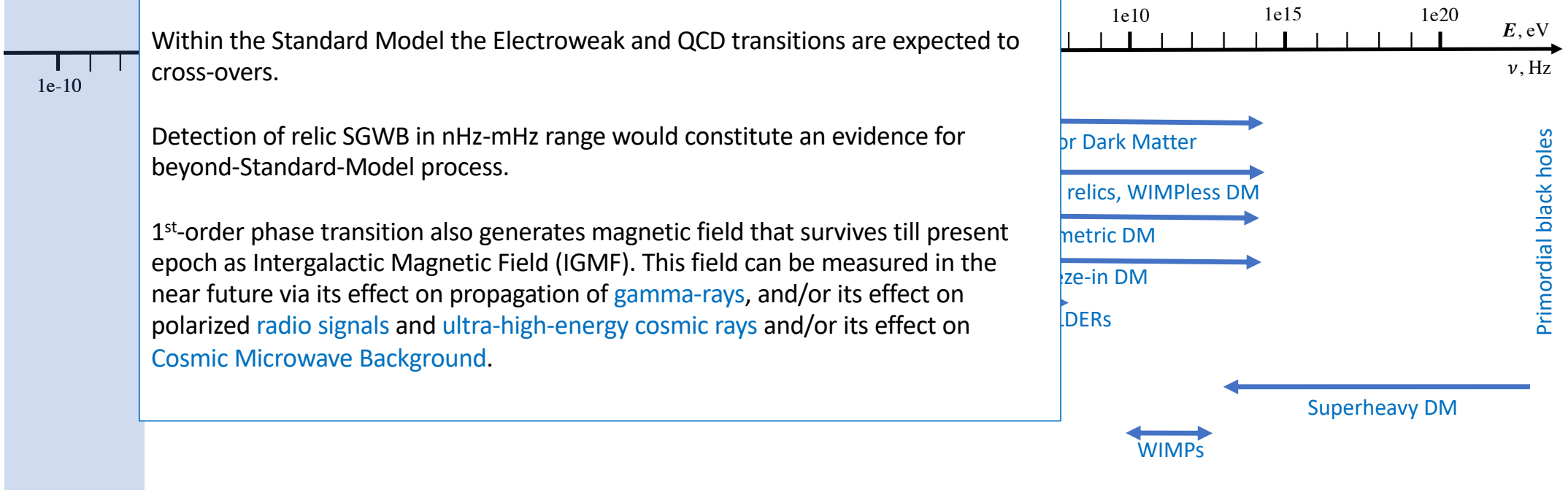

Neutrino astronomy

EM: electromagnetic

GW: gravitational wave

NU: neutrino

CR: cosmic ray

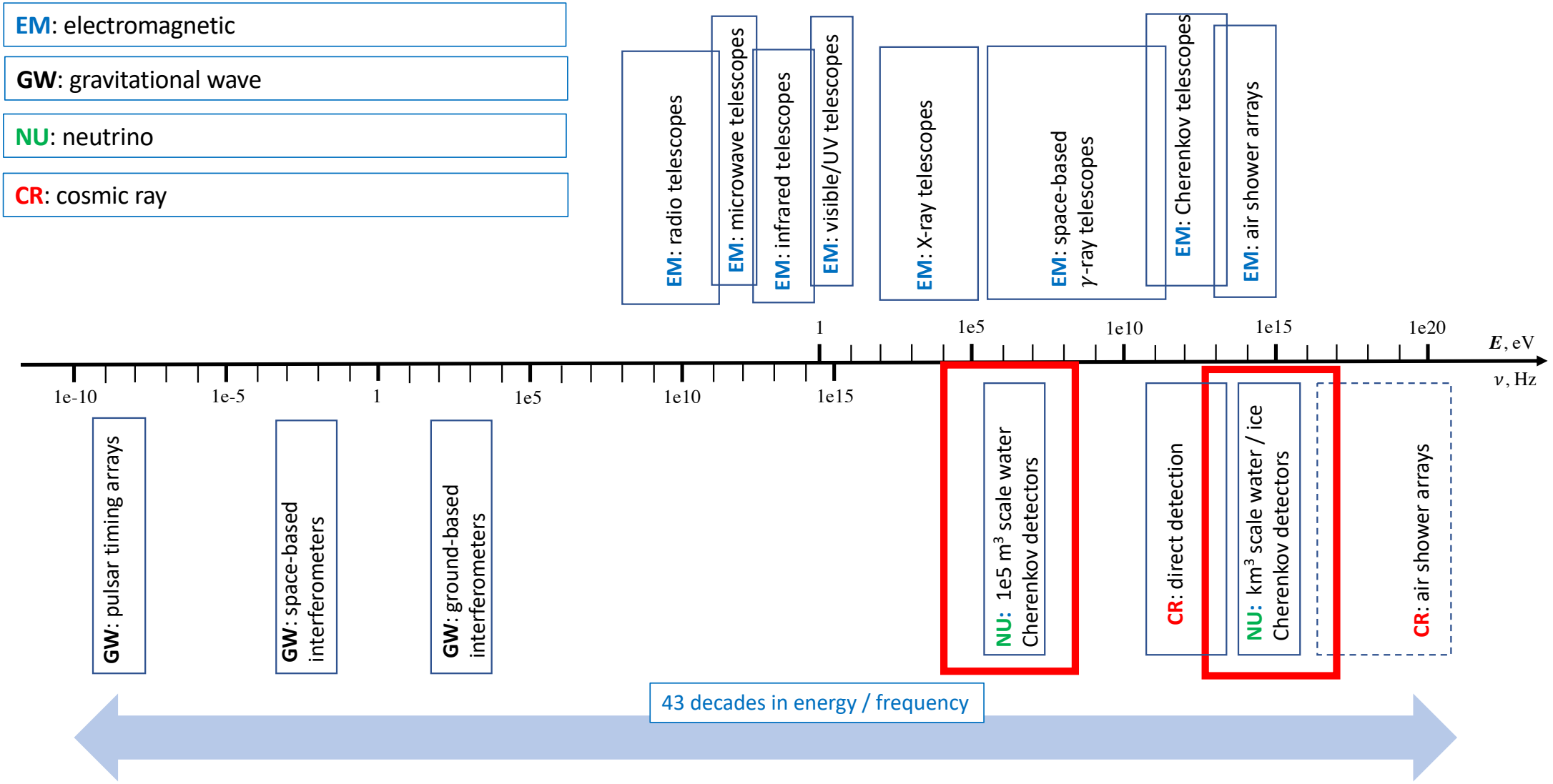

”low-energy” neutrino astronomy

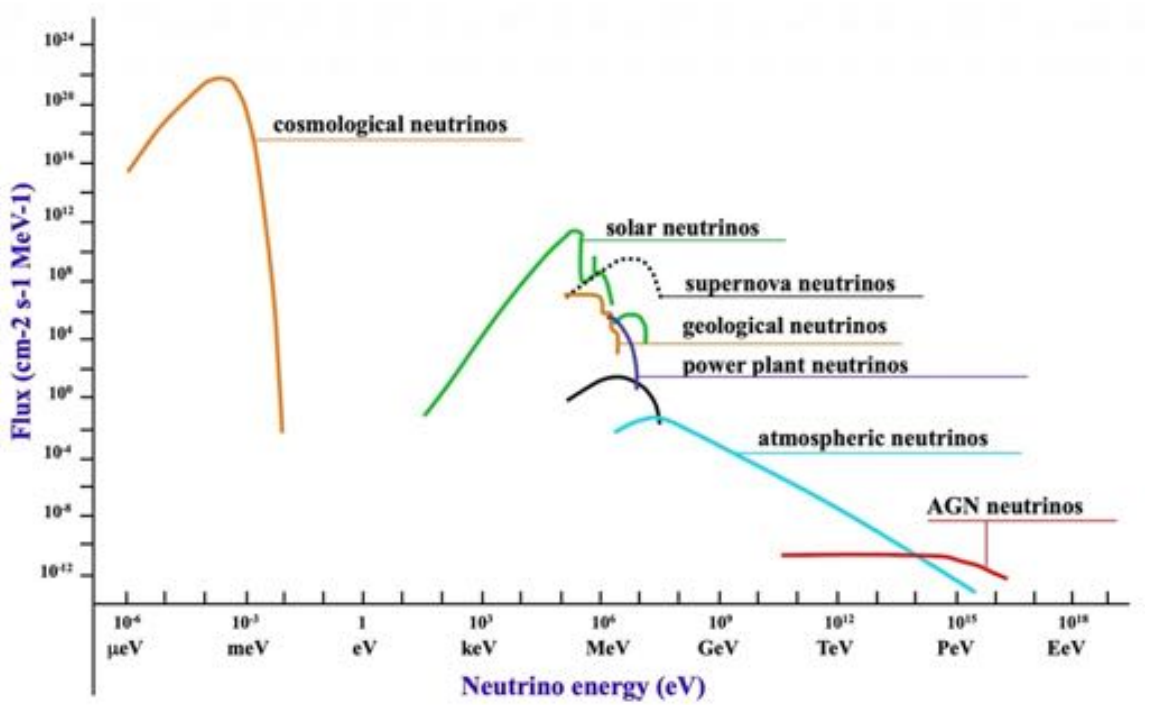

Stars, including the Sun, produce neutrinos in nuclear reactions in their cores. Solar neutrinos are detected by detectors like Super-Kamiokande, SNO.

Gravitational collapse of cores of massive stars and formation of neutron stars leads to production of neutrinos. Neutrino emission is the only mechanism that dissipates gravitational energy liberated by the gravitational collapse, of the order of

$$E_{grav} \sim \frac{GM_{NS}^2}{R_{NS}} \sim 10^{53}\ \mathrm{erg}$$

”low-energy” neutrino astronomy

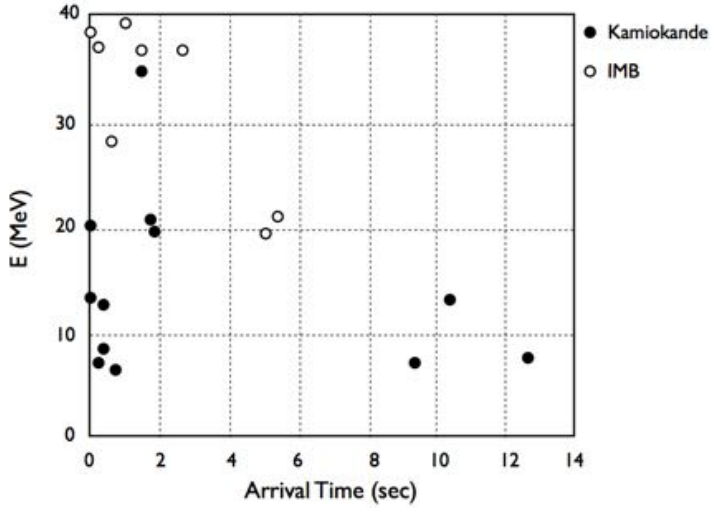

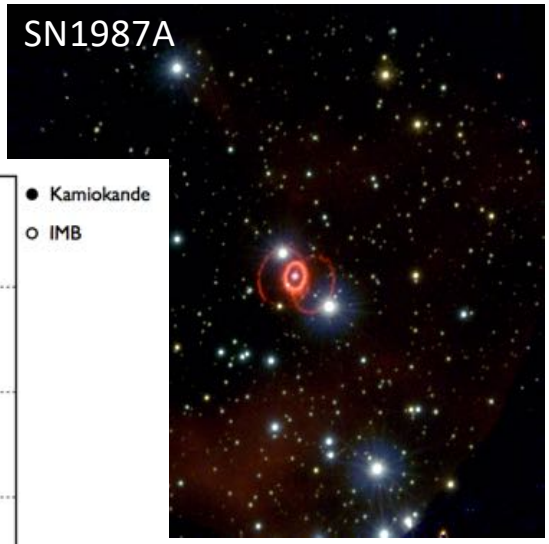

Gravitational collapse of cores of massive stars and formation of neutron stars leads to production of neutrinos. Neutrino emission is the only mechanism that dissipates gravitational energy liberated by the gravitational collapse, of the order of

$$E_{grav} \sim \frac{GM_{NS}^2}{R_{NS}} \sim 10^{53}\ \text{erg}$$

Neutrinos from the gravitational collapse, followed by supernova explosion, were observed once, from SN1987A, in the Large Magellanic Cloud (a satellite galaxy of the Milky Way).

The rate of supernova explosion in the Milky Way is 2-3 per century….. the neutrino signal from a supernova lasts ~ 10 s. A network of neutrino detectors monitors the neutrino flux with nearly 100% duty cycle (SNEWS, Supernova Early Warning System: Super-Kamiokande, SNO+, KamLAND, NOvA, XENONnT, LZ, PandaX-4T, KM3NET, ICECUBE.

Very-high energy neutrino astronomy

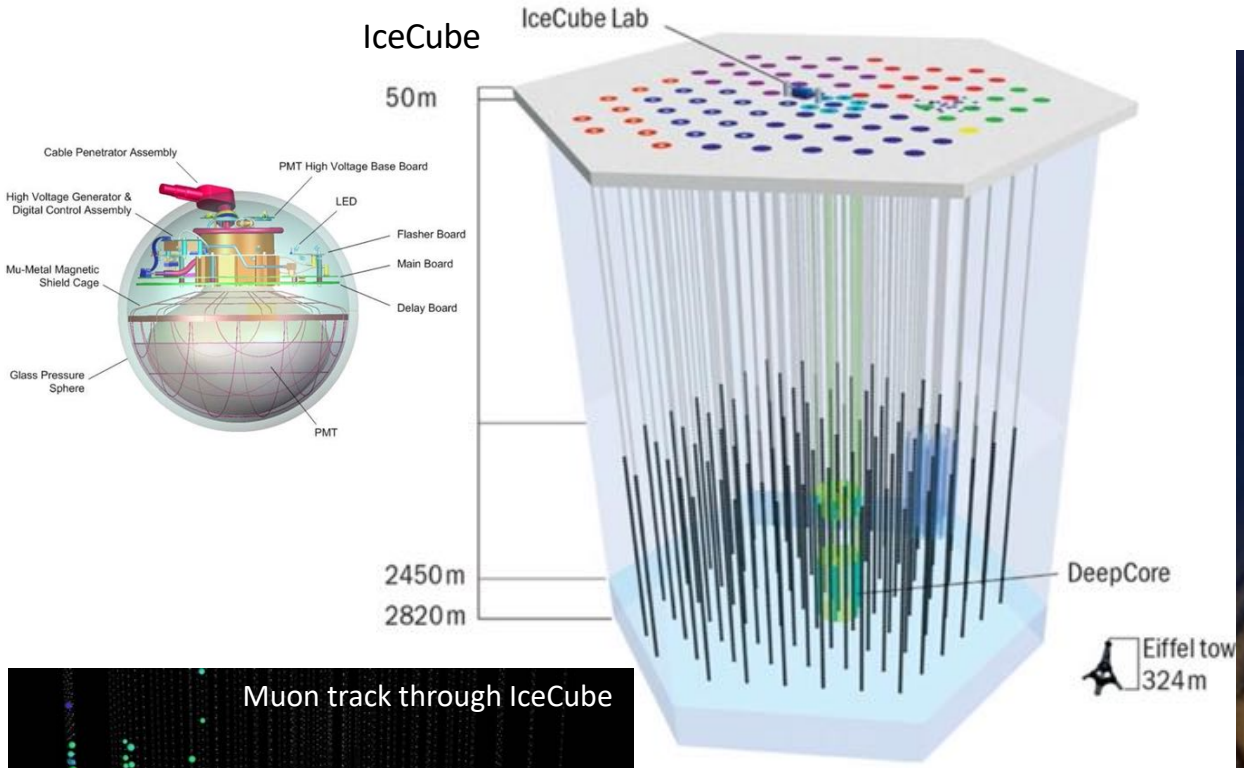

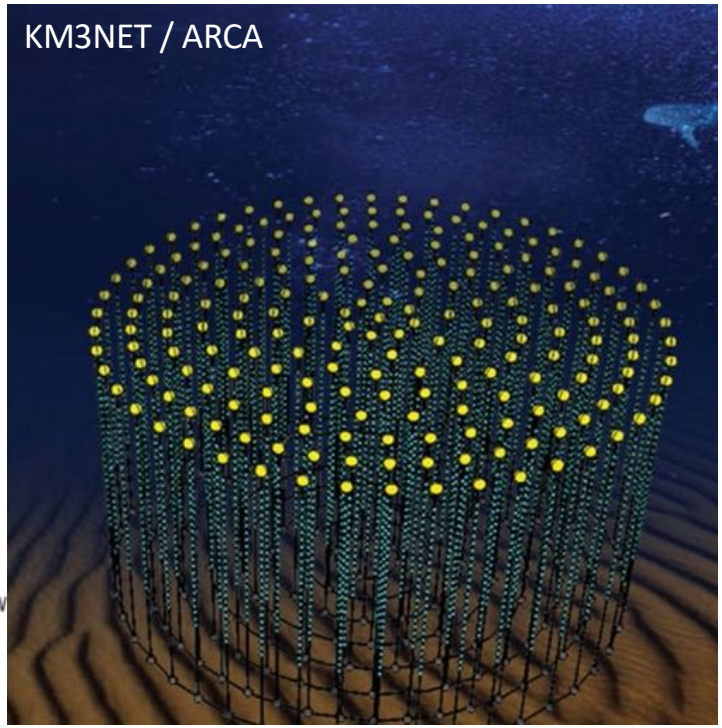

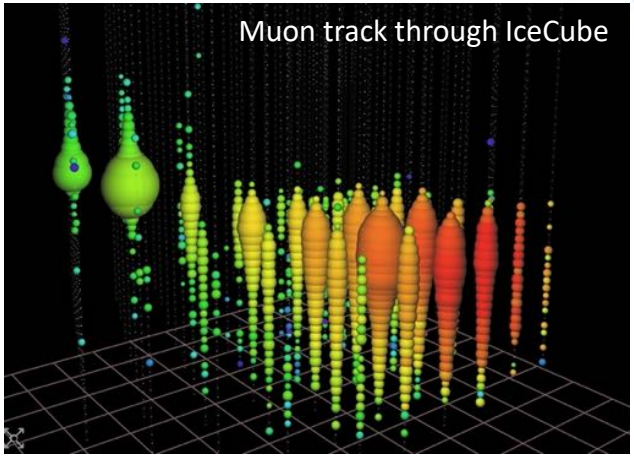

Km^3 scale detectors, arrays of large photomultiplier assemplies in ice (IceCube) or water (ANTARES, KM3NET, Baikal-GVD) are used for detection of neutrinos in the 100 GeV – 10 PeV energy range.

Muon neutrinos can be detected via “tracks” produced by muons from charged current interactions. Electron and tau neutrinos are detectable as “cascade” events from CC interacitons. All flavours are detectable as cascades from NC interactions.

Very-high energy neutrino astronomy

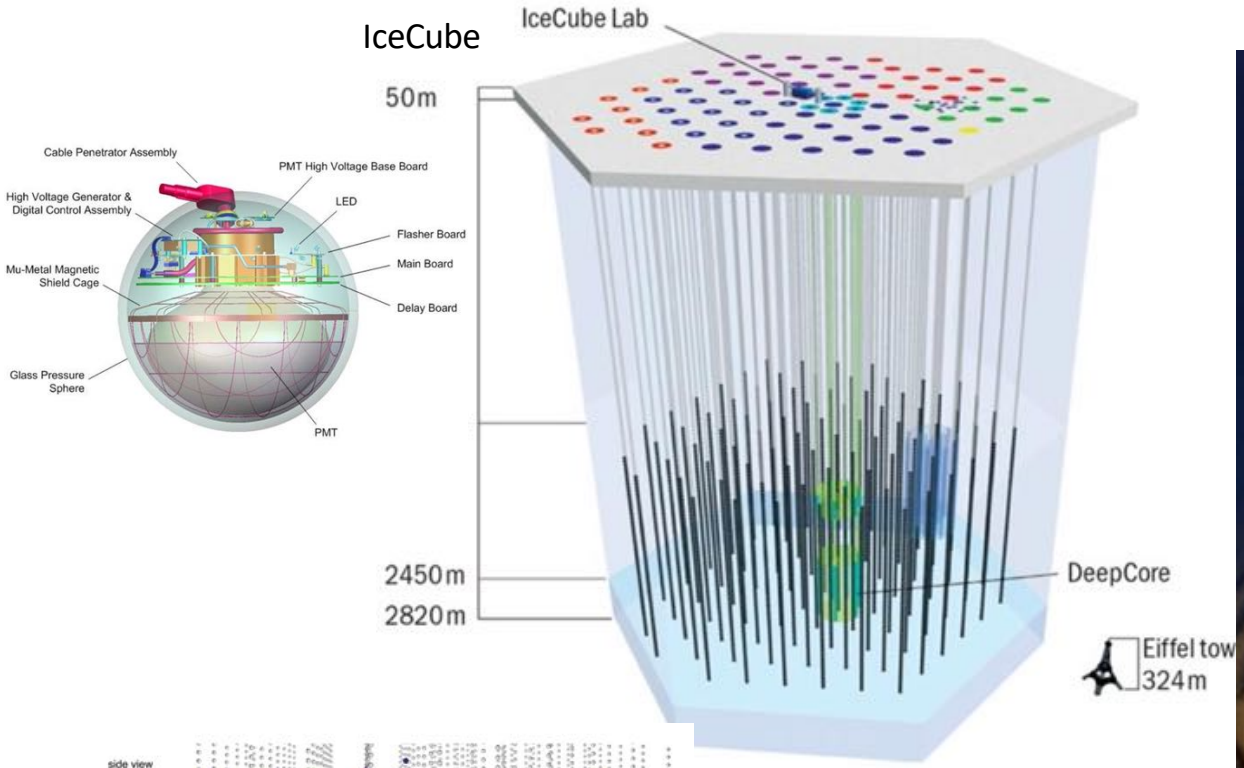

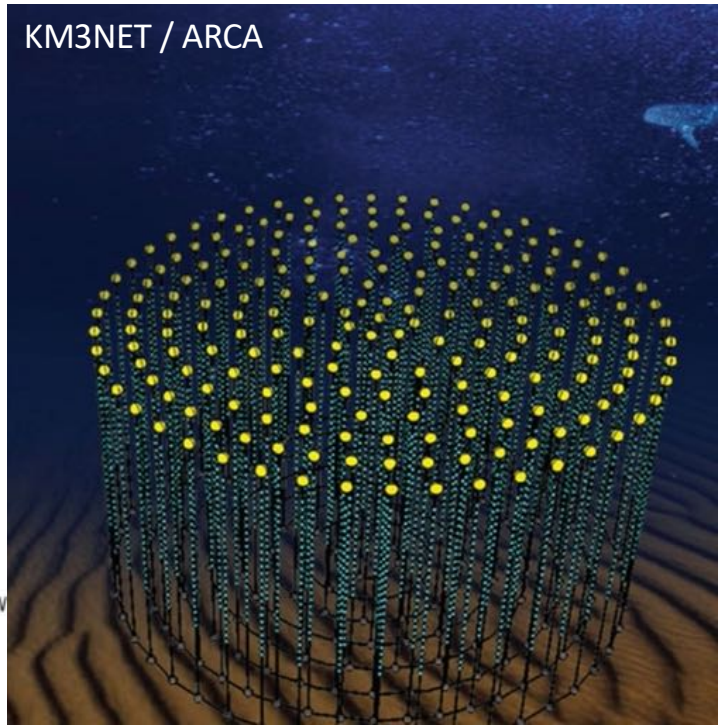

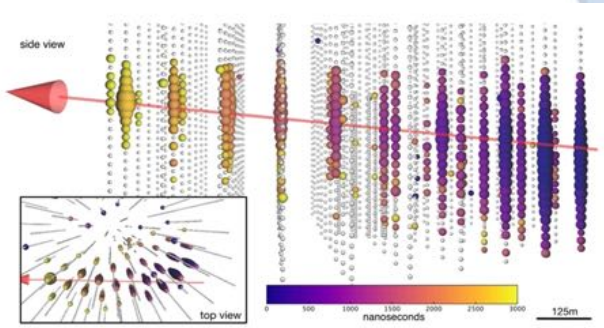

"Track" detection channel is characterized by good angular resolution (better than 1°), but poor energy resolution (muons are produced and loose energy outside the detection volume before entering the detector).

"Cascade" events provide poor angular resolution (ten(s) of degrees in ice, several degrees in water), but good energy resolution (the events are contained in detector volume)

Astrophysical neutrino signal

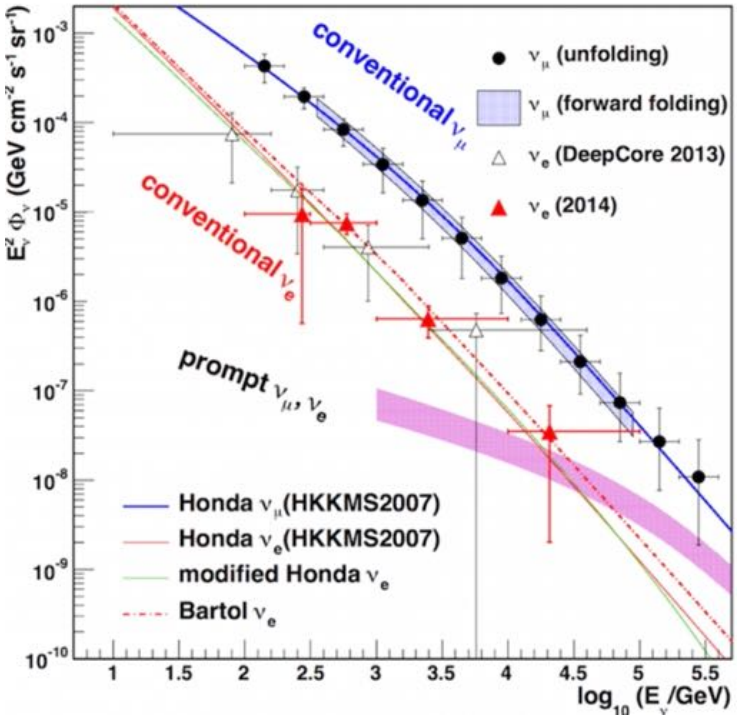

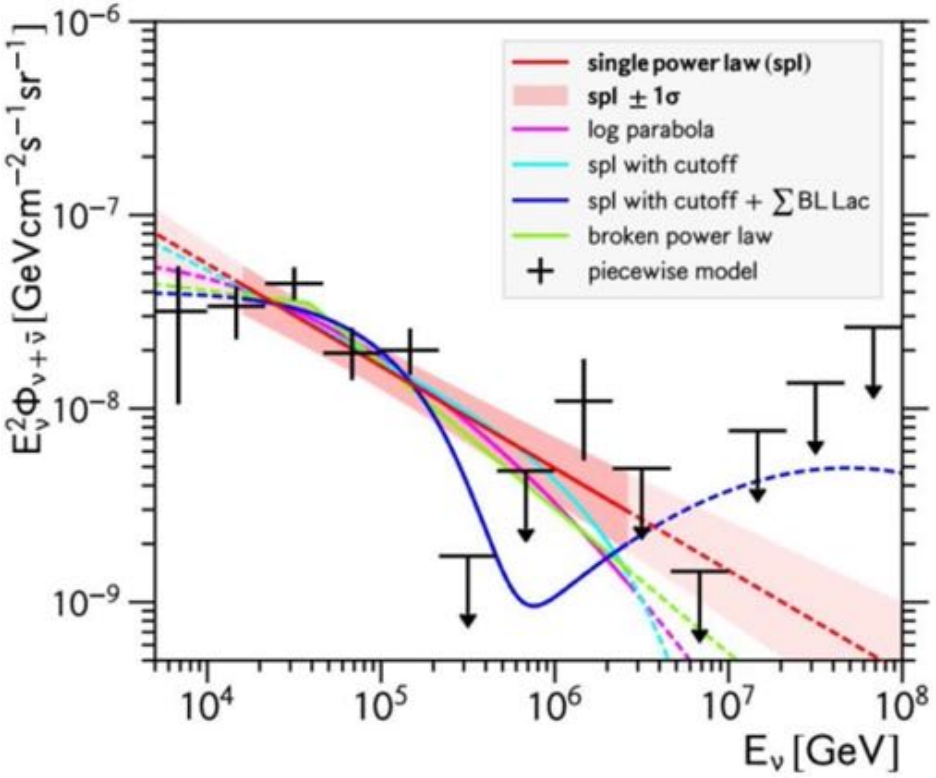

Astrophysical neutrino signal of uncertain origin (right) has been discovered by IceCube telescope. It is observed on top of the atmospheric neutrino background.

Astrophysical neutrinos in 10 TeV - 10 PeV range

Possible origin:

a) A contribution from cosmic ray interactions in the interstellar medium of the Milky Way
b) Extragalactic flux, e.g. from a population of AGN
c) "exotic" component like dark matter particle decays

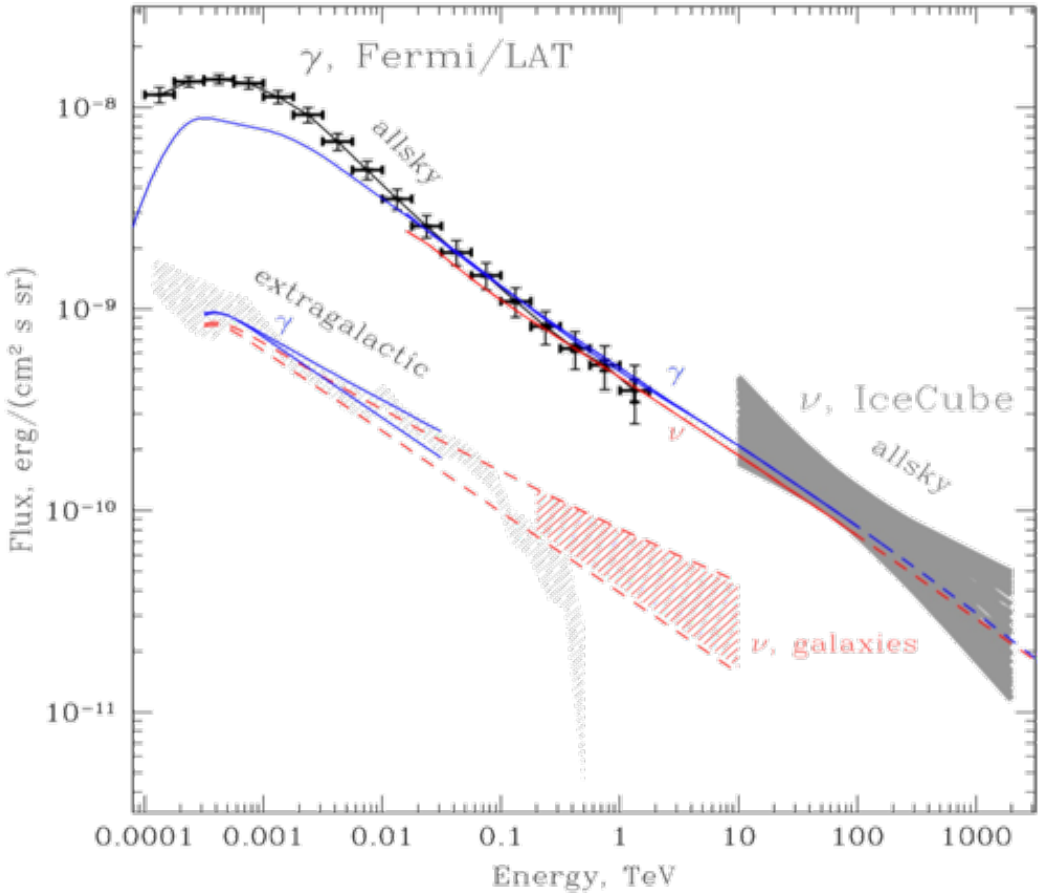

Neutrinos from AGN

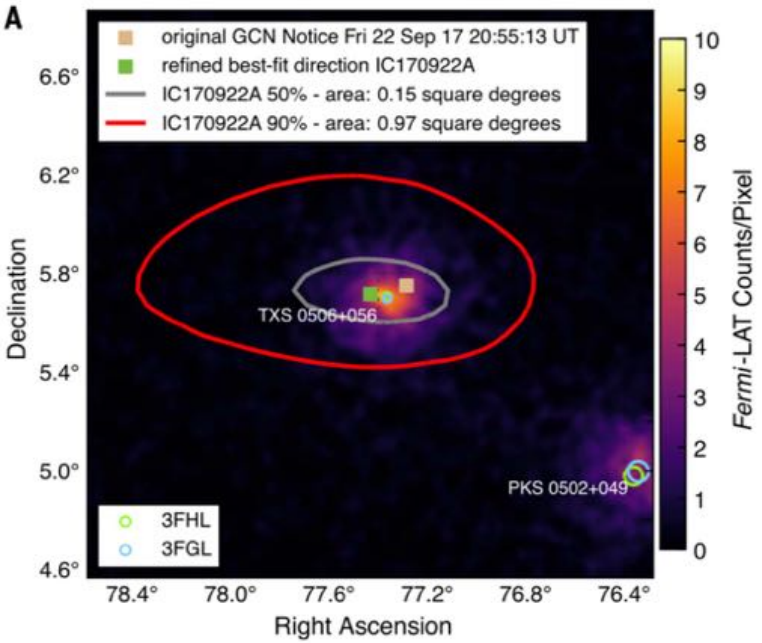

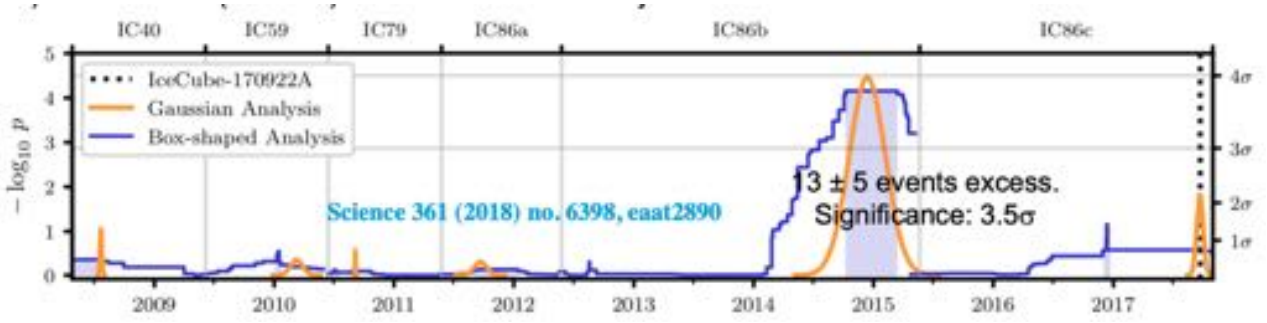

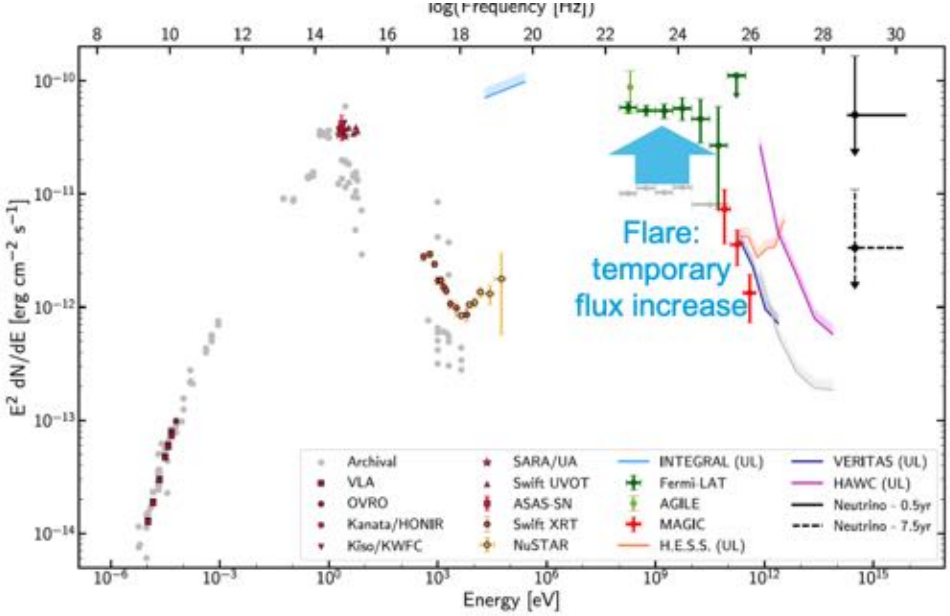

An evidence for neutrino arrival at the moment of a gamma-ray flare has been reported from TXS 0506+056, a distant “blazar” type AGN with powerful jet aligned along the line of sight.

An independent evidence for enhanced neutrino emission not accompanied by a gamma-ray flare has been reported by IceCube from the same source.

Neutrinos from AGN

An evidence for persistent neutrino signal from NGC 1068 a nearby AGN of the type “Seyfert galaxy”, with weak jet and weak gamma-ray flux (perhaps from starburst activity unrelated to the jet emission).

…. Higher statistics neutrino data are needed for firm identification of neutrino sources and clarification of the origin of the astrophysical neutrino signal.

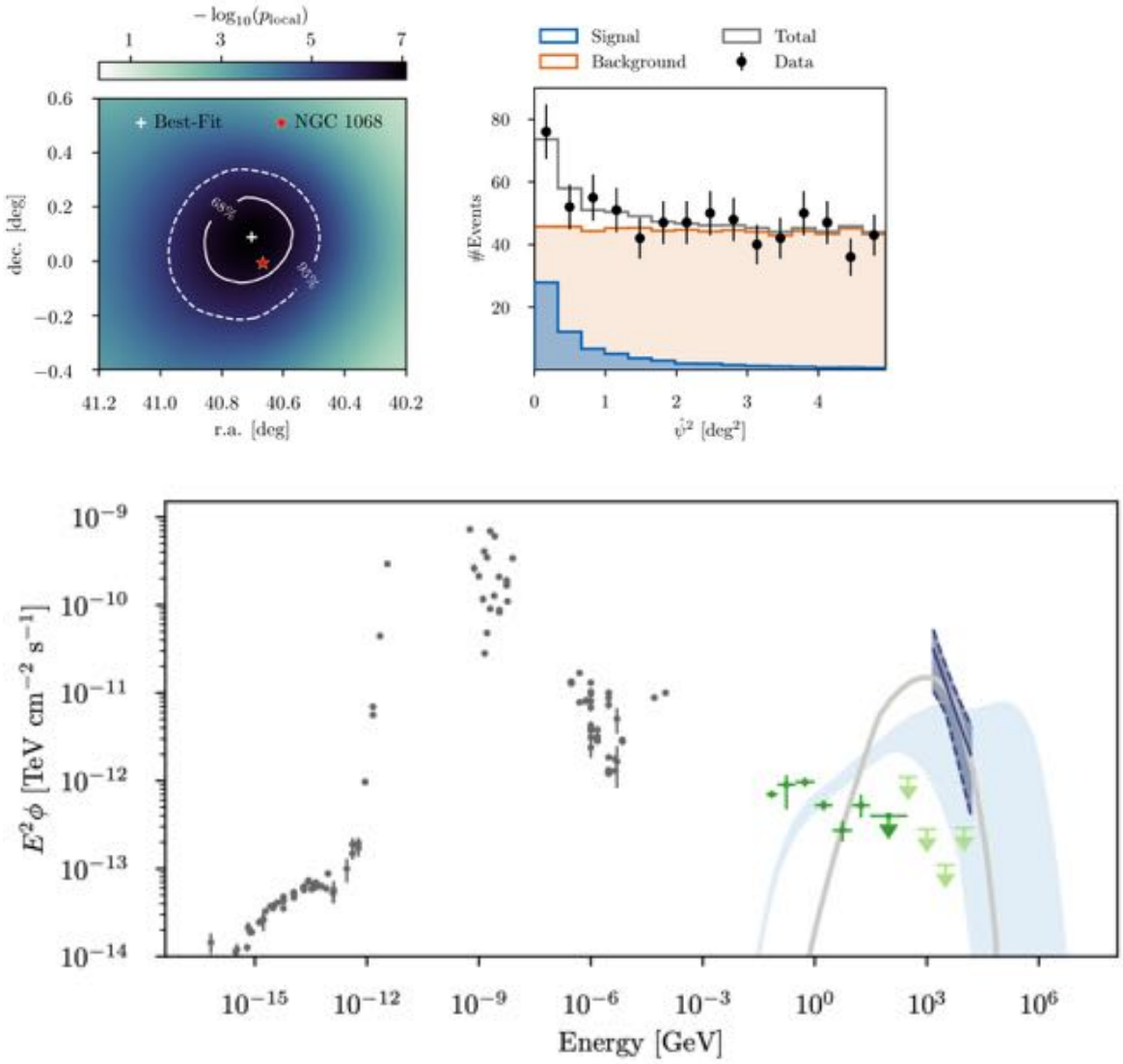

Next generation instruments (high-energy neutrinos)

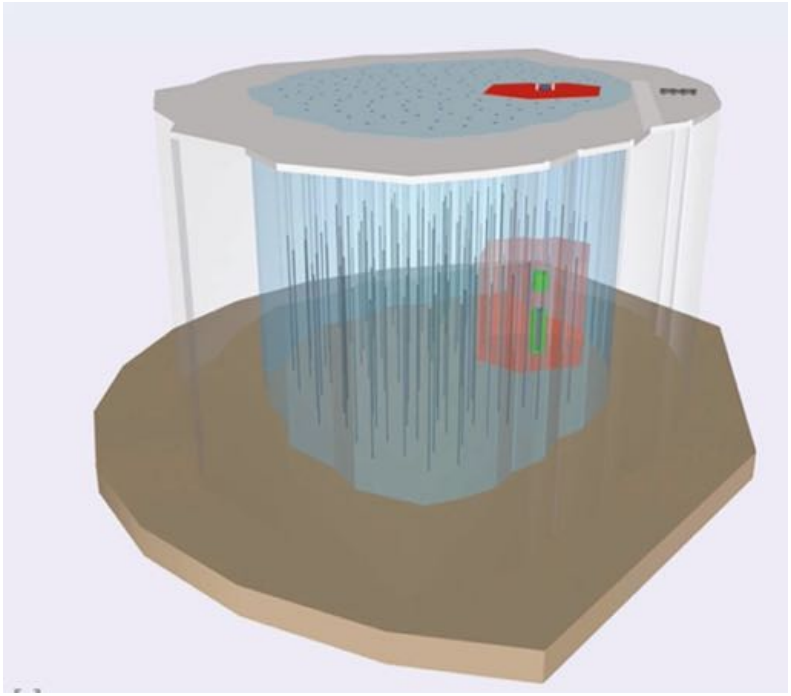

IceCube Gen-2, a 10 km^3 scale detector at IceCube site 2030th

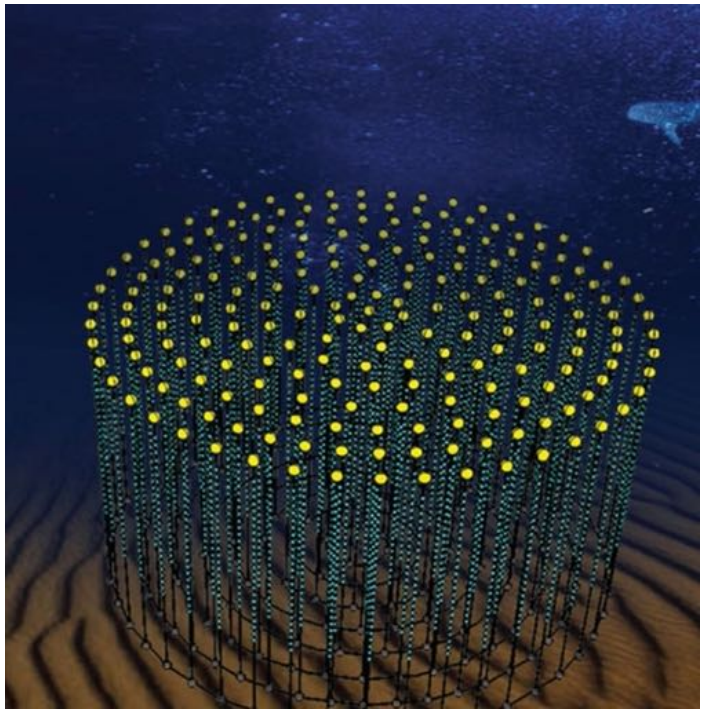

KM3NET / ARCA, a km^3 scale detector in Mediterranean (under construction)

Next generation instruments (gamma-rays)

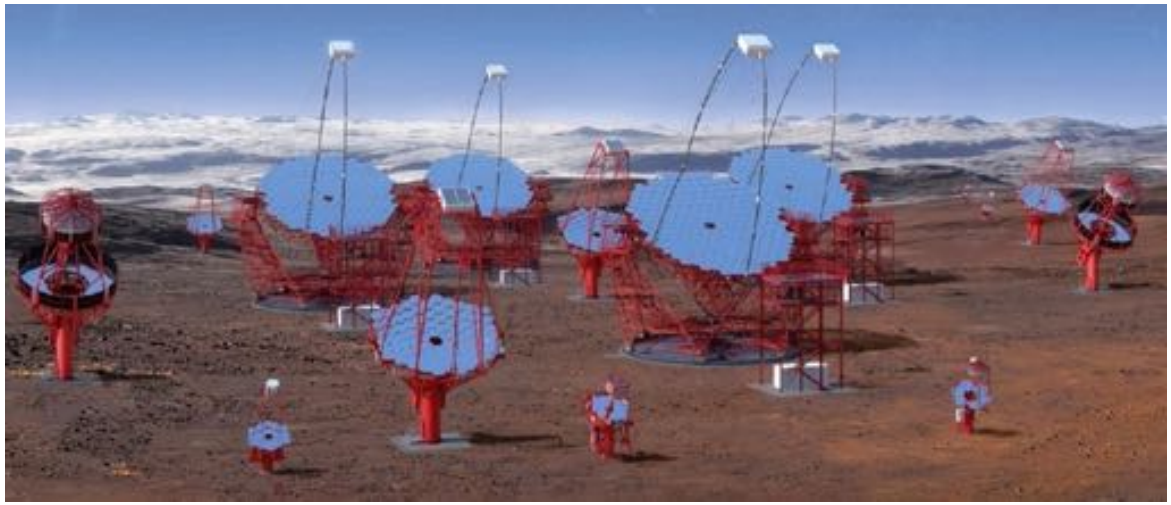

Cherenkov Telescope Array (CTA): IACT system on two sites (La Palma Canary island, Paranal, Chile), with km^2 scale effective collection areas (under construction)

Next generation instruments (cosmic rays, gamma-rays)

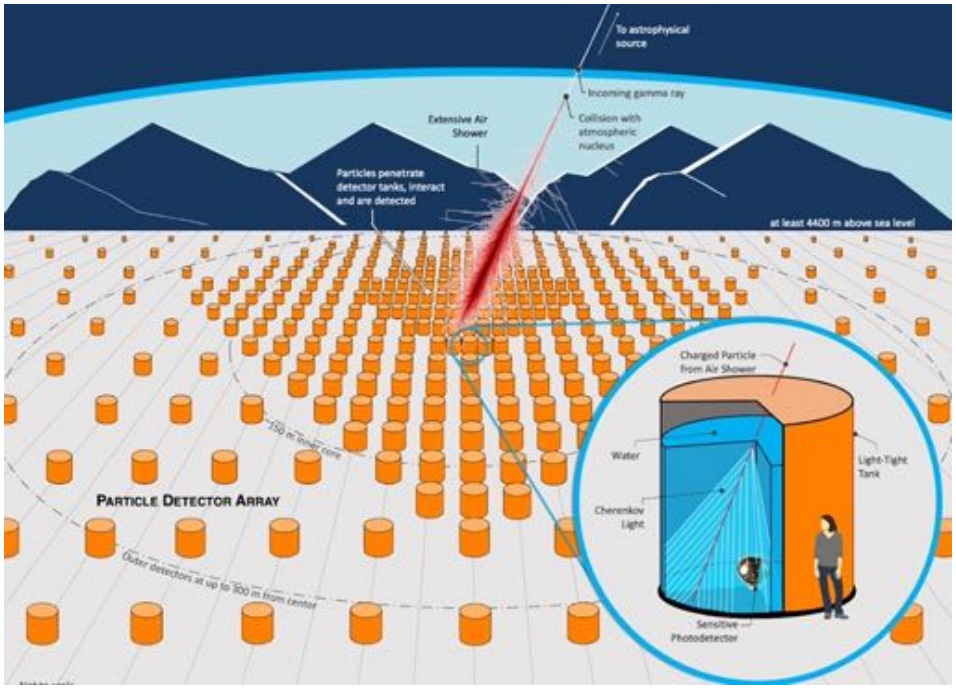

SWGO (Southern Water-Cherenkov Gamma-ray Observatory), an EAS array for PeV astronomy in Southern hemisphere (2030th).

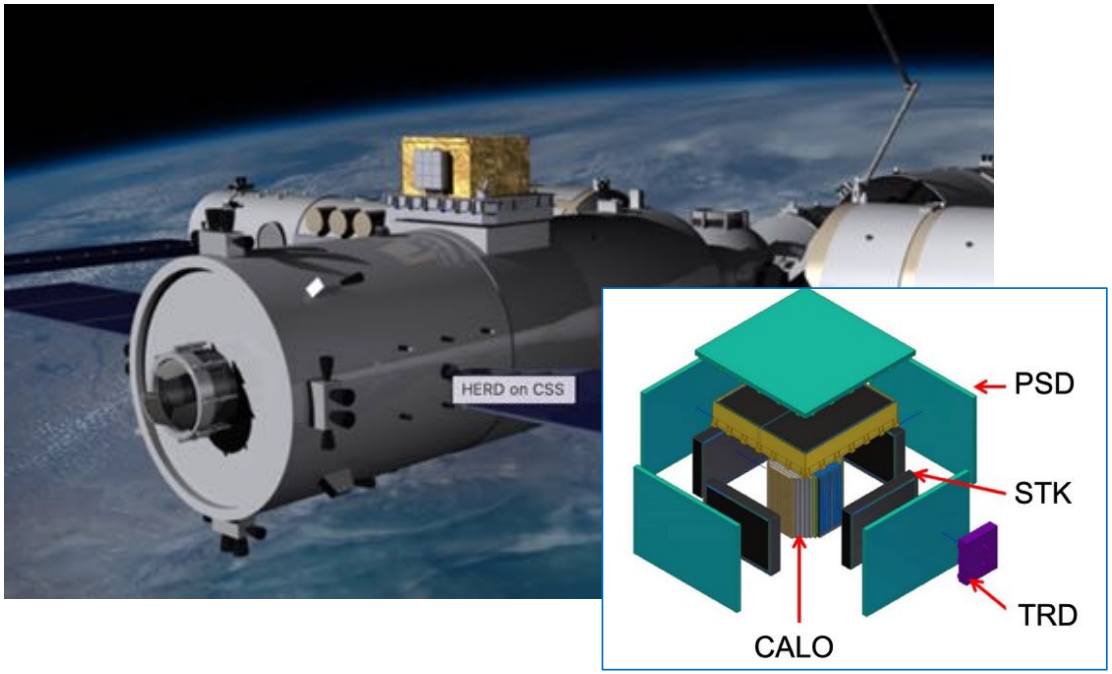

HERD (High-Energy Radiation Detector), cosmic ray detector and gamma-ray telescope for the Chinese space station (launch in 2027)

Next generation instruments (UHECR)

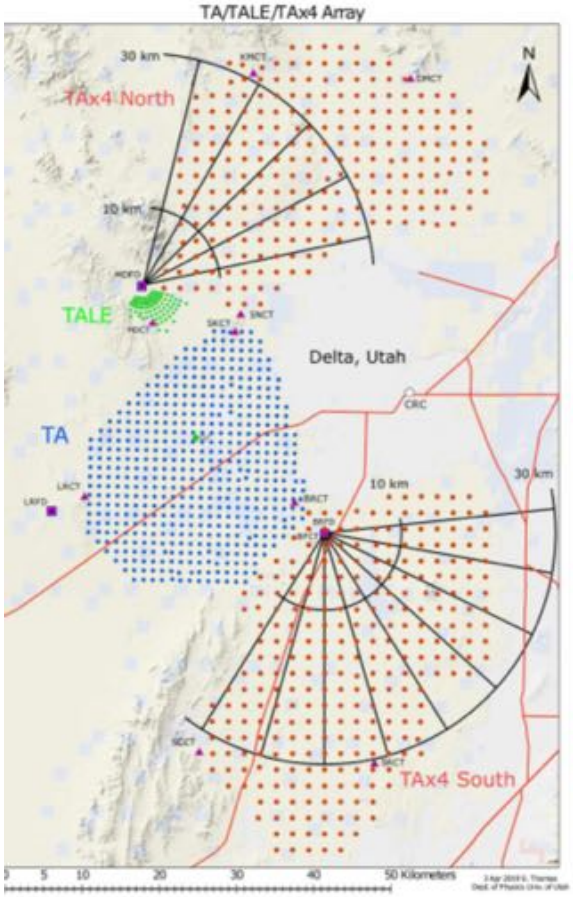

TAx4 (Telescope Array x 4 times), an upgrade of Telescope Array UHECR detector, with effective collection area 3000 km^3 in USA (Utah), starts data taking now.

Auger Prime, an upgrade of Pierre Auger Observatory (UHECR detector 3000 km^2 in Southern hemisphere), for improved measurement of UHECR composition, ready to start data taking.

Next generation instruments (mHz-kHz gravitational waves)

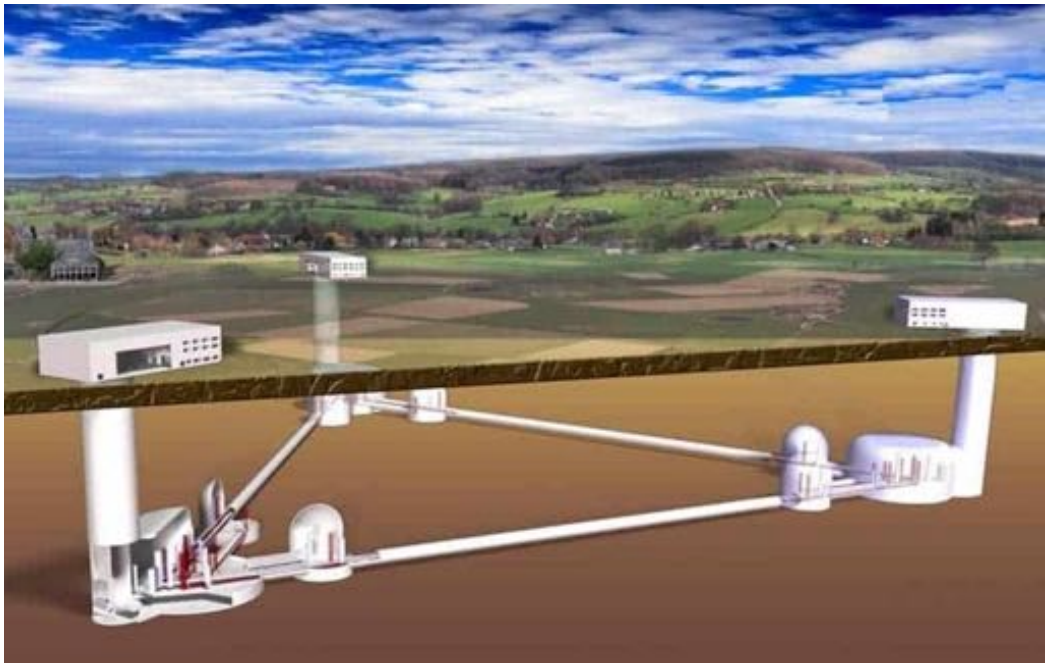

Einstein Telescope: 10 km scale interferometer for 1 Hz-10 kHz gravitational waves (2030th)

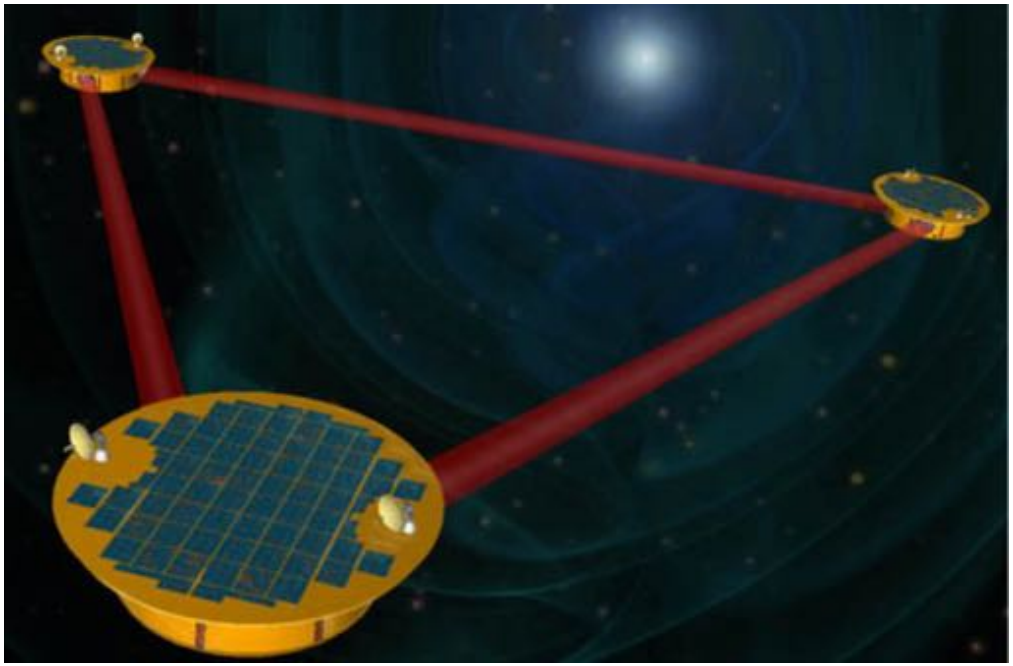

LISA, space-based interferometer with 10^6 km arms, for mHz gravitational waves (2030th)

Next generation instruments (nano-Hz gravitational waves)

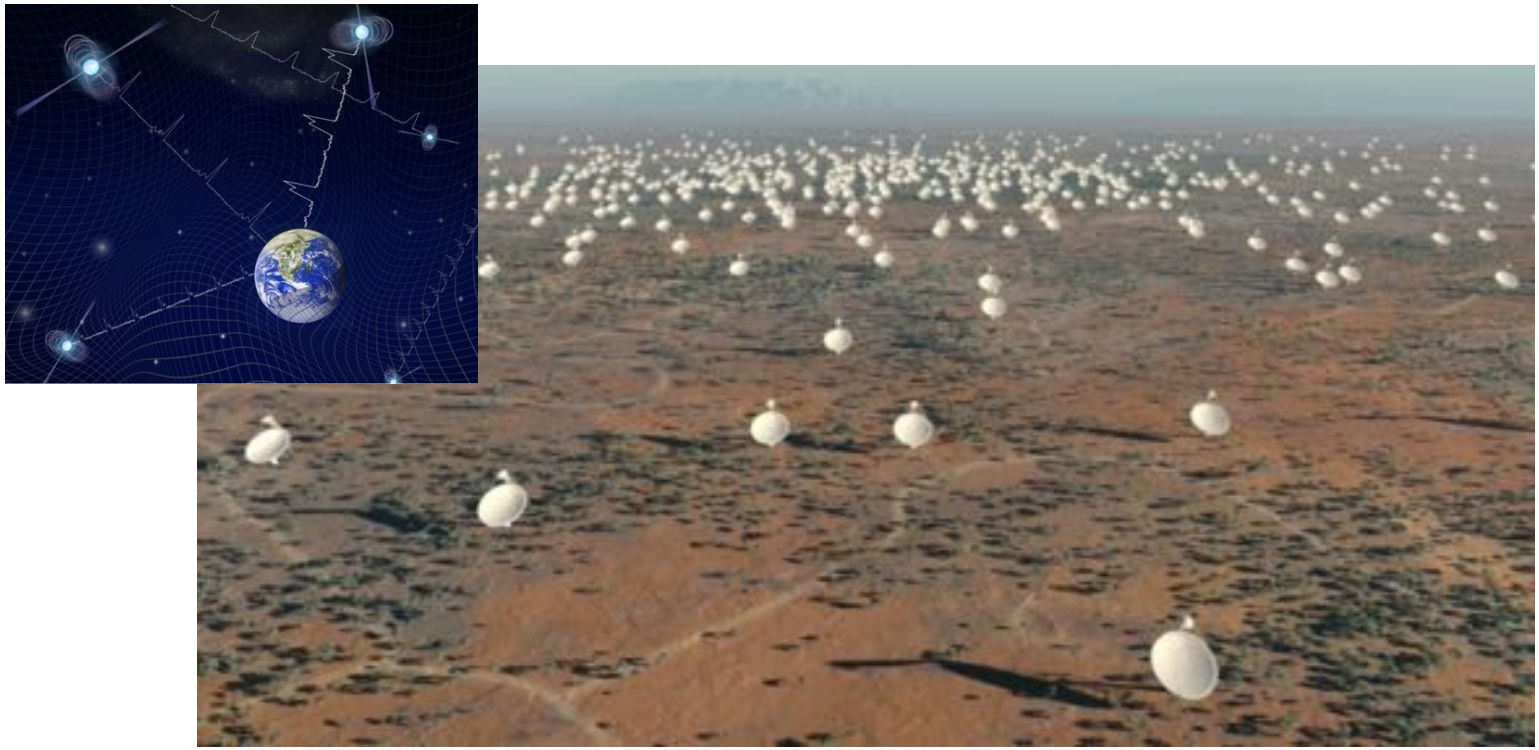

Square Kilometer Array radio telescope (in prototyping / construction) will serve as pulsar timing array, improving sensitivity of nano-Hertz gravitational wave measurements

Next generation instruments (direct dark matter detection)

https://lss.fnal.gov/archive/2022/conf/fermilab-conf-22-180-v.pdf

Name	Detector	Target	Active Mass	Location of Experiment	Status	Start.Ops	End.Ops
XMASS	Scintillator	LXe	832 kg	Kamioke	Ended	2010	2019
XENON10	TPC	LXe	62 kg	LNGS	Ended	2006	2008
XENON100	TPC	LXe	62 kg	LNGS	Ended	2012	2016
XENON1T	TPC	LXe	"1,995 kg"	LNGS	Ended	2017	2019
XENON1T (Ionization)	TPC Ionit.-only	LXe	"1,995 kg"	LNGS	Ended	2017	2019
XENONnT	TPC	LXe	"7,000 kg"	LNGS	Construction/Run	2021	2025
LUX	TPC	LXe	250 kg	SURF	Ended	2013	2016
LUX (Ionization)	TPC Ionit.-only	LXe	250 kg	SURF	Ended	2017	2019
LZ	TPC	LXe	"8,000 kg"	SURF	Construction/Run	2021	2025
PandaX-II	TPC	LXe	580 kg	CJPL	Ended	2016	2018
PandaX-4T	TPC	LXe	"4,000 kg"	CJPL	Running	2021	2025
LZ HydroX	TPC	LXe+H2	"8,000 kg"	SURF	R&D	2026	
Darwin / US G3	TPC	LXe	"50,000 kg"	LNGS/SURF/Boulby	Planning	2028	2033
DEAP-1	Scintilator	LAr			Ended	2007	2011
DEAP-3600	Scintillator	LAr	"3,300 kg"	SNOLAB	Running	2016	2028
DarkSide-50	TPC	LAr	46 kg	LNGS	Ended	2013	2019
Darkside-LM (Ionization)	TPC Ionit.-only	LAr	46 kg	LNGS	Ended	2018	2019
Darkside-20k	TPC	LAr	30 t	LNGS	Planning/Construct	2025	2030
ARGO	TPC or Scintillator	LAr	300 t	SNOLAB	Planning	2030	2035
GADMC	TPC	LAr			Planning	2030	
DAMA/LIBRA	Scintillator	NaI	250 kg	LNGS	Running	2003	
ANAIS-112	Scintillator	NaI	112 kg	Canfranc	Running	2017	2022
COSINE-100	Scintillator	NaI	106 kg	Yang'Yang	Running	2016	2021
COSINE-200	Scintillator	NaI	200 kg	Yang'Yang	Construction	2022	2025
COSINE-200 South Pole	Scintillator	NaI	200 kg	South Pole	Planning	2023	?
COSINUS	Bolometer Scintillator	NaI	?	LNGS	Planning	2023	?
SABRE PoP	Scintillator	NaI	5 kg	LNGS	Construction	2021	2022
SABRE (North)	Scintillator	NaI	50 kg	LNGS	Planning	2022	2027
SABRE (South)	Scintillator	NaI	50 kg	SUPL	Planning	2022	2027
CDEX-10	Ionization (77K)	Ge	10 kg	CJPL	Running	2016	?
CDEX-100 / 1T	Ionization (77K)	Ge	100-1000 kg	CJPL	Planning	202X	
SuperCDMS	Cryo Ionization	Ge	9 kg	Soudan	Ended	2011	2015
CDMSLite (High Field)	Cryo Ionization	Ge	1.4 kg	Soudan	Ended	2012	2015
CDMSLite (High Field)	Cryo Ionization	Ge	1.4 kg	Soudan	Ended	2012	2015
CDMS-HVeV Si	Cryo Ionization HV	Si	0.9 g	Surface Lab	Ended	2018	2018
SuperCDMS CUTE	Cryo Ionization / HV	Ge/Si	5 kg/1 kg	SNOLAB	Running	2020	2022
SuperCDMS SNOLAB	Cryo Ionization / HV	Ge/Si	11 kg/3 kg	SNOLAB	Construction	2023	2028
EDELWEISS III	Cryo Ionization	Ge	20 kg	LSM	Ended	2015	2018
EDELWEISS III (High Field)	Cryo Ionization HV	Ge	33 g	LSM	Running	2019	
CRESST-II	Bolometer Scintillation	CaWO4	5 kg	LNGS	Ended	2012	2015
CRESST-III	Bolometer Scintillation	CaWO4	240 g	LNGS	Ended	2016	2018
CRESST-III (HW Tests)	Bolometer Scintillation	CaWO4		LNGS	Running	2020	
COUPP	Bubble Chamber	CF_3I	4 kg	SNOLAB / Fermilab	Ended	2011	2012
PICASSO	Superheated Droplet	C_4F_{10}	3 kg	SNOLAB	Ended		2017
PICO-2	Bubble Chamber	C_3F_8	2 kg	SNOLAB	Ended	2013	2015
PICO-40	Bubble Chamber	C_3F_8	35 kg	SNOLAB	Running	2020	
PICO-60	Bubble Chamber	"CF_3I,C_3F_8"	52 kg	SNOLAB	Ended	2013	2017
PICO-500	Bubble Chamber	C_3F_8	430 kg	SNOLAB	Construction/Run	2021	
DRIFT-II	Gas Directional	CF_4	0.14 kg	Boulby	Ended		
NEWAGE-03b'	Gas Directional	CF_4	14 g	Kamioka	Running	2013	2023
MIMAC	Gas Directional	$CF_4+CHF_3+C_4H_{10}$		LSM (Modane)	Running	2012	
CYGNO	Gas Directional	$He + CF_4$	0.5 - 1 kg	LNGS	Planning	2024	
CYGNUS	Gas Directional	$He + SF_6/CF_4$		Multiple sites	Planning		
NEWS-G	Gas Drift	CH4		LSM	Ended	2017	2019
NEWS-G	Gas Drift	CH4		SNOLAB	Construction/Run	2020	2025
DAMIC	CCD	Si	2.9 g	SNOLAB	Ended	2015	2015
DAMIC	CCD	Si	40 g Si	SNOLAB	Ended	2017	2019
DAMIC100	CCD	Si	100 g Si	SNOLAB	Not Built		
DAMIC-M	CCD Skipper	Si	1 kg Si	LSM	Construction/Run	2021	2024
SENSEI	CCD Skipper	Si	2 g Si	Fermilab u/g	Running	2019	2020
SENSEI	CCD Skipper	Si	100 g Si	SNOLAB	Construction/Run	2021	2023
Oscura	CCD Skipper	Si	10 kg Si	SNOLAB	Planning	2024	2028
SNOWBALL	Supercooled Liquid	H2O			Planning		
ALETHEIA	TPC	He		China Inst. At. Energy	R&D		
TESSERACT	Cryo TES	He		LBNL	R&D		

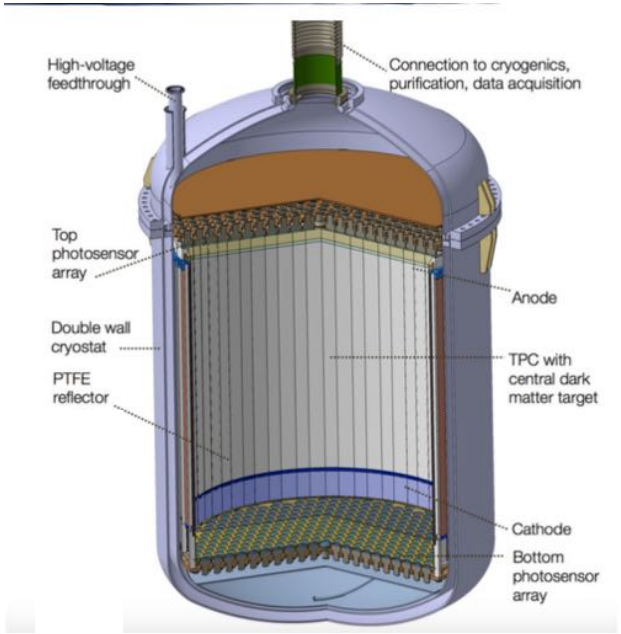

DARWIN (2028), tens-of-tonn scale dark matter detector